ESTIMATION OF DIFFERENT RECURRENCE INTERVAL FLOOD HYDROGRAPHS USING WMS AND GIS PROGRAMS IN JERASH, JORDAN

Albaraa SHANATI

2021
MASTER THESIS
CIVIL ENGINEERING

Thesis Advisor
Assist. Prof. Dr. Fatih SAKA

ESTIMATION OF DIFFERENT RECURRENCE INTERVAL FLOOD HYDROGRAPHS USING WMS AND GIS PROGRAMS IN JERASH, JORDAN

Albaraa SHANATI

T.C.
Karabuk University
Institute of Graduate Programs
Department of Civil Engineering
Prepared as
Master Thesis

Thesis Advisor
Assist. Prof. Dr. Fatih SAKA

KARABUK
June 2021

I certify that in my opinion the thesis submitted by Albaraa SHANATI titled "ESTIMATION OF DIFFERENT RECURRENCE INTERVAL FLOOD HYDROGAPHS USING WMS AND GIS PROGRAMS JERASH, JORDAN" is fully adequate in scope and in quality as a thesis for the degree of Master of Science.

Assist. Prof. Dr. Fatih SAKA .....
Thesis Advisor, Department of Civil Engineering

This thesis is accepted by the examining committee with a unanimous vote in the Department of Civil Engineering as a Master of Science thesis. June 28, 2021

Examining Committee Members (Institutions)	Signature
Chairman : Prof. Dr. Kasım YENİGUN (KU)	.....
Member : Prof. Dr. Tülay EKEMEN KESKİN (KBU)	.....
Member : Assist. Prof. Dr. Fatih SAKA (KBU)	.....

The degree of Master of Science by the thesis submitted is approved by the Administrative Board of the Institute of Graduate Programs, Karabuk University.

Prof. Dr. Hasan SOLMAZ .....
Director of the Institute of Graduate Programs

"I declare that all the information within this thesis has been gathered and presented in accordance with academic regulations and ethical principles and I have according to the requirements of these regulations and principles cited all those which do not originate in this work as well."

Albaraa SHANATI

ABSTRACT

M. Sc. Thesis

ESTIMATION OF DIFFERENT RECURRENCE INTERVAL FLOOD HYDROGRAPHS USING WMS AND GIS PROGRAMS IN JERASH, JORDAN

Albaraa SHANATI

Karabuk University
Institute of Graduate Programs
Department of Civil Engineering

Thesis Advisor:
Assist. Prof. Dr. Fatih SAKA
June 2021, 110 pages

Jordan is a Middle Eastern country located in the south of Syria and west of Palestine, which was disturbed by sudden floods because it is located in an arid region that is permanently and severely exposed to weather factors. This thesis has been prepared to create a simulation model of the flash floods affecting Jordan, to show how the developing technology can be used for this purpose, to analyze the various factors that cause such natural disasters to occur. In one such event, more than 21 people died in 2020 due to the occurrence of rapid and short-term floods. During the hydrological study of the Jerash Basin area, we obtained rainfall records from the Jordanian Ministry of Water and Irrigation for 6 rain stations, where these records were 31 years for four stations and 17 years for two stations, and two of the 6 stations were inside the study area, while 4 stations were surrounding the study area. In this study, 12.5 m x 12.5 m

resolution (Aster) images were used to model the Jerash Basin. Depending on the altitudes, the direction of the flow and the catchment area were determined, and the study area was found to be 101 square km. In the process of analyzing the rainfall records, the average, the largest, and the lowest values of precipitation for all stations in the study area were calculated by using the pivot table in Microsoft Excel. And by communicating with the University of Jordan, we obtained a soil map in addition to the hydrological classification of the soil of the study area, and we also obtained a land-use map. Through the two maps, the curve number for the study area was calculated based on the WMS program. Gumbel Type I distribution was applied to calculate the intensity-duration-frequency (IDF) curves for repetition periods of 2, 5, 10, 50, 100, 1000 years for each station by using the largest amount of precipitation obtained. And after that, we calculated the amount of runoff based on SCS, through an analysis process of both the runoff and the IDF curves, hydrographs of the study area were obtained the via WMS for different recurrence intervals. Finally, model accuracies were determined with historical flood records.

Keywords **:** Jerash Basin, Hydrological Modeling, WMS, IDF, ArcGIS, Runoff, Hydrograph.

Science Code : 91106

ÖZET

Yüksek Lisans Tezi

CERAŞ, ÜRDÜN'DE WMS VE CBS PROGRAMLARI KULLANARAK FARKLI TEKERRÜR ARALIĞI TAŞKIN HİDROGRAFLARININ TAHMİNİ

Albaraa SHANATI

Karabük Üniversitesi
Lisansüstü Eğitim Enstitüsü
İnşaat Mühendisliği Anabilim Dalı

Tez Danışmanı:
Dr. Öğr. Üyesi. Üyesi Fatih SAKA
June 2021, 110 sayfa

Ürdün, Suriye'nin güneyinde ve Filistin'in batısında yer alan, sürekli ve şiddetli hava faktörlerine maruz kalan kurak bir bölgede yer alması nedeniyle ani seller görülen bir Ortadoğu ülkesidir. Bu tez, Ürdün'ü etkileyen sel baskınlarının simülasyon modelini oluşturmak, gelişen teknolojinin bu amaçla nasıl kullanılabileceğini göstermek, bu tür doğal afetlerin meydana gelmesine neden olan çeşitli faktörleri analiz etmek amacıyla hazırlanmıştır. Böyle bir olayda, hızlı ve kısa süreli sellerin meydana gelmesi nedeniyle 2020'de 21'den fazla kişi ölmüştür. Jerash Havza alanının hidrolojik çalışması sırasında, 6 yağış istasyonu için Ürdün Su ve Sulama Bakanlığı'ndan yağış kayıtları alındı, bu kayıtlar dört istasyon için 31 yıl ve iki istasyon için 17 yıl ve bu 6 istasyondan ikisi çalışma alanı içinde, 4 istasyon ise çalışma alanını çevrelemektedir. Bu çalışmada Jerash Havzasını modellemek için 12,5 m x 12,5 m çözünürlüğe sahip (Aster) görüntüleri

kullanılmıştır. Rakımlara bağlı olarak akışın yönü ve su toplama alanı belirlendi ve çalışma alanı 101 km² olarak bulundu. Yağış kayıtlarını analiz etme sürecinde, çalışma alanındaki tüm istasyonlar için ortalama, en büyük ve en düşük yağış değerlerini Microsoft Excel'deki pivot tablo kullanılarak hesaplandı. Ayrıca Ürdün Üniversitesi ile temasa geçtik ve çalışma alanı zemininin hidrolojik sınıflandırmasına ek olarak bir zemin haritası ve arazi kullanım haritası elde ettik. İki harita aracılığıyla, WMS programına dayalı olarak çalışma alanı için eğri numarası hesaplanmıştır. Elde edilen en büyük yağış miktarı kullanılarak her istasyon için 2, 5, 10, 50, 100, 1000 yıllık tekerrür periyotları için şiddet-süre-frekans (IDF) eğrilerini hesaplamak amacıyla Gumbel Tip I dağılımı uygulanmıştır. Daha sonra, hem akış hem de IDF eğrileri yardımıyla SCS'ye dayalı akış miktarını hesapladık, farklı tekerrür aralıkları için WMS aracılığıyla çalışma alanının hidrografları elde edilmiştir. Son olarak tarihsel taşkın kayıtları ile model doğrulukları tespit edilmiştir.

Anahtar Sözcükler : Jerash Havzası, Hidrolojik Modelleme, WMS, IDF, ArcGIS, Akış, Hidrograf.

Bilim Kodu : 91106

ACKNOWLEDGMENT

First and foremost, praise be to God, who made everything easy. I would like to thank Associate Professor Fatih SAKA for his supervision, advice and guidance, as we had a father before he was our teacher, and all thanks and gratitude to Prof. Dr. Mustafa AL KUISI from the University of Jordan, who provided me with the data in the way to make this thesis successful, and I cannot forget my family, which is everything to me as they are the encouraging and the first source of strength for me in this life. I thank all of my colleagues and friends who were brothers in this life.

CONTENTS

Page

Page

Page

Page

LIST OF FIGURES

Page

Page

Page

Page

LIST OF TABLES

Sayfa

PART 1

INTRODUCTION

1.1. GENERAL

Jordan is one of the four countries of the Levant, which connects it to the Kingdom of Saudi Arabia from the south, Jordan is a water-poor country, which is considered one of the driest countries in the world, and has been exhausted by global warming, which has led to a decrease in the amount of rain, an increase in temperature rates, and an increase in weather fluctuations during periods of precipitation. Hydrological and meteorological factors are among the factors that are relevant to the occurrence of a flash flood (Youssef, et al., 2015). Floods in Jordan have increased due to climate fluctuations, and this indicates that time expectations for the impact of climate change on Jordan no longer accommodate sudden floods, and all of this is either due to natural action such as volcanoes and natural changes in greenhouse gas concentrations, and the human activities affecting global warming such as using Fossil fuels and gases from factories and cars, The Intergovernmental Panel on Climate Change (IPCC) of the United Nations has defined climate change as “climate change over time”, whether by natural or human (IPCC, 2007) the report of the Intergovernmental Panel on Climate Change also revealed some of the impacts of climate change that can be avoided by limiting global warming to 1.5 degrees Celsius instead of 2 degrees Celsius, and limiting reckless weather conditions, which bring disasters such as floods (IPCC, 2007) The difference in geomorphological structures causes climatic fluctuations that contribute to extremely heavy rainstorms, which in turn cause rapid floods of short duration in the valleys. As for flash floods, they are known as rapid generation flows, meaning that they are short-term floods with relatively high peak discharge. Other factors that cause floods in Jordan must be mentioned, which are the surrounding environment and the morphology of the

watershed (poor vegetation, low infiltration, steep slopes, and human activities) (Youssef, et al., 2015).

1.2. EFFECT OF CLIMATE CHANGE ON FLOODS

After a period of time after the industrial revolution, the world began to face a serious challenge, which is the phenomenon of climate change, which led to an Acceleration of snowmelt in the North and South Poles (Arctic and Antarctica), decreasing amounts of rain, increasing fluctuations in weather conditions, and this led to the drying of many streams and the decrease in the quantities of groundwater to low levels (Green, et al.,2011) in addition to the difficult climatic conditions, high temperatures in summer and flash floods in winter (Sippel, et al., 2015).

Therefore, Jordan turned to policies aimed at promoting the use of renewable energy, Interest in agriculture and gradually moving away from the use of greenhouse gases, because annual precipitation rates clearly indicate a continuous decline overtime at a rate of 1.2 mm per year, And, in a report issued by the United Nations Intergovernmental Panel on Climate Change, it says that the average temperature is increasing 0.2 degrees / year, humidity is also increasing at a rate of 0.08%, and rain will witness a decrease in precipitation rates, with more intense rains (Namrouqa , 2018).

1.3. FLASH FLOODS IN JORDAN

Flash floods are like other natural disasters come without warning and may occur in all countries of the world, and their consequences are disastrous for the environment and infrastructure (The National Severe Storms Laboratory, n.d.). In October 2018, the weather was sunny and there were no factors indicating rain, suddenly the sky turned black and clouds gathered in the sky where a thunderstorm occurred followed by heavy rain, as the amount of rain reached 43 mm within 22 minutes, and this storm caused a flash flood, and water entered the homes of the people of the area, killing 4 people, including two students And the results reached that it became catastrophic due to several

factors (heavy rainfall, the degree of saturation of the soil with water, lack of knowledge of how the land is used, the terrain, the type of vegetation cover, etc.) (The New York Times, 2018).

We can see one of the floods that occurred in Jerash in 2020 in Figure 1.1 below, and Figure 1.2 Flood in Jerash city in 2021 shows what happened in February of 2021. In Figure 1.3 the Arab News wrote" Two women and a girl died in severe floods in Dabaa, and another girl died in Madaba, floods come two weeks after 21 people, mostly children, were killed in flash floods near the Dead Sea" (Arabnews, 2018).

Figure 1.1. Flood in Jerash in 2020 (Tashta, 2020).

Figure 1.2. Jerash in 2021 (Toaimat, 2021).

Figure 01.3. Flash floods in Petra in Jordan (Arabnews, 2018).

1.4. STUDY PROBLEM

Climate change in Jordan will lead to an increase in the flood problem in the coming years, and this phenomenon poses a threat to Jordan, Jordanians and tourists who are the first financial resource for the Jordanian economy. Studies confirm that Jordan and all countries of the world will continue to suffer from these flaws oods if the world does not find a solution to the phenomenon of global warming. So, the causes of floods and the factors related to climate change should be known, where plans and measures should be developed to mitigate the size of material and moral damage to try to avoid the danger of floods in the area.

1.5. OBJECTIVES OF THE STUDY

- A study of the geology and geography of the area in order to form an idea about the hydrology of the area
- Analyzing the data coming from the meteorology authority for the study area.
- Detecting the reasons for flash floods in the study area and studying its consequences resulting from climate change
- Calculating flood quantities by constructing a hydrological model for it
- Using technology to predict floods caused by storms, and trying to know the hydrological conditions that help in these floods

1.6. PREVIOUS STUDY

Many authors have studied flash floods as an issue concerning various disciplines such as geology, hydrology, geomorphology, water resources, geography, and many more. The following is a summary of the literature review and previous work.

Rimawi and Salameh (1988) studied the hydro chemicals of the groundwater system in the Zara-Zarqa Ma'in thermal field. They concluded that the high salinity of the Zarqa Ma'in thermal waters is caused by their mixing with the waters of the Dead Sea.

Sawarieh (2005) carried out a detailed hydrogeological and hydrochemical study on the thermal water in Central Jordan (Wadi Zarqa Ma'in and Wadi Waleh). The investigation concluded that the thermal water in the Jiza region caused from mixing between the bicarbonate water of the upper aquifer with the thermal chloride water of the lower aquifer across faults, resulting in a high-water temperature near these faults.

Abu-Allaban and Jaber (2009) analyzed the trend in weather parameters in Jordan. Six meteorological stations distributed all over Jordan were taken to analyze the data using some parametric and nonparametric statistical methods. The results presented that no visible trends are demonstrating a decrease or an increase in the yearly rainfall and maximum temperature. Though, there are good to strong trends indicating that the yearly temperature range has decreased in the last decade while the yearly minimum temperature has increased. The temperature in the Earth's atmosphere showed a significant decrease, which means that the atmosphere has become more efficient in catching terrestrial infrared radiation, which is responsible for global warming.

Alhasanat (2014) evaluated the risk caused by possible Flash Flood risks in Wadi Mousa. He worked to quantify flows of flash flood hazards and to create floodplain zone maps for specific flood return periods of 25, 50, 75, and 100 years. The surface drainage is divided into sub-catchments which are Wadi Khaleel with Wadi Jelwakh, Wadi Al-Maghir, Wadi Als-Sader. The area of the study area is 53.3 km2 and it consists of flash floods resulting from heavy rainstorms over the watersheds and flows into Wadi Araba. The average yearly precipitation of Wadi Mousa was computed at 178 mm, and the average yearly evapotranspiration is 1300 mm per year.

Youssef, et al. (2015) studied the various factors that caused flash floods in two main flash flood events in the city of Jeddah from 20 November 2009 to January 2011. These

factors were categorized into geomorphological features, network and watershed factors, human activities, and climate change and precipitation factors.

In this study, remote sensing RS, and geographic information systems (GIS), integrated topographic with geological maps, precipitation data, climate change data, and field investigations were used.

Farhan and Anbar (2016) conducted a study to evaluate the flash flood in Wadi Yutum catchment, southern Jordan. GIS and remote sensing techniques were used combined with geological and geomorphical data to test the possibility of flood risk spatially. The El-Shamy's approach and morphometric ranking method were utilized for seventeen sub-basins of the Wadi Yutum to assess flood risk. Both methods utilized twenty morphometric parameters to estimate flood risk. Through the two methods, they were able to identify the branch basins with a high potential of flash flooding. GIS and morphometric analysis were used to produce flood hazard maps showing sub-basins vulnerable to damaging floods in the Wadi Yutum. The aim of this work is to help decision-makers and planners understand the spatial distribution of flood risk conditions and this is to reduce the negative effects of frequent floods on the population and infrastructure of the city of Aqaba.

Twumasi, et al. (2017) studied the impact of climate change causing floods in the Southern African area using GIS and remote sensing data. The results of the study revealed significant damages to the natural environments and society, with flood risk areas in the study area.

Lababneh, et al. (2019) conducted a study about hydrological modeling for the Al Hasa watershed area using the GIS. They used three methods for flood computations, namely: time of concentration, unit hydrograph, and SCS curve number methods. They concluded that the results of the three methods were close and acceptable, though, time of concentration method has the greatest value as it takes all ideal variables considered and ignored external variables impacts.

Abdallah (2020) studied the climatic trends of the important climatic factors in Jordan mainly precipitation and temperature. Trend analysis revealed obvious decreasing trends in the precipitation, while temperatures showed increasing trends. These conditions are prompt results of climatic changes affecting in recent times.

1.7. GIS IN HYDROLOGY

The Geographic Information Systems (GIS) program is defined as a realistic technology program that simulates spatial data, displays it, stores it, and performs the process of analysis and processing of this data. It has been adopted by many government institutions such as universities and institutions related to geography, water, and geology. As we know, the GIS program is concerned with surface and groundwater, but it can represent population features (National Geographic, n.d.).

In recent years, a large number of individuals have noticed the tendency to create hydrological models through the use of (GIS), after they realized the value and benefit of integrating hydrological modeling with (GIS), and this is what explained when he mentioned that GIS is one of the best tools, if not the best (Al-Smadi, 1998).

To carry out an information gathering process in order to obtain the best hydrological models. Several authors have stated that there is an importance of using a geographic information system to study the connection between changes in land use and flood risks through analysis (Chang et al., 2009). In Recent Times, GIS has been utilized to delineate watersheds and compute morphometric parameters. During this study, geographic information systems were the tool that determines the hydrological parameter of the Jerash Basin area. (DEM) was used in the various branches of hydrology, and the analysis of drainage, watersheds and slope hydrology was largely based on the digital elevation model (DEM) (Naidu, 2015). In Figure 1.3 we can see a simple summary about what is GIS.

Figure 1.4. Summary of GIS (gisgeography, 2021).

PART 2

GEOLOGICAL INFORMATION OF STUDY AREA.

2.1. LOCATION STUDY AREA

The northern Jerash Basin area is located at 32º 17′ 45.566″ North and 35º 53′ 39.8116″ East, where it is 48 km away from the capital Amman, and its altitudes range between 261 m to 1268 m above sea level. In this area, the catchment area can be categorized as an arid and semi-arid .The following map is portrayed by a sub-dendritic to dendritic drainage network with two main trends, and Jerash is distinguished from other governorates of Jordan by the purity of its springs, as shown in Figure 2.1 below (Wienner, 2018).

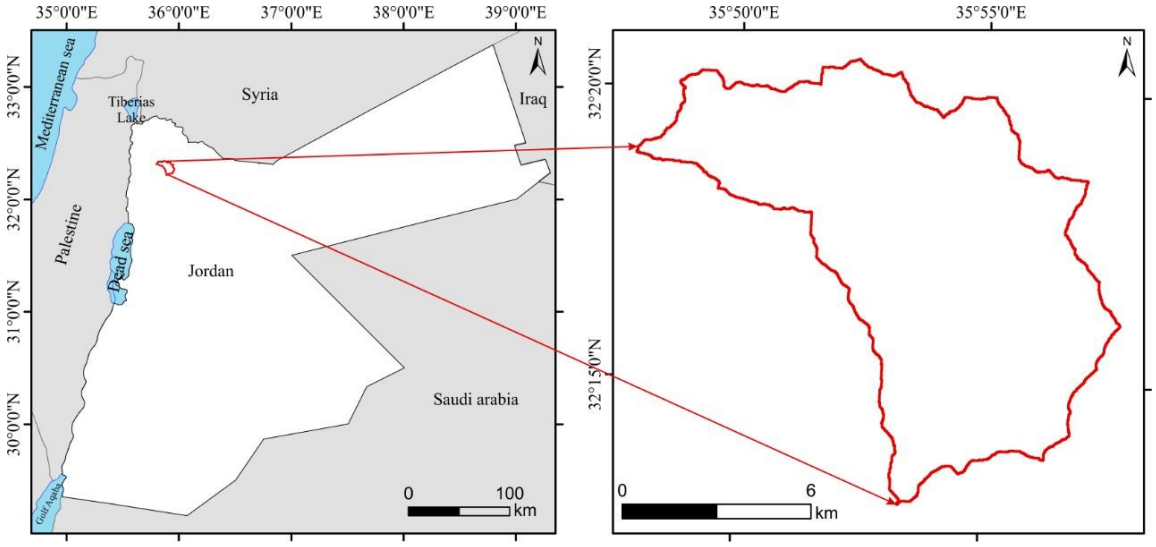

Figure 2.1. Location of the study area.

2.2. THE CLIMATE OF JORDAN

Jordan is known as a country with an arid and semi-arid climate, as it is characterized by having relatively high temperatures, which contributes to an increase in the amount of evaporation and a decrease in precipitation. Some areas of Jordan derive humidity from the Mediterranean region, which is what we see in the northwestern regions, while the surrounding desert regions affect it and give it a dry climate, this includes the rest of Jordan and what distinguishes these areas is that the rate of evaporation in them is higher than the rates of rain. (Britannica, n.d.) Temperatures in it range from a few degrees in winter to 46 degrees Celsius in summer. As for rain, it is distributed according to regions. In desert areas, precipitation ranges at 50 mm / year, while in the northwestern highlands it reaches 600 mm / year where our study area is located, in Figure 2.2 we can see how are the bioclimatological regions distributed in Jordan. As for the study area, it is dominated by the Mediterranean climate, and as is known about this region, its rains are in the spring and winter seasons, and the precipitation rates vary according to the terrain, in the low areas it is 250 mm / year and in the high areas it reaches 450 mm / year. (Sawarieh et al., 2009).

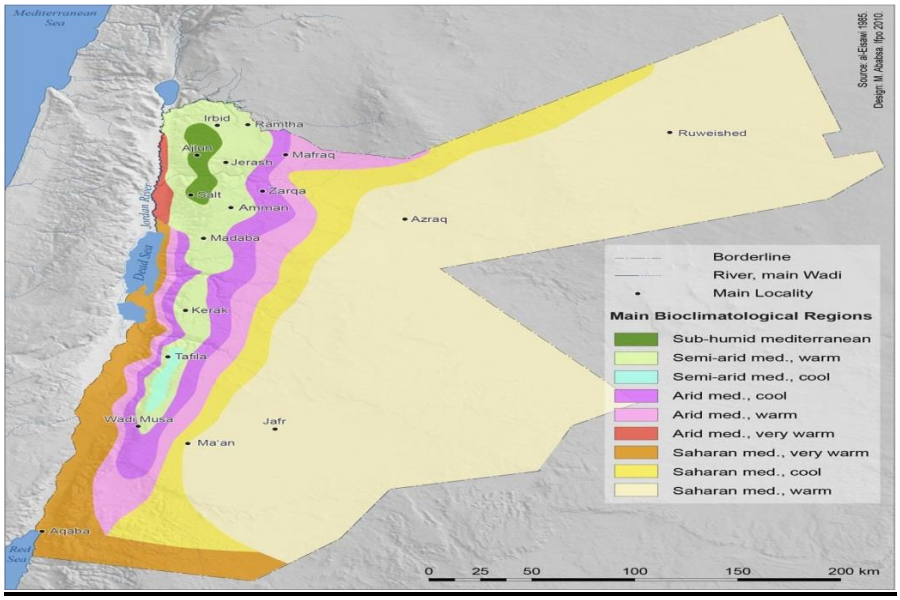

Figure 2.2. Climate Regions in Jordan (Ababsa, 2013).

2.3. TOPOGRAPHY

The northern Jerash basin is located in a mountainous area that includes many valleys, where its heights start from 261 m to 1268 m above sea level. This indicates that there is a topographic diversity, but it is not large, but it can change quickly and this is what the slope map shows, where the ArcGIS program provided us, Map showing the regressions after using DEM. In figure 2.3 Slope angles over the study area was shown as the slope angles over the study area and we slope is decreasing in the middle and increasing in the south-west.

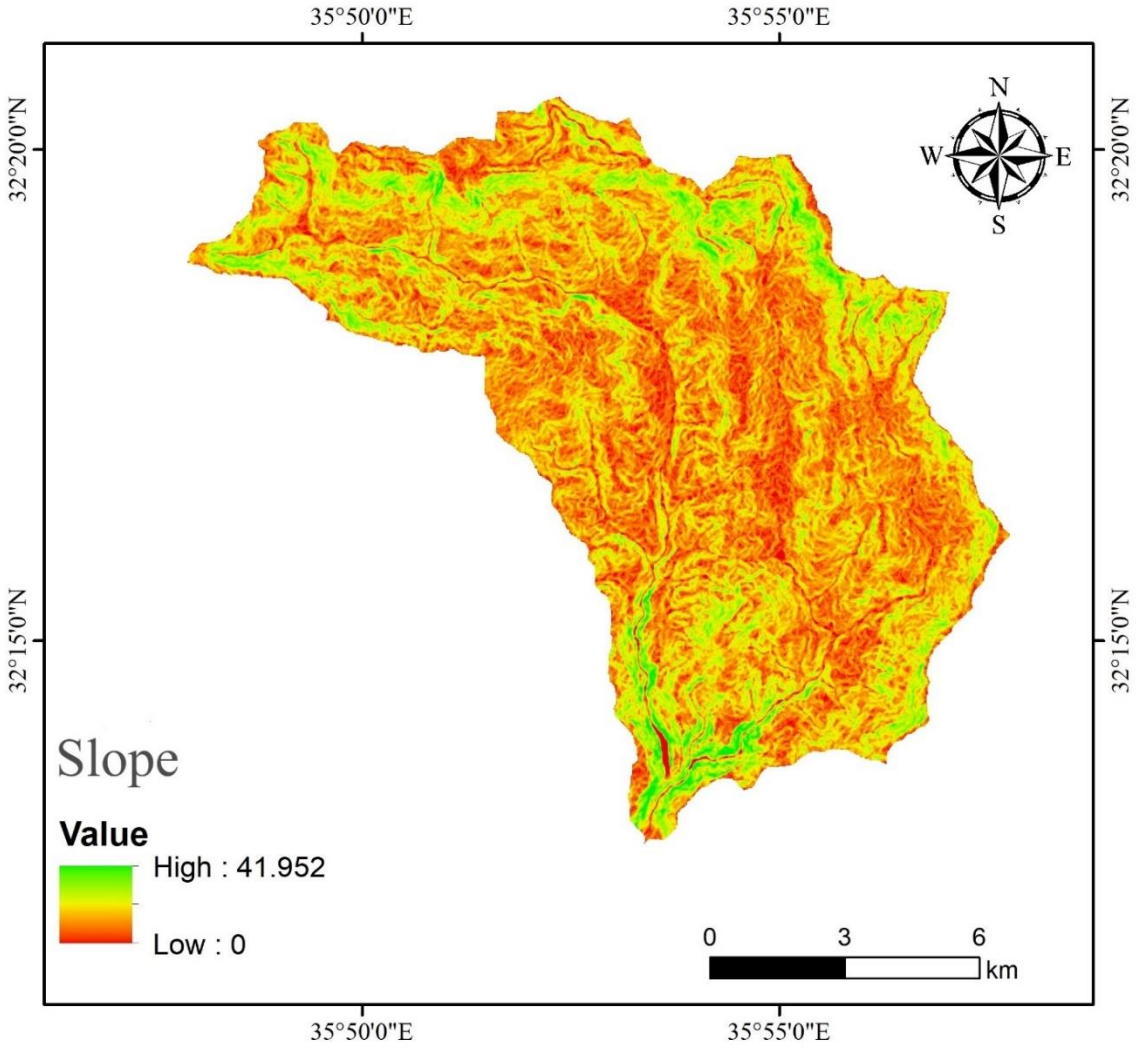

Figure 2.3. Slope map of study area.

2.4. LAND USE

Land use in Jerash is divided into four parts: built-up lands, agricultural lands, forests, and unused lands:

- The built-up lands include vital places in the governorate such as urban, rural, roads and the industrial zone in the east of the governorate, as well as tourist and commercial places, and this area constituted a total of 1% of the total area of the governorate in 1952, and continued to expand until it reached 8% Of the total area of Jerash governorate in 2019 (Zregat, 2014).
- Agricultural lands where olive, citrus, and vegetable trees abound, in addition to wheat and barley fields. Combined agricultural lands constituted an area of 33% of the general area of Jerash Governorate in 1952, and this figure indicates that a large percentage of the area's population are farmers, and with the Jordanian government’s move to reclaim lands, the area of agricultural land increased over the previous years until it reached Equivalent to 48% of the total public health package in 2009.
- Forests: The forests in Jerash governorate are found in all regions of the governorate, and oak and pine trees grow in them, and cultivated forests have recently spread in them. With regular slopes and harsh slopes, as it formed in 1952 an area of 8% of the general area of Jerash Governorate, but in 2009 it became a total of 14% of the general area of the governorate (Zregat, 2014).
- Unused lands: they are lands that are not used except by livestock herders and are characterized by having steep slopes. They constituted a total of 58% of the general area in 1952, then this area began to shrink until it reached the equivalent of 30% of the general survey of the governorate in 2009. Jerash, the researchers have explained that the retreat of unused land to the expansion of built-up lands, the exploitation of these lands for the benefit of agricultural lands, and the tendency to cultivate them on steep slopes to try to protect the soil from erosion. (Zregat, 2014).

2.5. GEOLOGY OF JORDAN AND STUDY AREA

Jordan is characterized by the presence of thick sedimentary sequences and being located to the northwest of the Arabian Peninsula, it includes three topographic regions starting from the south to the north, the heights in its center, the rift in the west of the kingdom, in addition to the plateaus in its east. It was also noted that there are rocks more than 600 million years old that formed in the Arab-Nubian Shield and are located in southern Jordan. (Abed, 2000). Figure 2.4 Geological Map of Jordan and Figure 2.5 Explanation of Geological Map of Jordan Show us the geological situation of Jordan and its explanation, and we can see that the study area is locating between KS1 (varicolored argillaceous sandstone, white sandstone silicified sandstone, and brown coarse-grained sandstone) and KS2 limestone, sandy limestone, dolomite, nodular limestone, shale and gypsum. (Abed, 2000).

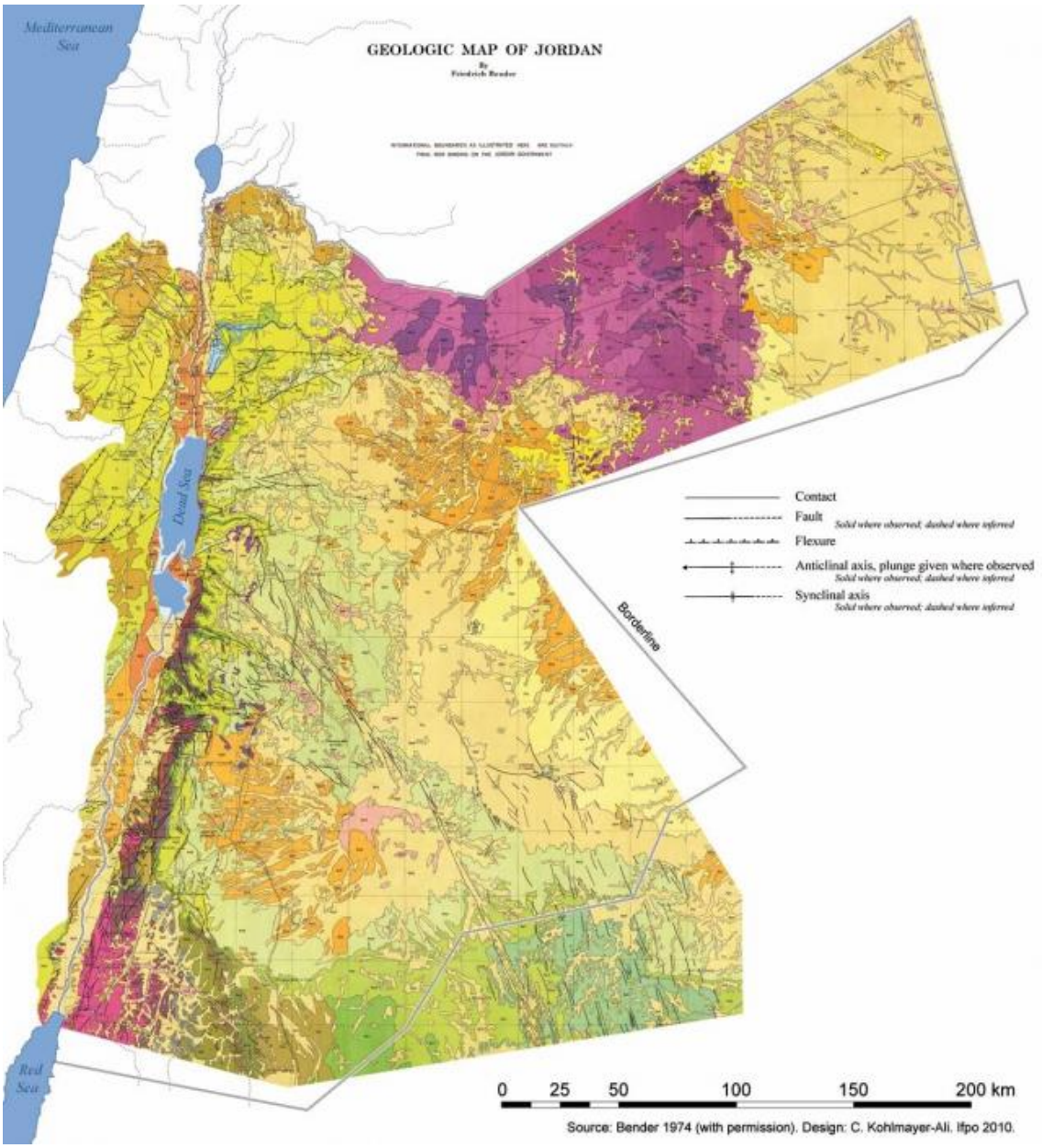

Figure 2.4. Geological map of Jordan (Ababsa, 2013).

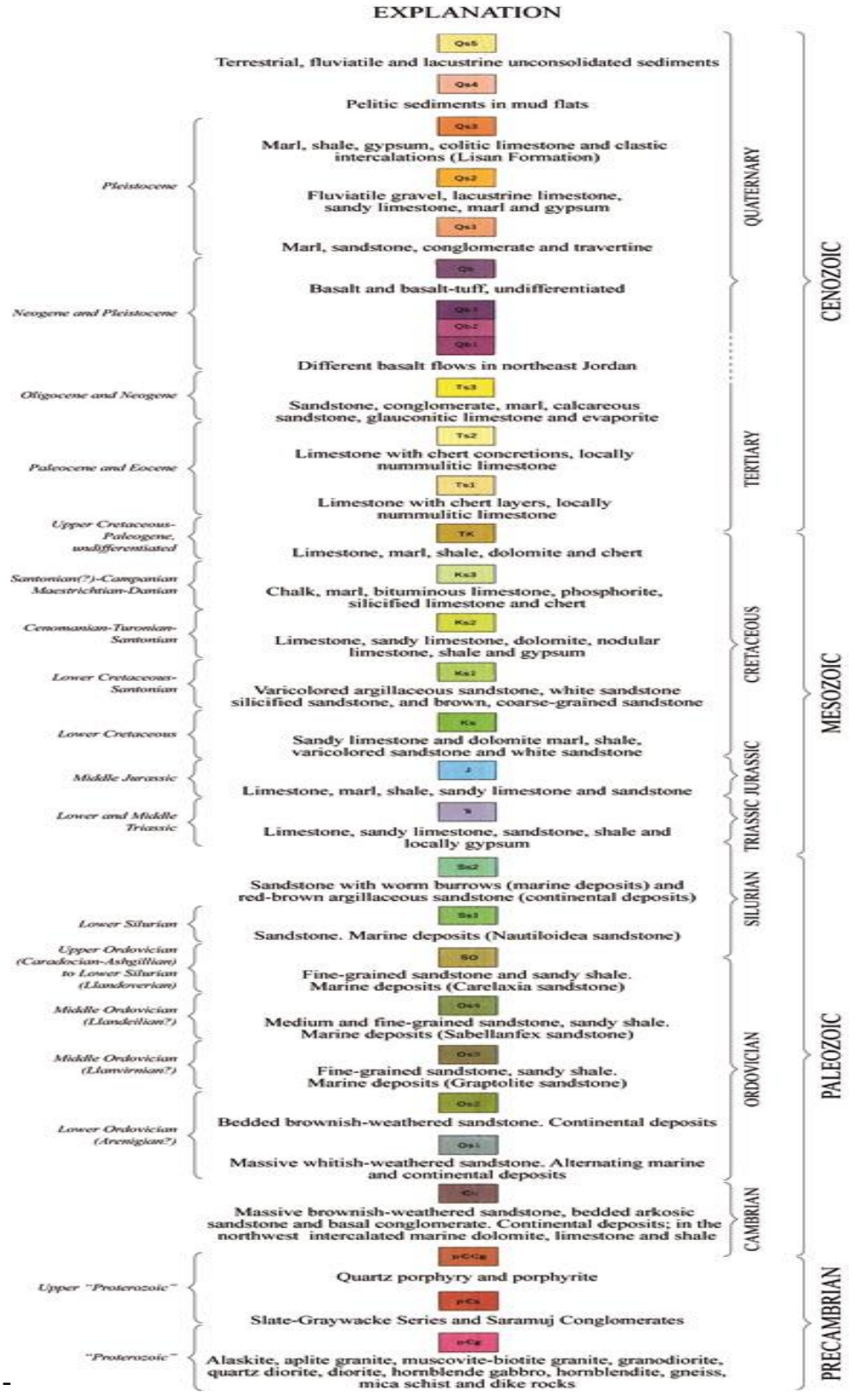

Figure 2.5. Explanation of geological map of Jordan (Ababsa, 2013).

The geology of the study area was divided geologically according to the neighboring regions. In the following map, we note that there are two rock formations appearing in most of the study area, which are the Na'ur formation and the Fuheis formation, while the sandstone appears in the southern part of the study area, In Figure 2.6 The geological map of the study area we can see the formation of the study area, Na'ur Formation is biggest formation according to its area which is located at the middle of the study area, Kurnub Sandstone is located at the south-west and Amman Formation is located on the northern border of the study area (Moumany, Abed, & Ibrahim, 2011).

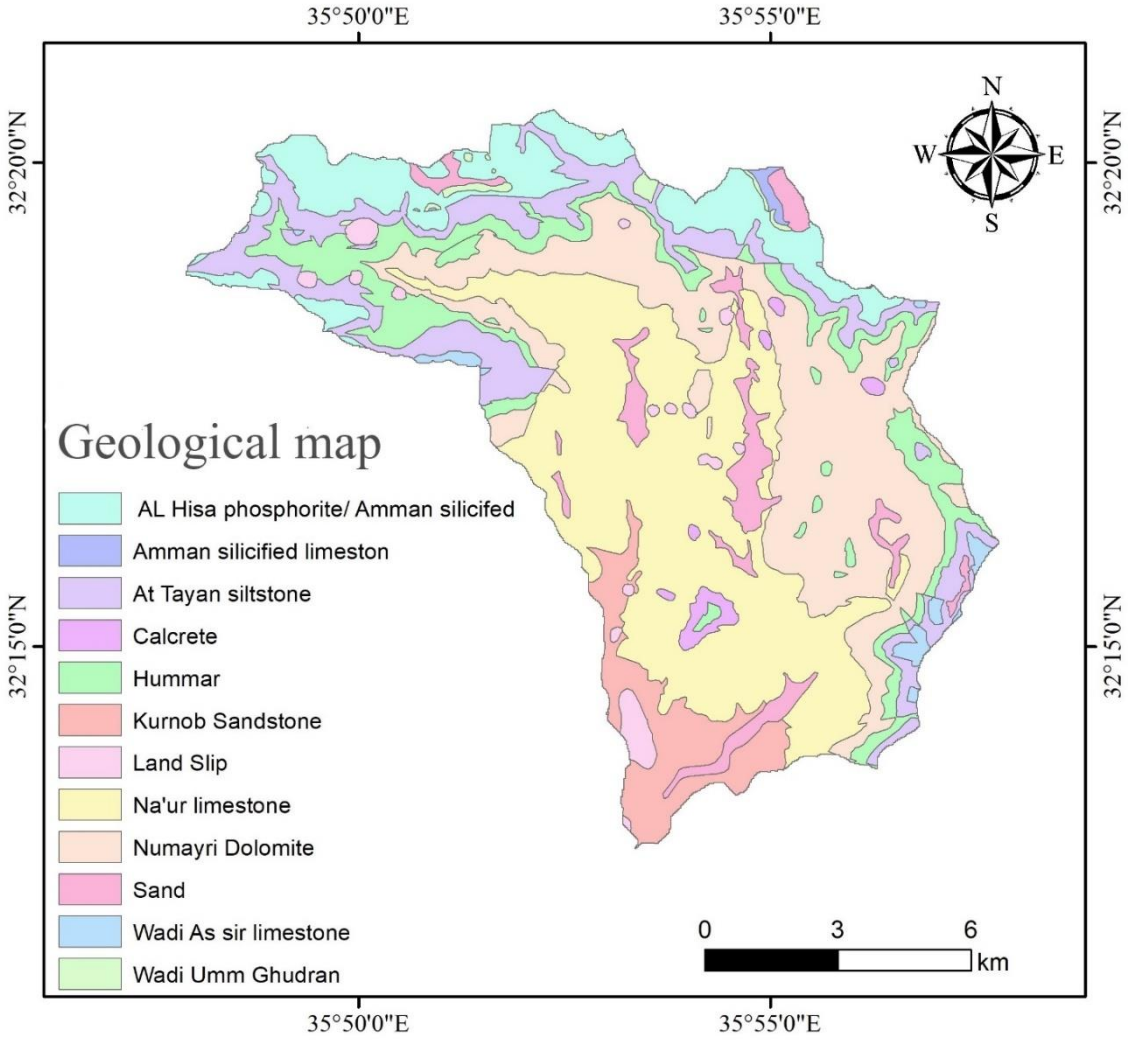

Figure 2.6. Geological map of study area (Bender, F. 1974).

2.5.1. Kurnob Formation

In the valley of the valleys of the western Jordan mountains from Ajloun in the north to the south of Grindel, the Wadi Araba is hardly without the exposures of the Kurnob group. Then it unfolds along the precipice of the Negev head- The belly of the ghoul and to the east of that and in many locations south of that cliff. Moreover, isolated excavations were found in the pebble's sepals southeast of Bayer and in Wadi Arnah east of Al-Jafr. And since the description here is general, it can be said that the Kurnob group consists of two clear sand units, a white mass sand unit at the bottom and a multicolored sand unit at the top. (Abed, 2000) This description is good in the middle and south of Al-Azden from the Madaba region almost to the south. In the north, as it enters the content of the Kurnob group, several marine levels made up of dolomite, limestone, gluconate, and others, alternate with the sandy rocks we know that make up the Kurnob. (Abed, 2000)

2.5.2. Alna'ur Formation

It can be said that the formation of the Na'ur was composed of a succession of levels of different thicknesses (not exceeding 30 m) of limestone (or dolomite) with marl. This is the general picture of the composition, but that is in detail. The Naour Formation was divided into four rock units from the bottom, A – D:

Unit A: It is the bottom. I have been given a Juhra Member Profile and this unit is part of the Cabbage Group.

Unit B: The beginning of this lower unit is the true beginning of the formation of Na'our, meaning it is the lower boundary of the formation of Na'our. It is a solid carbonate cliff-forming unit over the cabbage collection consisting of dolomite, dolomitic limestone and limestone with few flint nodules. This unit begins with fossil limestone (oysters and oyster) topped by dolomitic bulk limestone rich with traces of fossils in the form of

bifurcated cylindrical worm pits with a diameter of up to several cm. These traces are made of dolomite while the rest of the rock is limestone (Abed, 2000).

Unit C: is a soft unit made of green marl, silt limestone, soft clay limestone and a few layers of delicate dolomitic limestone. The thickness of the unit does not change much north to south

Unit D: is a unit composed of carbonates generally of gray dolomite, dolomitic limestone, limestone and some nodules of flint. It is made of cliff-forming calcareous rocks above the soft C unit and under the soft fuhayes marley formation. This unit constitutes the summit of the Naour formation, and this unit can be traced from northern Jordan to Ras al-Naqab, and it is the unit on which the Mujib Dam was built (Abed, 2000).

2.5.3. Hummar Formation

The main characteristic of the formation of Hummar is that it is a solid cliff-forming lime above the soft, Marly formation of Fuheis. Hummar consists of gray stone, fine dolomitic limestone and dolomite. With these hard carbonate rocks there are thin layers of clay or marley limestone towards the base of the formation. In the section of Umm al-Dinanir, west of al-Baqa'a, formation begins with the Marley limestone rich in fossils of molluscs and the abdomen, over al-Fuheis Marl (18 AD). Then the limestone and dolomitic limestone predominate, with only a companion level (2 m) of marl being cut. And at the end of the formation (the top five ms) is the Marley limestone (Abed, 2000).

2.5.4. Wadi As Sir Formation

The formation was named after the town of Wadi Al-Seer, west of Amman, and this formation was called limestone, the limestone unit. This designation includes the chalk mud above the Wadi Al-Seer formation. This formation is characterized by having a thickness of 80-90 m. The lower part is made of limestone (Abed, 2000) .Well applied, a

soft limestone facet (mikrit) that does not contain fossils predominates in this part, it is topped with a layer of peloidal grain stone, then there are a few meters of thin-layered limestone in which the miliolid limestone predominates (Abed, 2000).

2.5.5. Al_hisa Phosphorite/Amman Silicifed

The content of the Amman Formation changes horizontally from northern to southern Jordan. However, these changes are minimal when measured by changes in the composition of ALghudran (below) and by the changes in the composition of phosphates (above). The flint is the main rock in this formation, so if the Oman Formation was mentioned, the flint would come to mind. Flint is found in the formation of Oman and everywhere in it, alternating with limestone rocks that may be cocaine, chalk and dolomite. Flint is usually brown and may be black or white. It is present in layers of different thicknesses between the thickness which may be more than a meter and between the laminates. Even some of the thicker flint can be laminated or cross-laminated. Some types of bulk flint do not show internal sedimentary structures. Others are bedded brecciated chert (Abed, 2000).

2.5.6. Wadi Umm Ghudran

Oil shale is the main component of this formation and is characterized by its proximity to the surface of the earth and spread in the central and northwestern regions of Jordan, and it is what the Jordanian people rely on in order to improve their economic affairs, and it is expected that it will be used in order to bridge Jordan's energy shortage at the long term (Abed, 2000).

2.5.7. Numayri Dolomite

Dolomite is known as sedimentary rocks that precipitate like limestone, dolomite usually consists of 50% of calcite and dolomite, while pure dolomite consists of 30% of CaO,

47% of CO2 and 21% of MgO and is widely distributed in Karak and Ma'an. It can be observed in the rest of Jordan over a few areas (Abed, 2000).

2.5.8. Calcite

Calcrete spreads in Jordan in many areas clearly, which are the Rumman, Marsa, and Wasfi al-Tal forest, and its thickness ranges from 3-10 meters. Texture and around the granules there is a coagulated nodular tissue (Abed, 2000).

2.5.9. Sand

Jordan is an extension of the Hawran plains to the north and the Arabian Desert in the south, and because of the diversity of the regions surrounding Jordan, we see the overlap of types of rocks in several areas, where sand is found in southern Jordan and extends downward to the north, and the source of sand is the Paleozoic era rocks east of Wadi Araba, and red sand is found in the Al-Quwirah region (Abed, 2000).

2.6. UNDERGROUND WATER

Underground water is defined as the water that moves from the surface of the earth to the ground through the pores on the surface of the earth, and collects in the datum, and this water comes out to the surface of the earth either on its own as in springs, valleys, and rivers, or comes out by human action by drilling wells and extraction using pumps from the ground to the surface of the ground (Shawabkeh, 1998).

In the area of our study, the underground water is divided into two parts: the unconfined upper aquifer, and the lower confined aquifer.

2.6.1. The Upper Aquifer

The upper aquifer constitutes 45% of the total groundwater in the study area, and is characterized by the thickness of the aquifer in it ranging from 170 meters to 327 meters.

2.6.2. The Lower Aquifer

It constitutes 25% of the groundwater. It is distinguished by the fact that the thickness of the groundwater in it reaches 600 meters in a certain Zarqa Valley. (Akkawi & Hadadin, 2009) It is also distinguished by the fact that the water comes out to the surface of the earth in the form of thermal springs. (Shawabkeh, 1998)

2.6.3. Aquitards

The aquitards are distinguished in the study area that it divides the aquifer into two parts and consists of limestone and marl from the Cretaceous period.

2.6.4. Springs

Because of the high temperature that characterizes Jordan, and the high flow rates, thermal springs were formed, which provide Jordan with a source of thermal energy, and contain a number of springs of up to 60 thermal springs, and these springs reach a water temperature of approximately 63 degrees Celsius (Abed, 2000).

In Figure 2.7, we can see the springs that participate in the flood waters when heavy rainfall occurs, and these springs, as we can see, are located on the underground flow lines in the study area, in order to know the amount of water flowing from these springs, we note in Table 2.1 , which gives us the flow value for each of the springs shown in Figure 2.7, and we took this table as a hand file from Jordanian MWI.

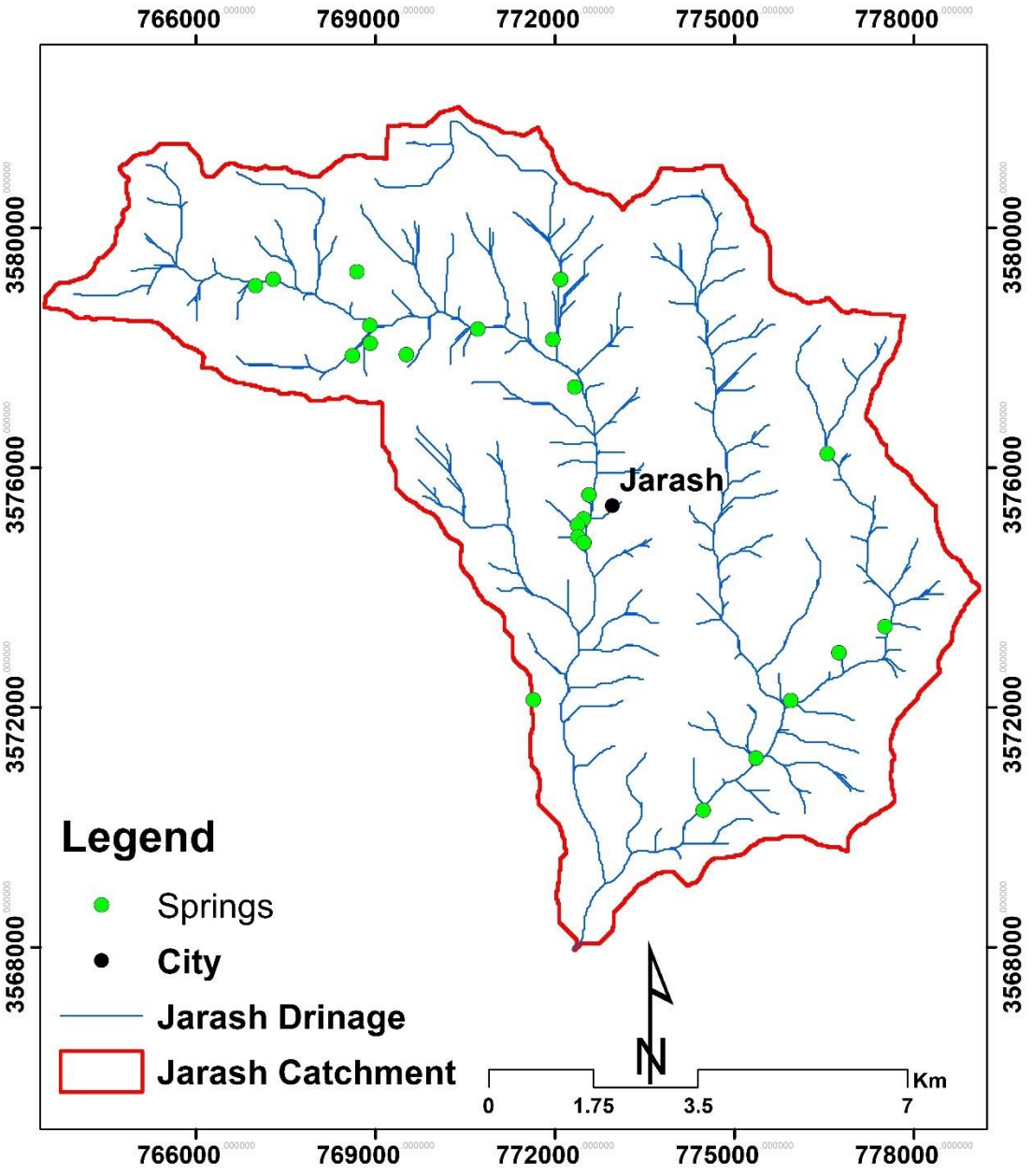

Figure 2.7. Springs of the study area.

Table 2.1. Spring discharge.

Discharge (m^3/h)	
10.50	
20.5	
20	
1	
1.5	
30	
21	
6	
2.6	
3	
15	
38	
4	
22	
37	
12	
6	
10	
10	
6.5	
6.65	
20	
7	
310.2	Total Discharge / Hour
2.72 MCM	Total Discharge / year

PART 3

METHODOLOGY AND DESCRIPTION OF THE STUDY AREA

3.1. DATA COLLECTION

This study included an examination of the Jerash Basin by using natural data such as soil type, terrain, elevations, land use, vegetation cover, runoff, rain and data issued by the Meteorological Authority.

3.1.1. Hydrological Data

To study the process of rainfall-runoff relationship hydrological data were collected that included the annual precipitation rate, surface water runoff data, data related to temperature, and we obtained these data from the Ministry of Water and Irrigation (MWI) and Jordan Meteorological Department (JMD). As for precipitation rates, we took measurements of rainfall stations (Ajloun, Jerash, Kittah, Midwar, Prince Feisal Nursery, and Qafqafa), the data were inspected and analyzed, and the smallest parts of the Pivot Table data were focused on in order to obtain accurate results, and (17-31) years were used from daily, monthly, and annual rainfall data records according to its establishment, these climatic data informed us by calculating the averages, maximum, and minimum precipitation. We will calculate each of the Curve number (Rainfall-Runoff model approach), Time of Concentration, and Unit hydrograph method by using the data we obtained from (JMD), and it will be clear in the next paragraphs.

3.1.2. Geological Data

We took geological maps that include the northern region of Jerash Governorate, with an area of 101.66 square kilometers for the study area, and the maps were obtained them from the Department of Geography and Geology of the University of Jordan in Amman.

3.1.3. Soil Map

This type of map is available at the Jordanian Ministry of Agriculture, where it is easily provided in order to develop studies that contribute to increasing the amount of information that allows Jordan to try to avoid disasters such as soil erosion and try to prevent the risks of flash floods through a project that named: National Soil Map and the Land Use Project, this is what helped us to achieve the success of the study by knowing the composition of representative samples.

We see the explanation of the soil map in Figure 3.1 and soil characteristics in Table 3.1.

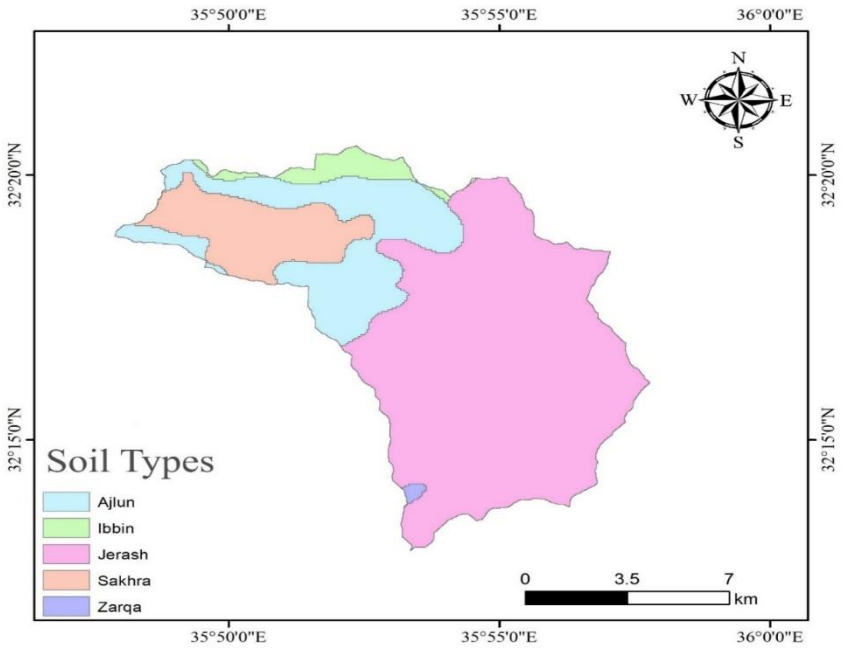

Figure 3.1. Soil map of study area (Abed, 2000).

Table 3.1 Soil characteristic of the study area.

Name	Soil Texture	Hydrological Soil Group (HSG)
Ajloun	Clay Loam and Clay	D
Ibbin	Silty Clay Loam	C
Jerash	Silty Clay and Clay	C
Sakhra	Silty Clay and Clay	C
Zarqa	Silty Clay and Clay	C

3.1.4. Landuse Map

We created a landuse map in the northern Jerash basin area, after we verified the existence of a land cover and obtained many pictures that will help in understanding landuse in Jerash, we will see in detail in the next paragraphs because understanding the landuse map helps greatly and is considered one of the most important factors affecting flash floods. Figure 3.2 shows the landuse in the study area, and we can see that the tree crops form the largest portion of landuse map.

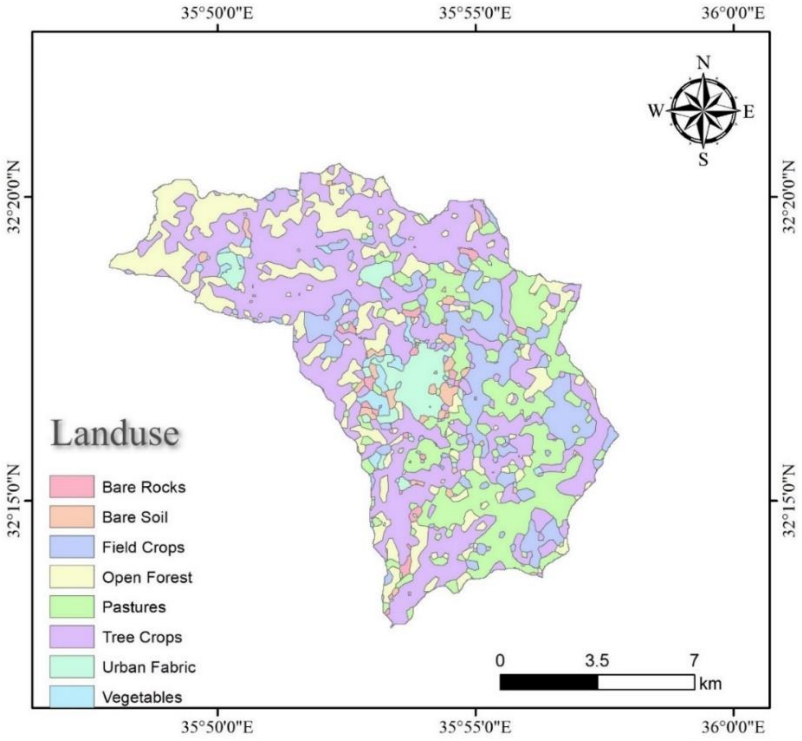

Figure 3.2. Landuse map for study area (Zregat, 2014).

3.1.5. Digital Elevation Model (DEM)

The Vertex website of NASA allowed us to obtain the DEM that we want with a resolution of 12.5m x 12.5m by using the search engine ALOS PASLAR, which had a great role in the success of the study completion by using it. In Figure 3.3 we can see the Dem map for the study area which is taken from ArcGIS, and we can see that the elevation in the study area ranges between 261 m and 1268 m.

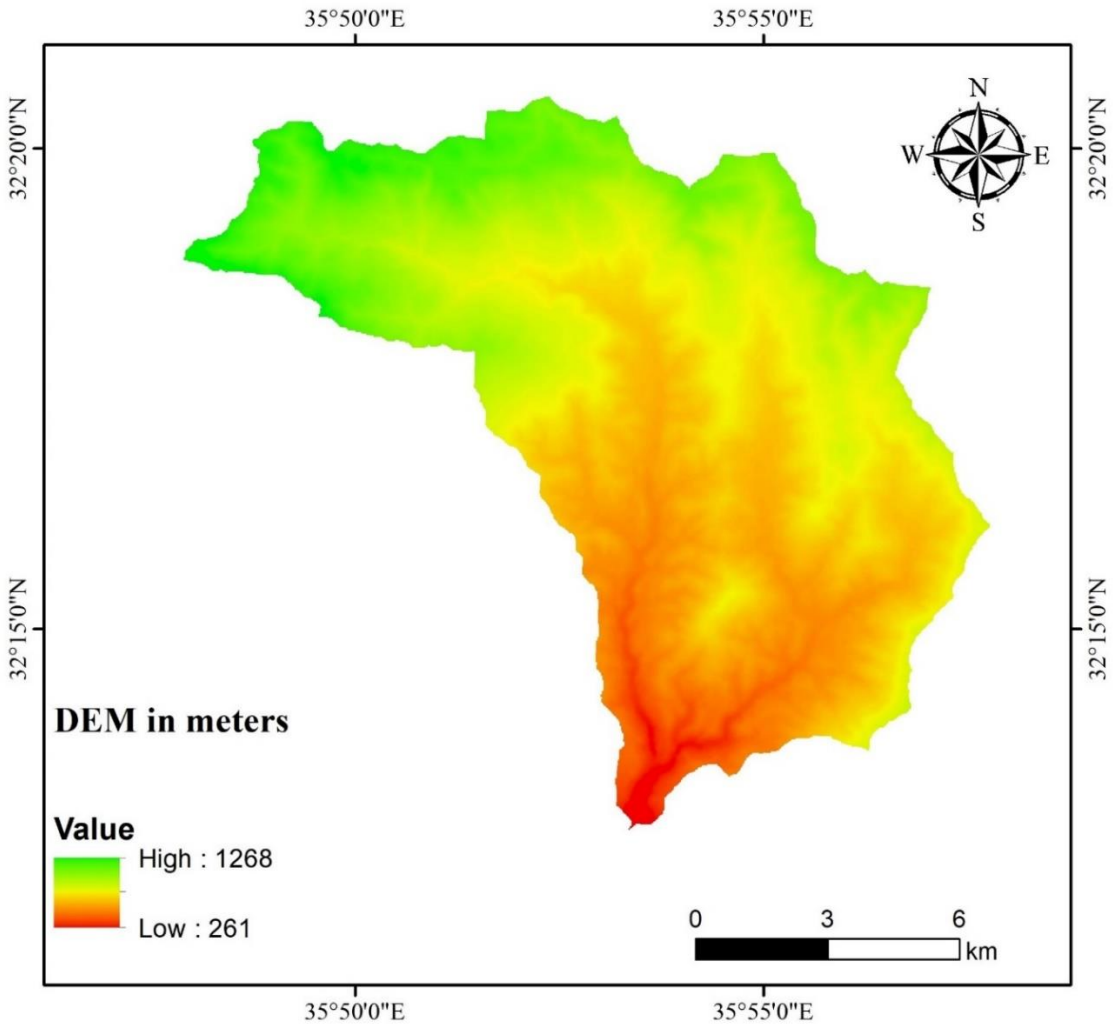

Figure 3.3. Digital Elevation Model (DEM) of study area (Earth data, n.d.).

3.1.6. Data Analysis and Interpretation

Below we will see a diagram of a hydrological model, where both Watershed Modelling System (WMS) and ArcGIS programs were worked on, depending on the DEM that was taken from the Vertex website.

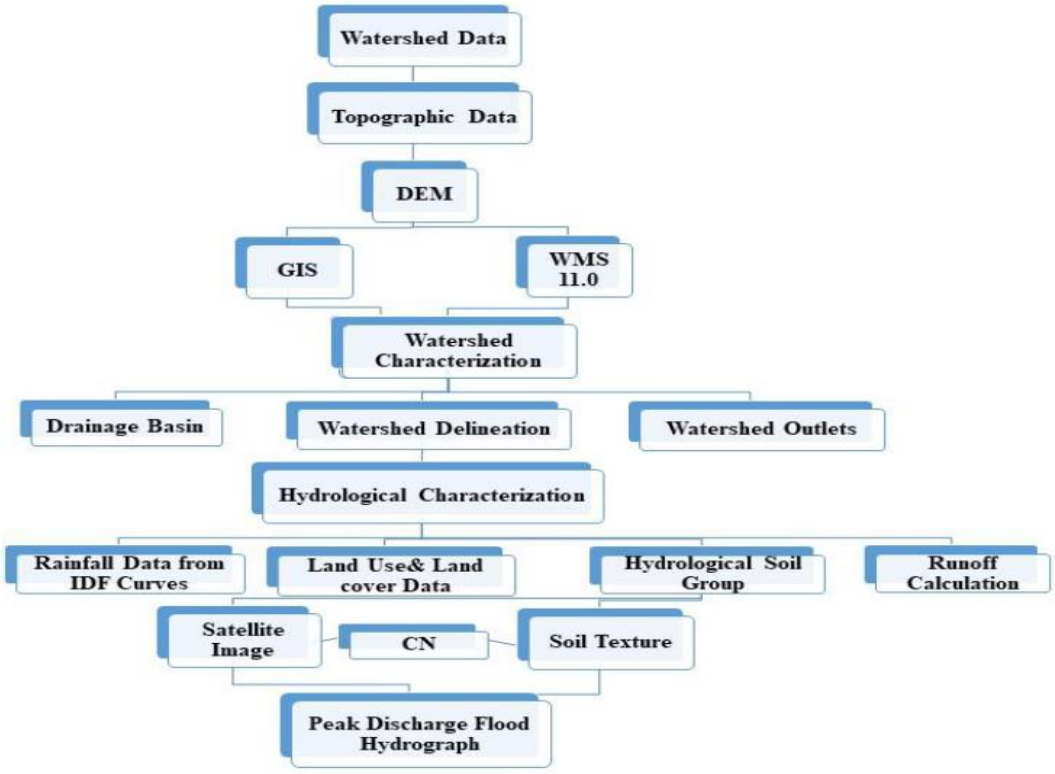

Figure 3.4. Methodology of study.

3.1.6.1. Arcgis

Basis of Hydrological Studies as they called it, we used GIS for mapping, that gave us an interpretation of the data and it was visible. That is informed us about how the land use changed in the study area, and helped us by showing the locations of the rain stations. (ESRI, n.d.).

3.1.6.2. (WMS)

WMS is the program of the water basin modeling system, as it provided us with an advanced graphical environment that helped us in the work of hydrological and hydraulic calculations, and it is characterized by providing a fast and easy process in building hydrological and hydraulic models, and mega projects have been applied to it, such as simulating the impact of a terrorist attack on water projects in America in 2002, and simulated flash floods in Iran on the Dez River in 2007. (Aswathy, Sajikumar, & Mehsa, 2016)

3.1.6.3. Hec Ras

This program is used to know the extent and length of the flood, as it provides cross-sections that extend along the reach, and it can present a cross-section that is used alongside the water surface during the direction of the floods during the return periods, and it shows the maximum features of the water surface for the periods of return that expected by the model.

PART 4

HYDROLOGY OF STUDY AREA

4.1. SUMMARY

During a variety of hydrological conditions, hydrological factors were audited and analyzed by presenting water balance models. Water balance is considered one of the decision-makers in countries' policies and can be considered the cornerstone of management and policy-making for managing water resources, providing pallets for water supply and wastewater management (Anderson et al., 2006). Hydrological studies depend mainly on climatic factors, these factors are used to evaluate the fundamentals of the water system's balance, in Figure 4.1 and 4.2 there are simple models about watershed formation processes and influencing factors on watershed, water equation can be summarized as:

$P = R + Ea + I$; P = precipitation (mm),
R = runoff (mm),
Ea = Evapotranspiration (mm),
I = infiltration (mm).

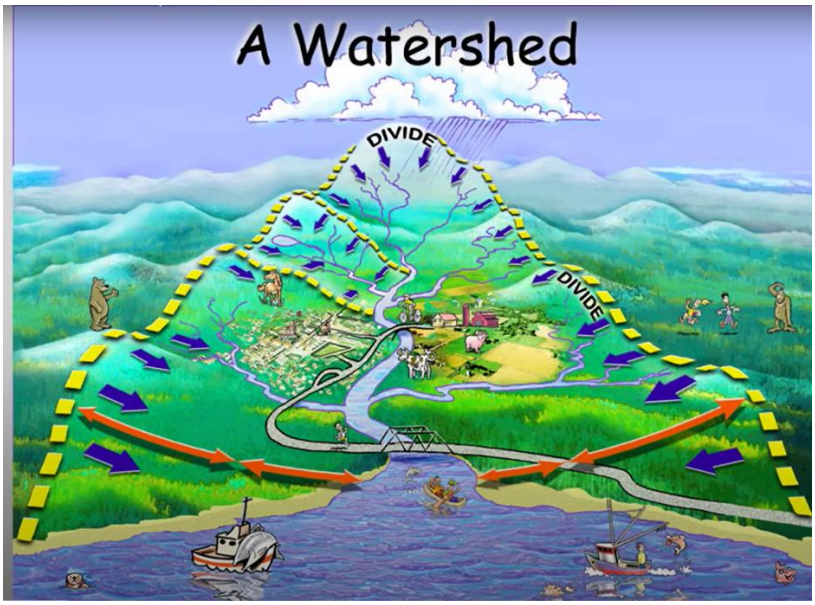

Figure 4.1. Watershed formation (Teach Engineering, n.d.).

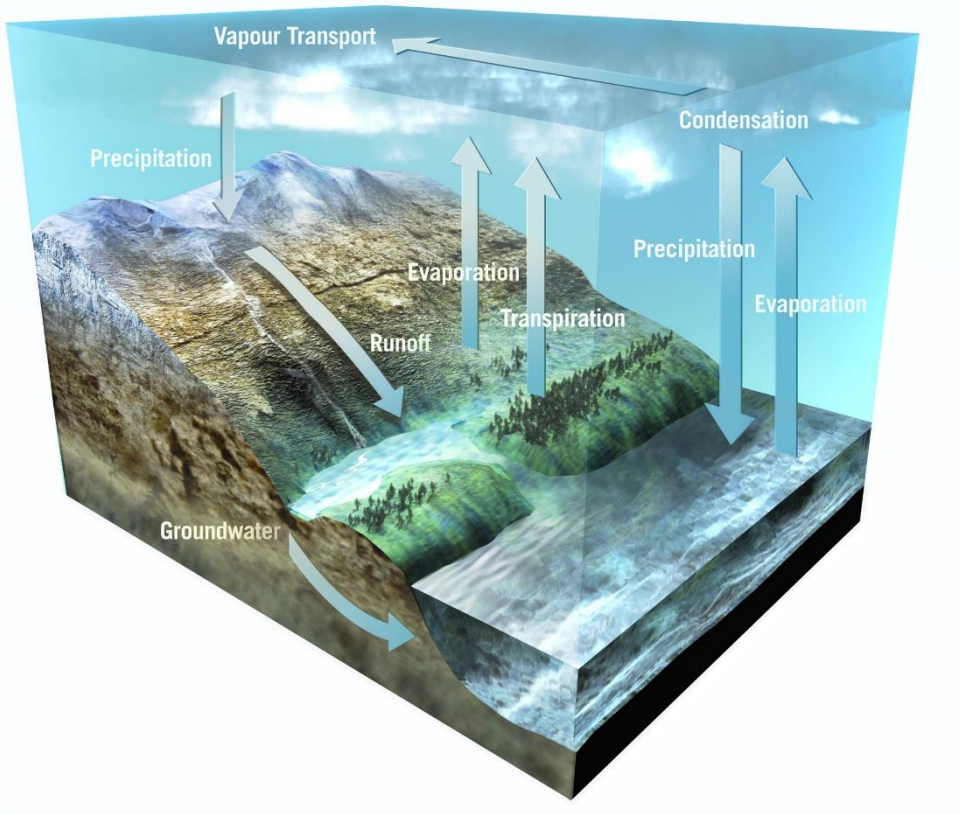

Figure 4.2. Watershed and Influencing factors (The European Space Agency, n.d.).

4.2. CLIMATE ANALYSIS

We obtained data that includes averages of (temperature, wind speed, evaporation rates and humidity) daily, monthly, and yearly from the Jordanian MWI, and the data was in MS Excel format. The data were obtained from the stations of (Ajloun, Jerash, Kittah, Midwar, Prince Feisal Nursery and Qafqafa) and were for the period (17 and 31 years according to their establishment date). We made a careful analysis by filtering the climate data and verifying its focus on the smallest parts of the pivotable. (IPCC, 2013)
Below we will see the drawings and calculations that we did according to the climate data

4.2.1. The Temperature

Jordan follows the Levant and is divided according to the temperature into two parts: a section belongs to the Mediterranean region and a section belongs to the desert region, where the northwestern region is characterized by a Mediterranean climate, while the rest of the country is dominated by the desert region, it is noticed in the northwestern region that whenever we head west towards the valley, the degree of the temperature rises because it is close to the Dead Sea, which is considered the lowest area on the earth's surface, and a large difference in temperature can be recorded between the highlands and the Ghor region, August is the hottest month in Jordan, where temperatures sometimes reach 40 degrees Celsius. In the study area, the average temperatures in the month of August reach approximately 33 degrees Celsius during the day and 18 degrees Celsius at night, while in winter the temperatures range between 10 degrees Celsius and can reach subzero degrees (and that is during snowstorms).

The following figures (4.3, 4, 5, 6, 7, 8, 9, 10, 11, 12, 13) show us the temperatures in Jerash. The figures show that in winter months the average temperature during the day is 11 c^{o} and at night (3-5 c^{o}), during the spring months the average temperature ranges from (13-25 c^{o}) during the day, and at night (5-15 c^{o}). And we focused on these months because these seasons are the rainiest seasons.

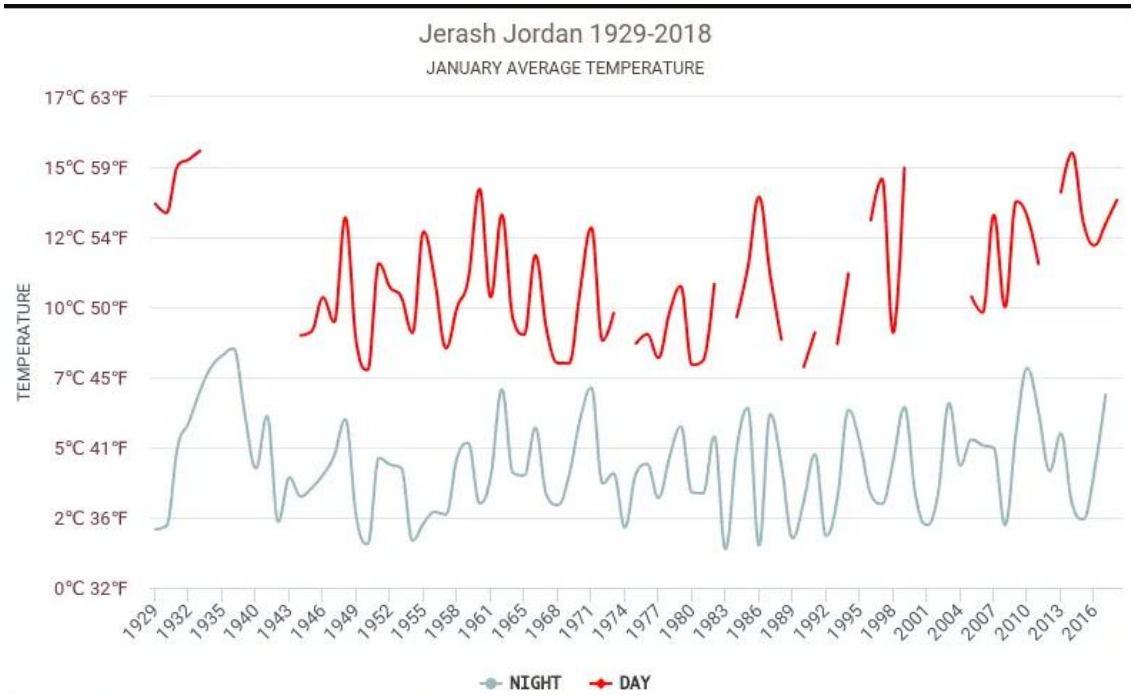

Figure 4.3. Temperature in Jerash in january (hikersbay, 2020).

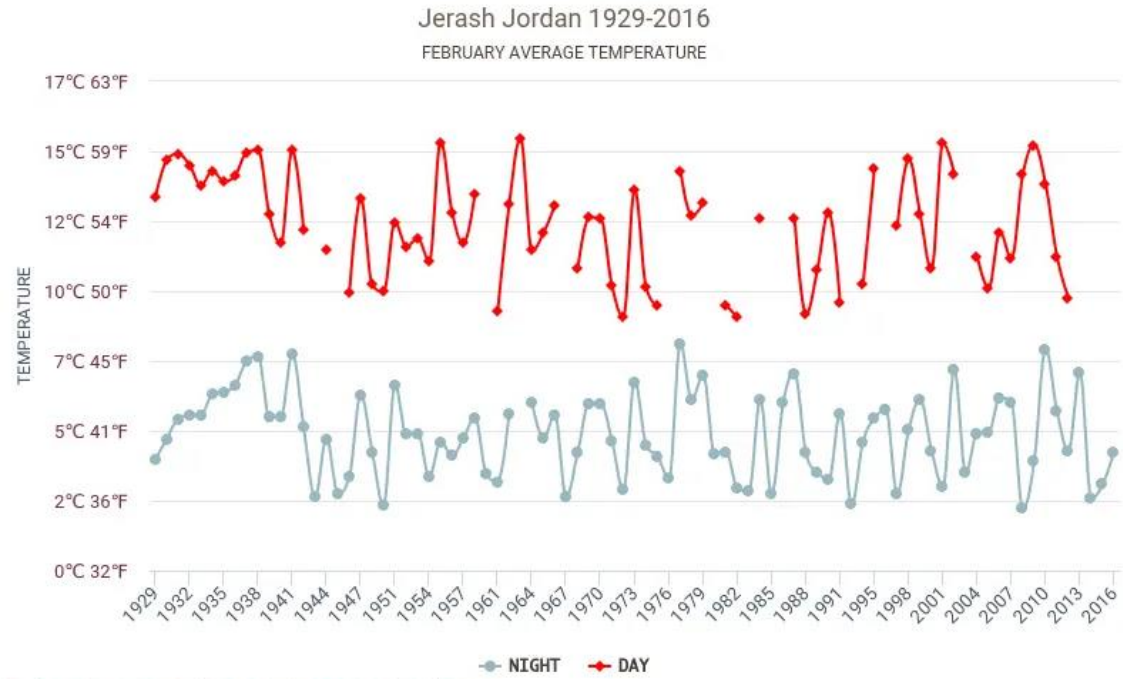

Figure 4.4. Temperature in Jerash in february (hikersbay, 2020).

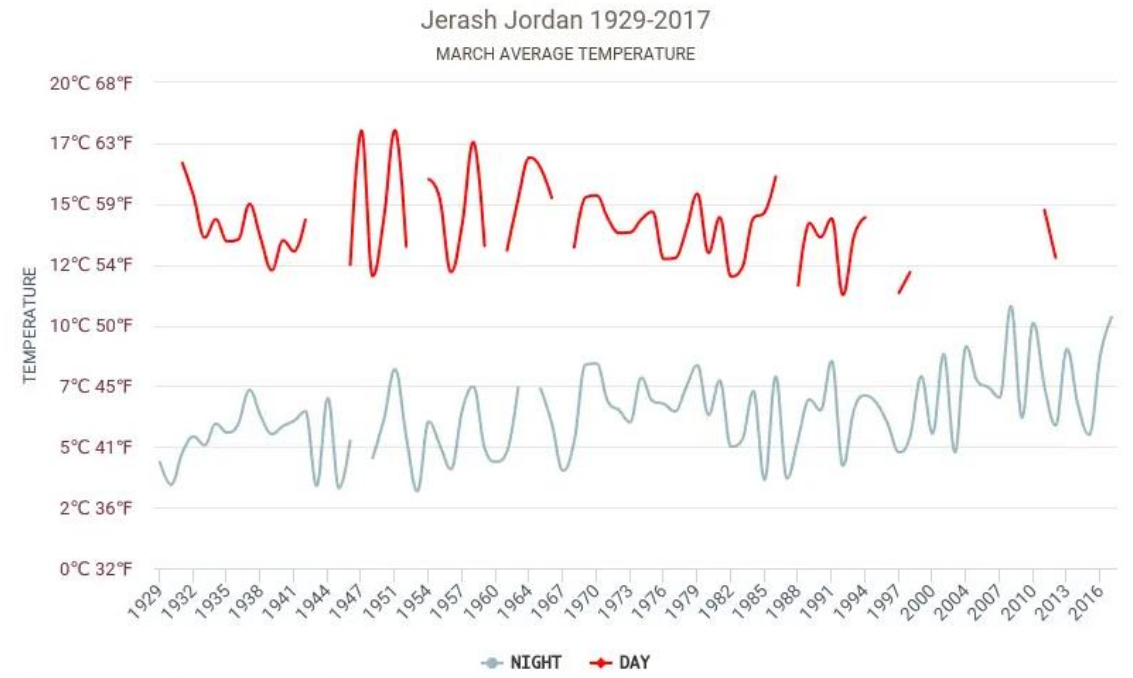

Figure 4.5. Temperature in Jerash in march (hikersbay, 2020).

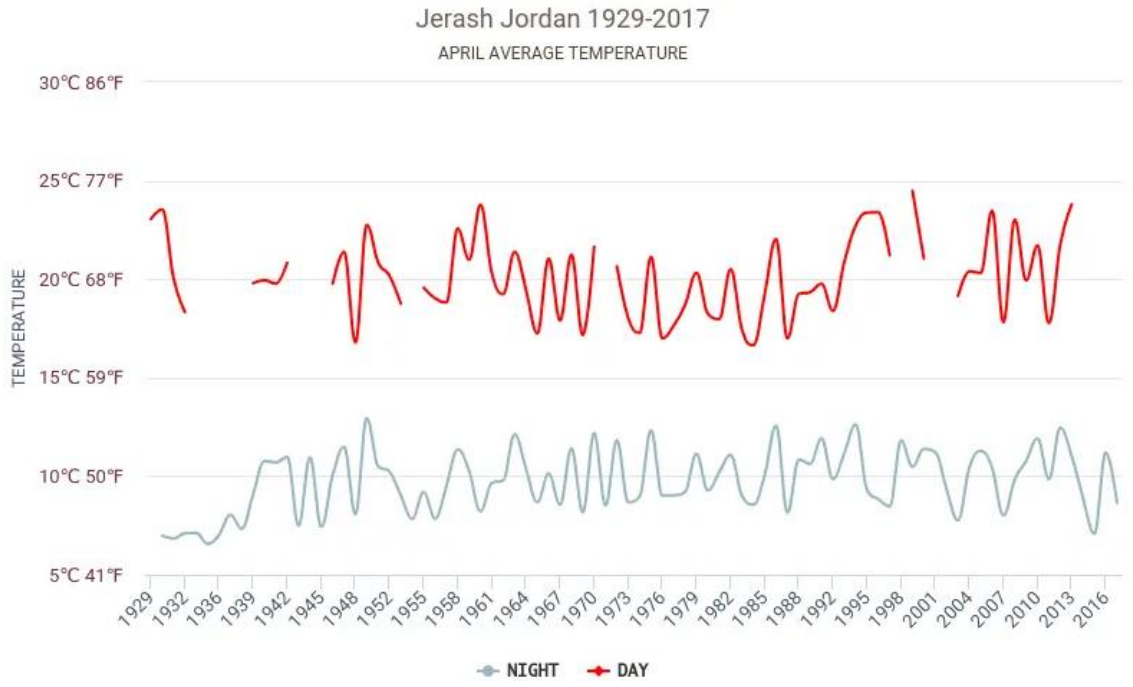

Figure 4.6. Temperature in Jerash in April (hikersbay, 2020).

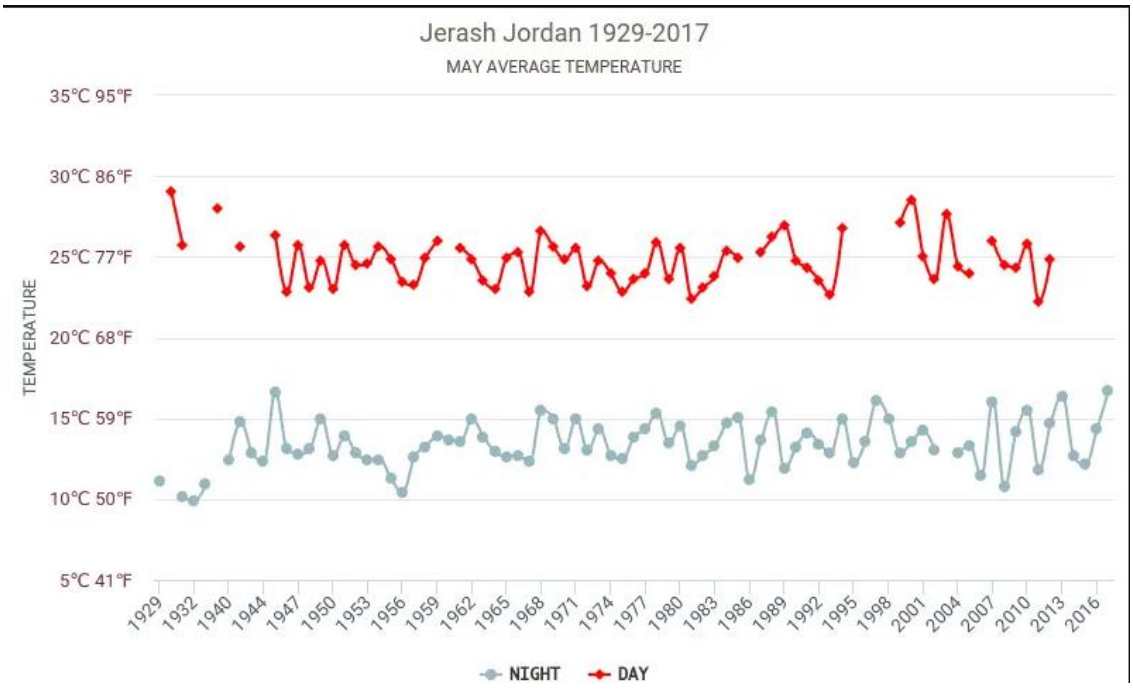

Figure 4.7. Temperature in Jerash in May (hikersbay, 2020).

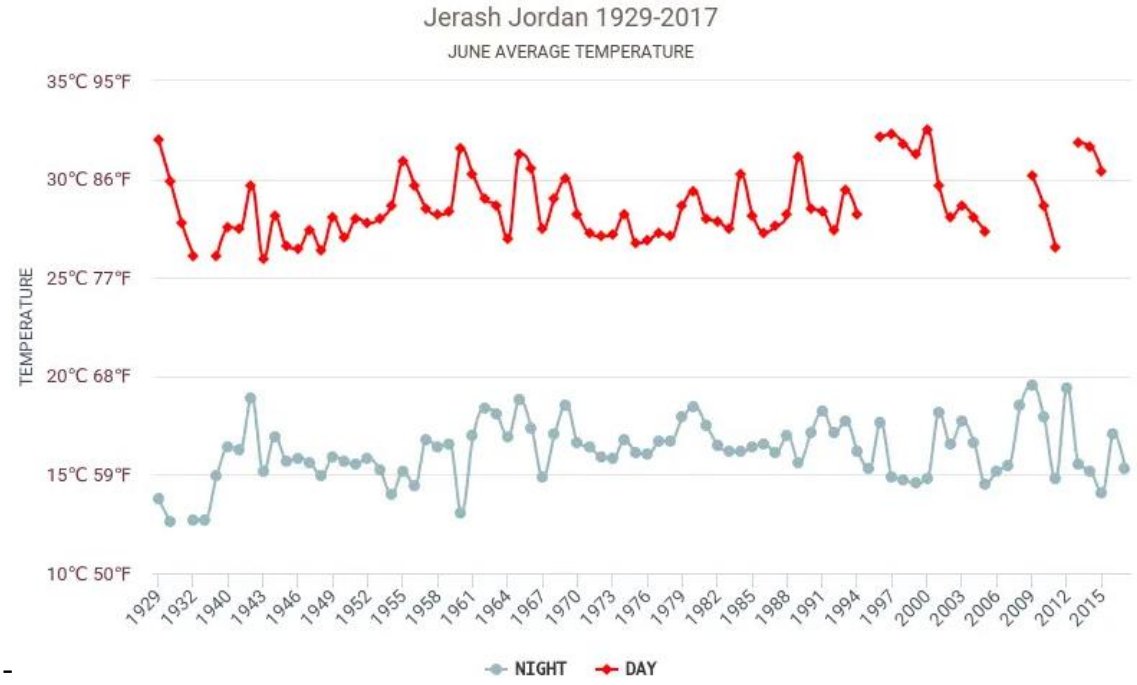

Figure 4.8. Temperature in Jerash in June (hikersbay, 2020).

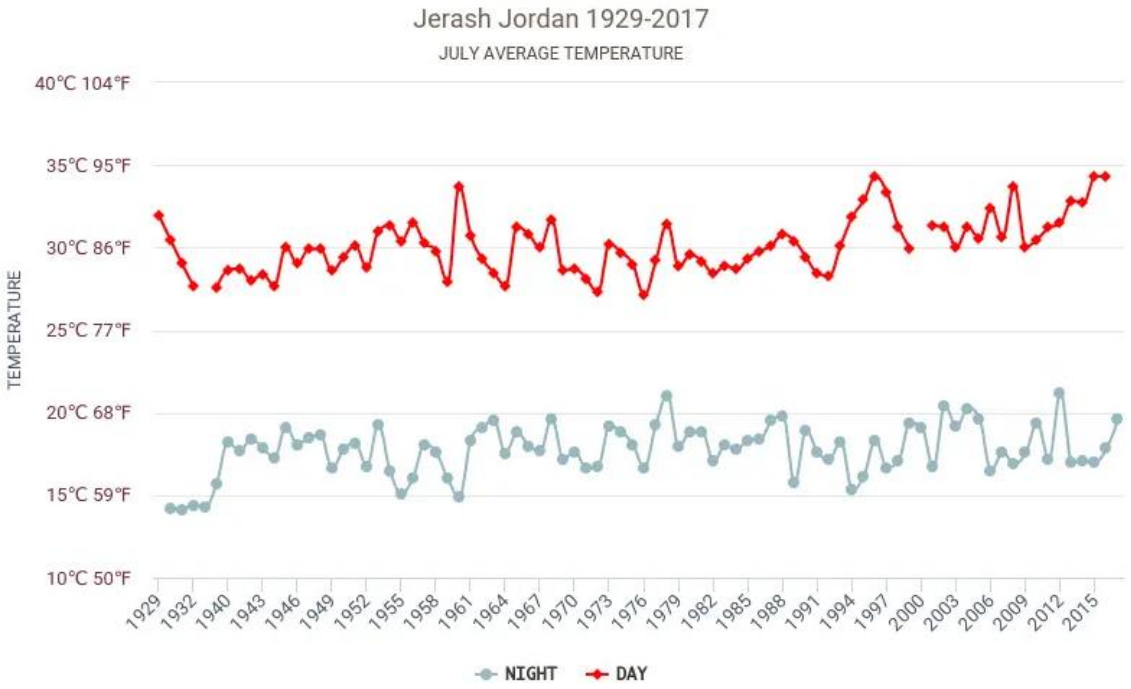

Figure 4.9. Temperature in Jerash in July (hikersbay, 2020).

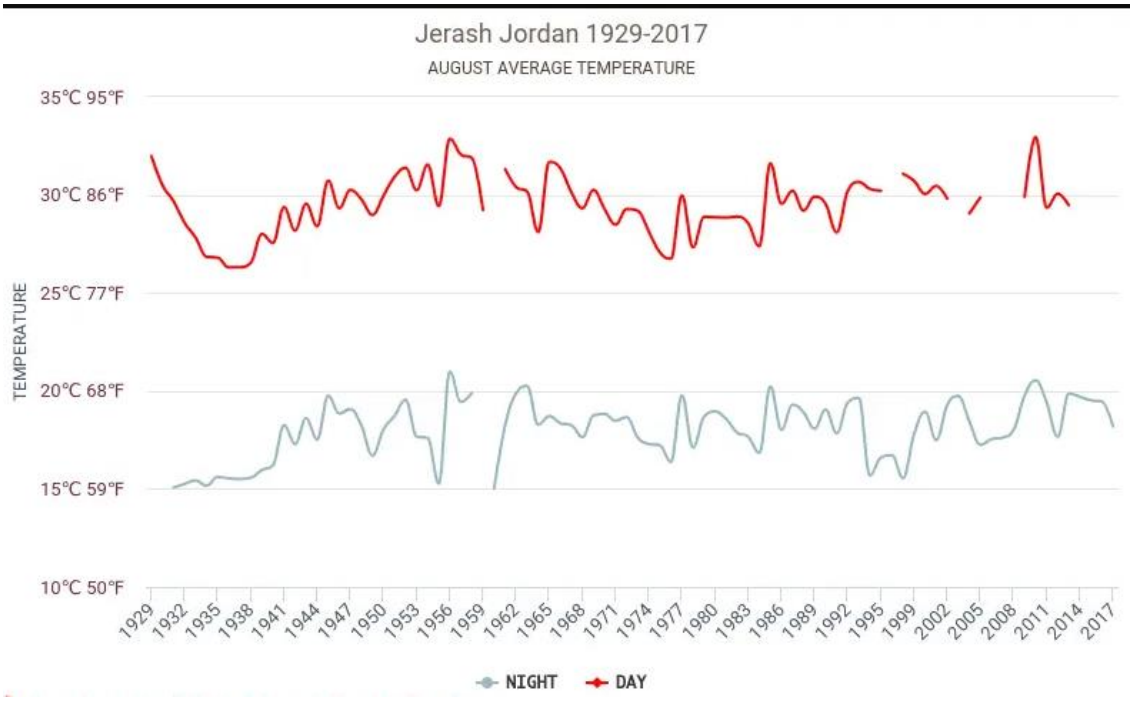

Figure 4.10. Temperature in Jerash in August (hikersbay, 2020).

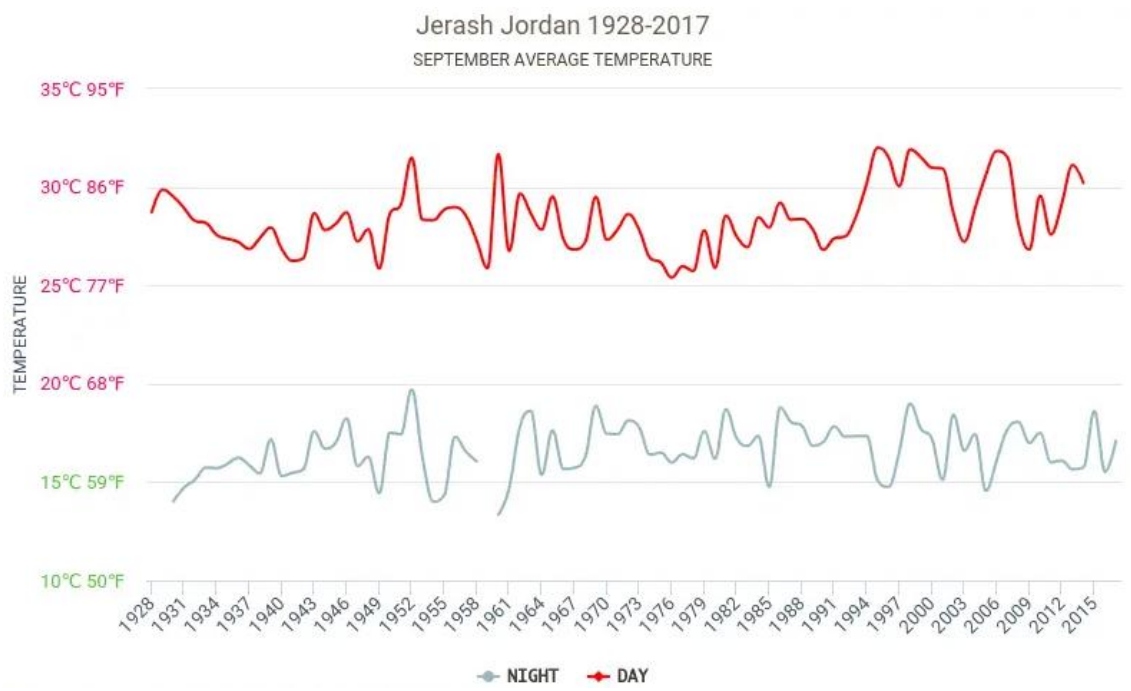

Figure 4.11. Temperature in Jerash in September (hikersbay, 2020).

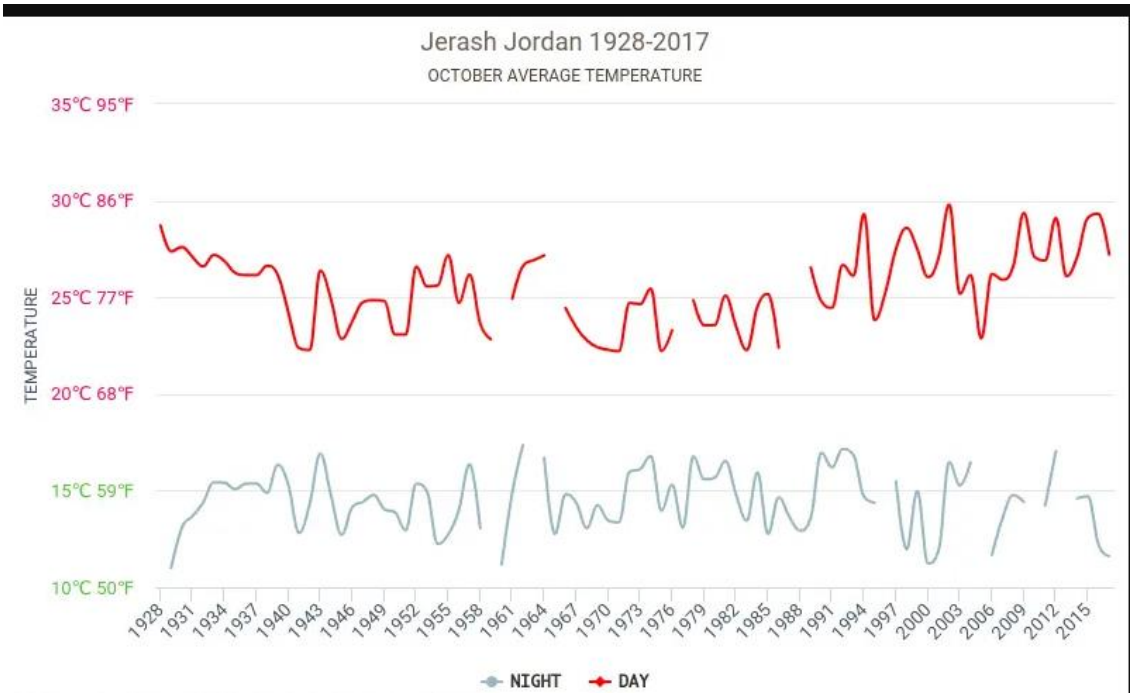

Figure 4.12. Temperature in Jerash in October (hikersbay, 2020).

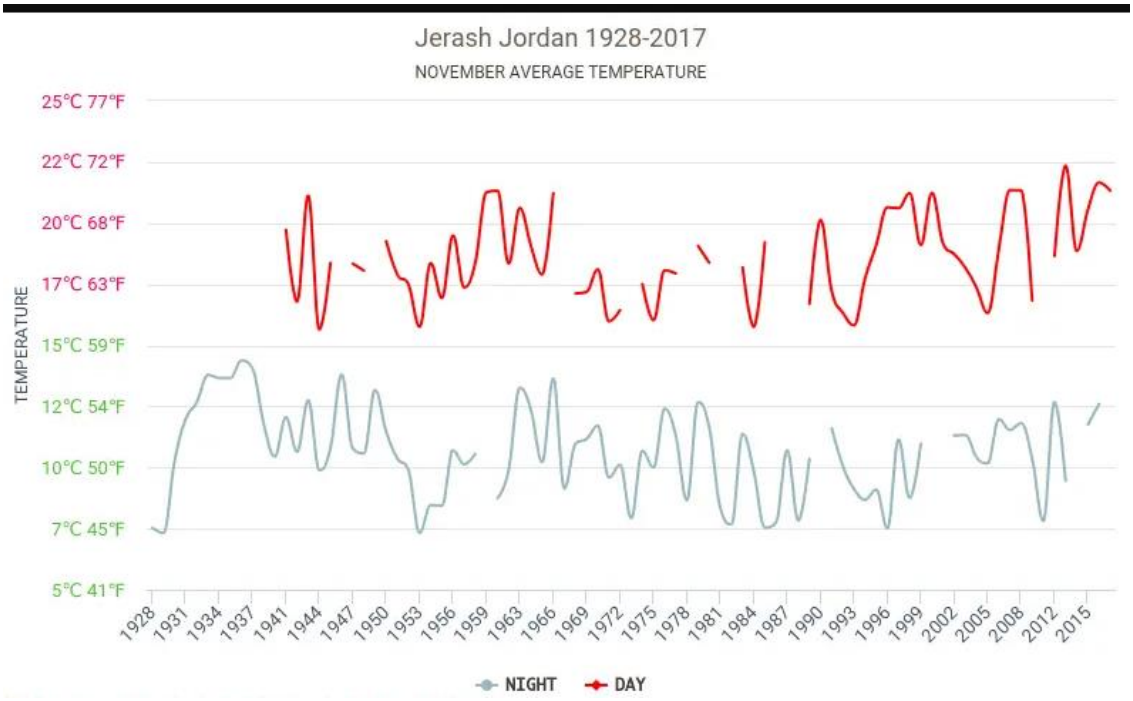

Figure 4.13. Temperature in Jerash in November (hikersbay, 2020).

4.2.2. Relative Humidity

The relative humidity is the percentage of water vapor in the air, and it is compared to the largest amount in which the air can be retained. The study area is located in the northwest of Jordan, it is considered relatively close to the Mediterranean Sea, which makes it slightly humid. The relative humidity in the study area ranges from 47% to 60% during the summer, while the relative humidity in the winter season, i.e., the months of December, January, and February, ranges from 69% to 81%. (Fardous, 2004).

4.2.3. Wind

In winter, Jordan is affected by the polar depressions and the Mediterranean lows, while summer is affected by high temperatures in both Iraq and the Arabian Gulf. This indicates that Jordan is affected by northerly and westerly winds in winter, and south and

eastern winds in summer. In the study area, the average wind speed is from October to May, respectively (6.74, 6.14, 5.7, 7.77, 7.12, 8.12, 8.46, 8.65 Km/hour)

4.2.4. Evaporation

What distinguishes the Mediterranean region is the distinct variation of the seasons, with moderate wet winters and hot dry summers. Since Jordan is close to the Arabian Gulf, it has 7 months of drought throughout the year, as rain decreases in these months and high temperature rates, and this means increased rates of evaporation in it, but in winter it decreases to its lowest levels due to low temperatures and precipitation.

According to a report issued by the Hashemite University in Jordan, the annual evaporation rate in the northwestern region reaches to very big number, which is a very large number compared to rainfall records, more than 65% of the amount of evaporation occurs between the months of May and October. The water flows in two ways, one of them heading to the desert areas located in the east of the Kingdom, and the other heading to the west to the Jordan Valley and eventually pouring into the Dead Sea. As for the water heading to the desert area, its way ends in barren lands, in addition to the large amount of evaporation, where the rate of evaporation in the eastern region reaches 4400 mm / the year (Fardous, 2004).

4.3. WATERSHED CHARACTERISTICS

The hydrological analysis is mainly based on identifying an area containing the catchment area that contributes to the runoff of the valleys. The main factor required to obtain accurate hydrolytic results and analyzes is the DEM. By using the DEM, we can obtain modeling purposes (terrain, elevations, slopes). We used a diameter of 12.5 m × 12.5 m, and we were able with WMS to obtain this image about the study area:

4.4. HYDROLOGICAL ANALYSIS

4.4.1. Rainfall Stations

Through the Jordanian MWI, we obtained the rainfall data for the required stations for the study area, which are in the table below, and these data were required an in-depth analysis to focus on the data after a process of filtering the hydrological data that we obtained. These data were daily, monthly, and yearly, and then we calculated the average precipitation for the study period. In Table 4.1 we can see the stations concerned with the study area, Table 4.2, we will see the years of the station's measurements (from the beginning to the end), in addition to the average annual rainfall, max. annual precipitation and min. annual precipitation, and Figure 4.14 shows the locations of rainfall stations.

Table 4.1. Rainfall stations for the study area.

Station Name	Station ID	Number of Years	Palestine North (m)	Palestine East (m)	Jordan North (m)	Jordan East (m)
Ajloun	AJ0001	17 years	1193500	221000	579043.438	382528.97
Jerash	AL0004	31 years	1187500	234500	572819.625	395926
Kittah	AL0005	31 years	1187000	229500	572403.063	390918.81
Midwar	AL0002	31 years	1188500	244000	573661	405440.16
P. N. F.	AL0036	31 years	1180500	234500	565821.313	395809.44
Qafqafa	AL0050	17 years	1195300	238800	580545.938	400355

Table 4.2. Station records of precipitation with average, maximum and minimum precipitation.

Station Name	Start	End	Number of Record Years	Yearly Average	Max. Year (mm)	Min. Year (mm)
Ajloun	2002	2018	17 years	598.18	823.1	326
Jerash	1987	2018	31 years	361.56	692	161.6
Kittah	1987	2018	31 years	498.93	862.5	194
Midwar	1987	2018	31 years	254.66	520.1	54.2
Prince Feisal Nursery	1987	2018	31 years	305.98	675.2	90.1
Qafqafa	2002	2018	17 years	336.16	487.7	120.7

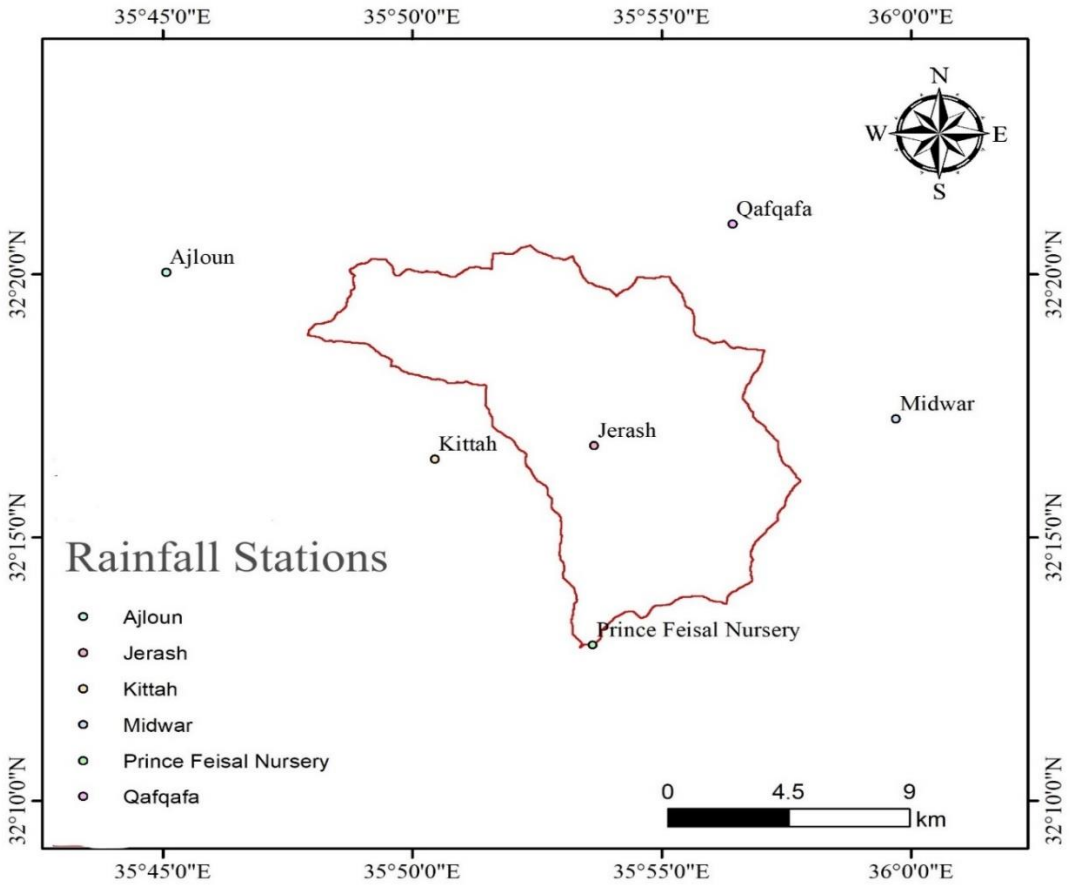

Figure 4.14. Locations of rainfall stations.

4.4.1.1. Daily Rainfall

As we have seen in Table 4.2 that we have six stations, 4 stations whose data were available for 31 years and two stations were for 17 years from the Jordanian MWI during the two periods (1987-2018) (2002-2018), we used this data in order to collect daily precipitation data for each month in order to produce the total monthly precipitation for each month of every year, then the monthly average precipitation for all years was calculated. It is evident that there has been an increasing trend of maximum daily rainfall over the study area during the last ten years that can be attached to climate change (Abdulla, 2020), In (Figure 4.15, 16, 17, 18, 19, 20) we can see the daily rainfall that registered from the stations, In Qafqafa and Ajloun stations we can see the reading for only 17 years from 2002 to 2018, and for other stations we can see that the records are for 31 years from 1987 to 2018. Figure (4.21, 22, 23, 24, 25, 26) Show the max. daily precipitation, and we can see that the max. precipitation of Ajloun Station was 2018, Jerash 1992, Kitta 1992, Midwar 2013, Prince Feisal Nursery 2003 and Qafqafa 2009

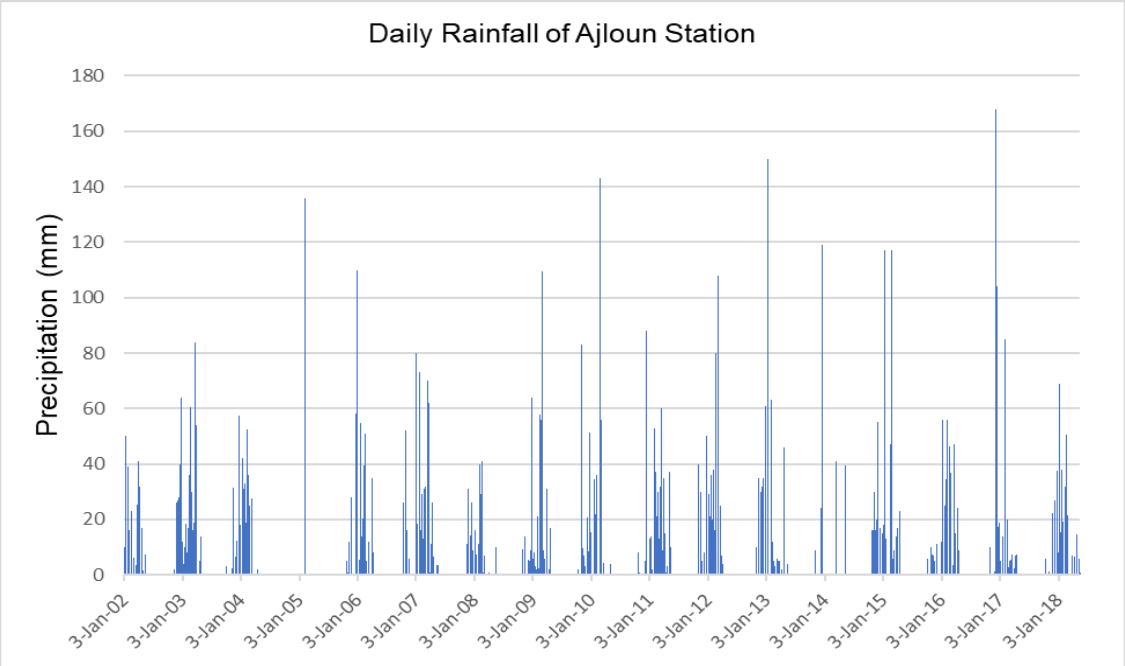

Figure 4.15. Daily rainfall of Ajloun station

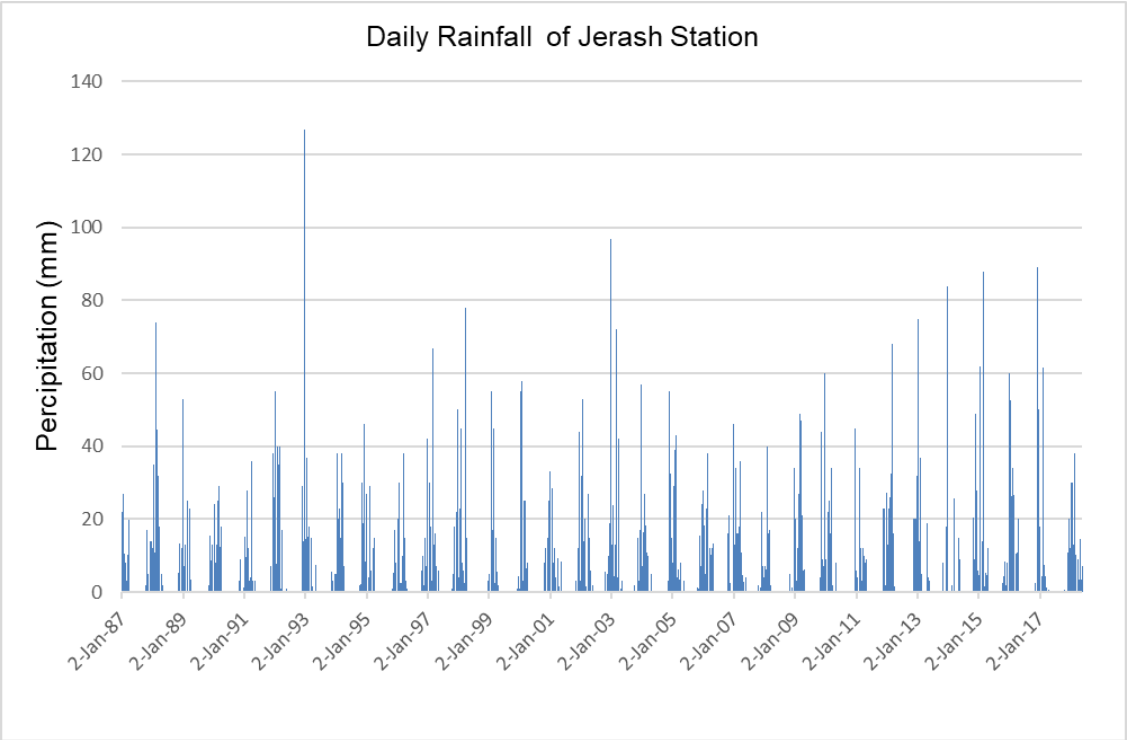

Figure 4.16. Daily Precipitation of Jerash station.

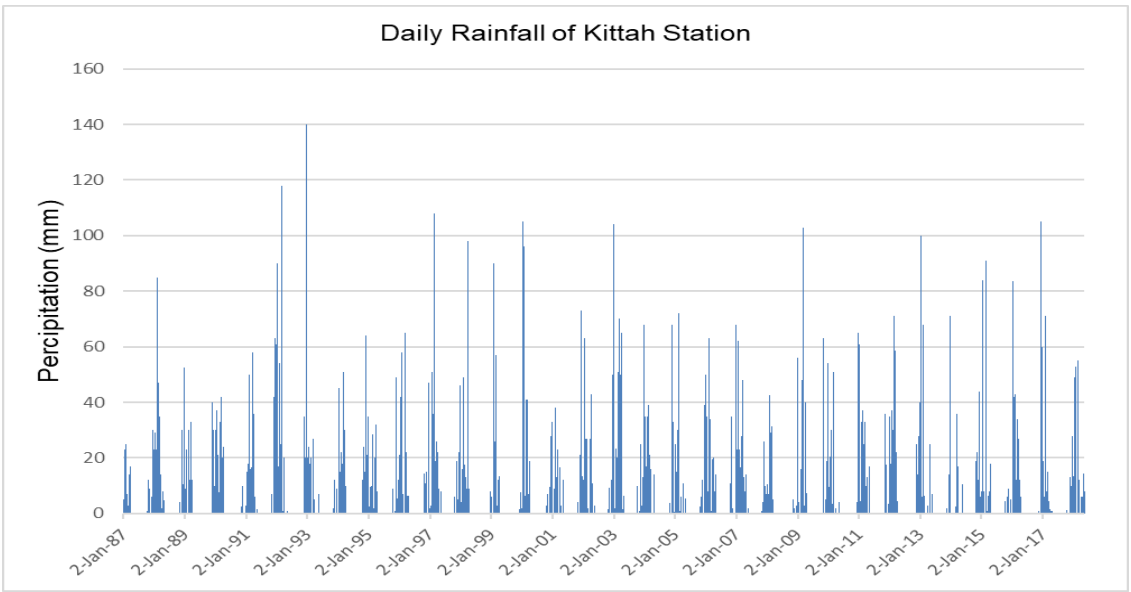

Figure 4.17. Daily Precipitation of Kittah Station

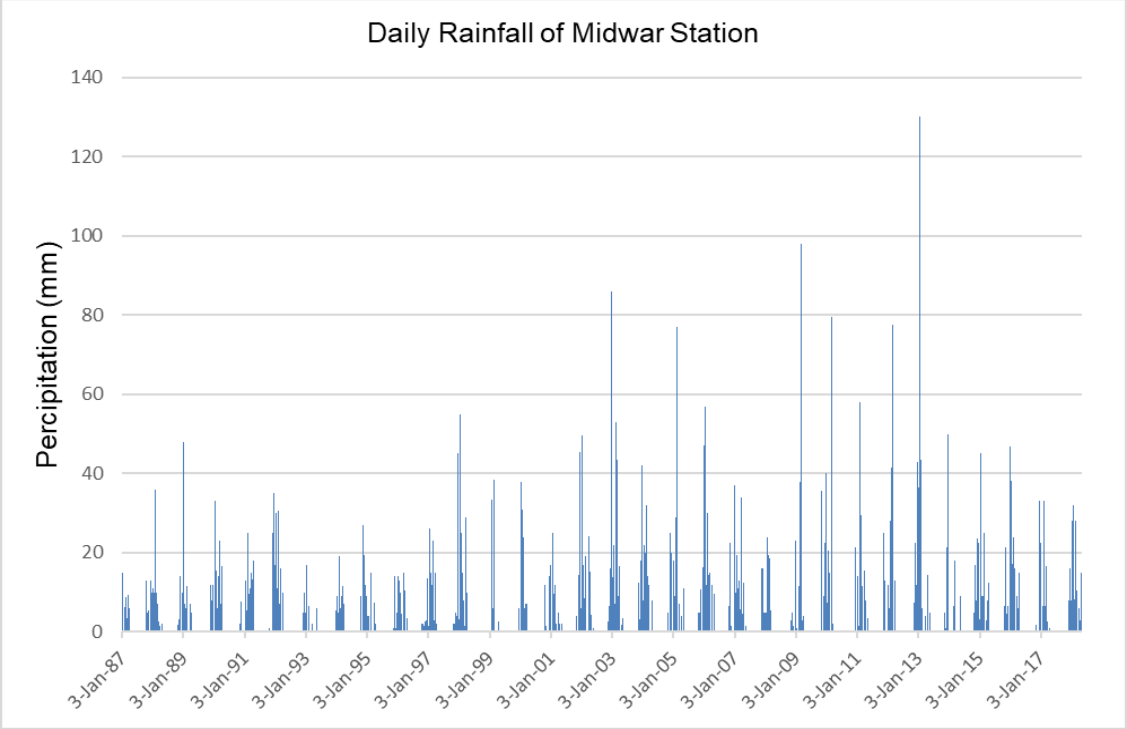

Figure 4.18. Daily Precipitation of Midwar station.

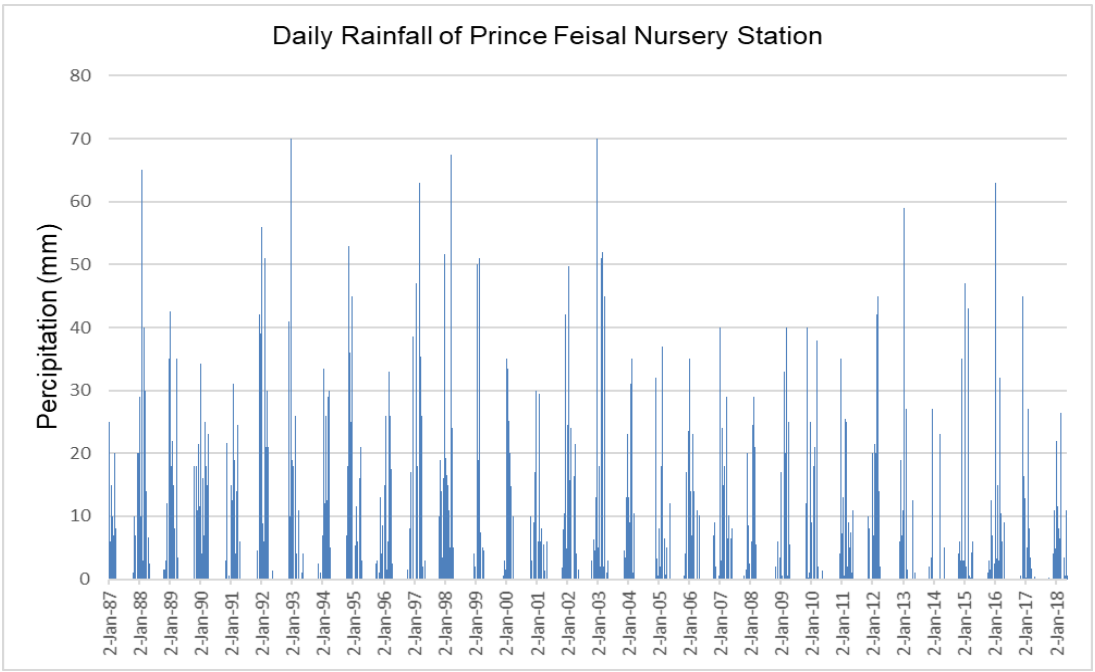

Figure 4.19. Daily Precipitation of Prince Feisal Nursery station.

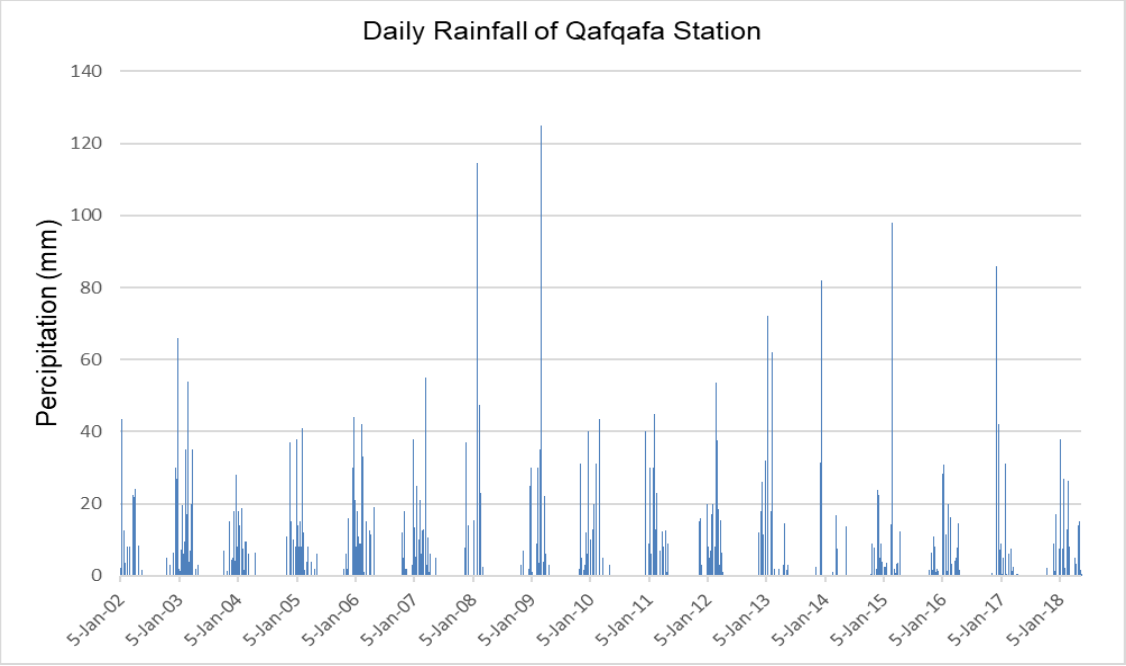

Figure 4.20. Daily Precipitation of Qafqafa station.

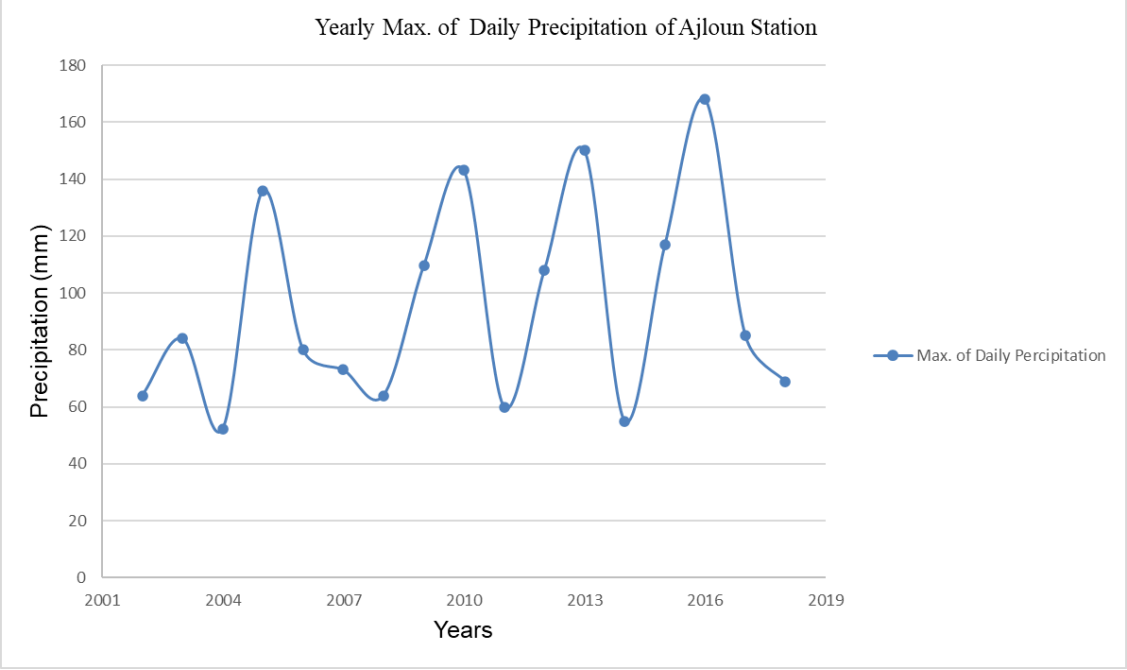

Figure 4.21. Yearly Max. of Daily Precipitation of Ajloun station.

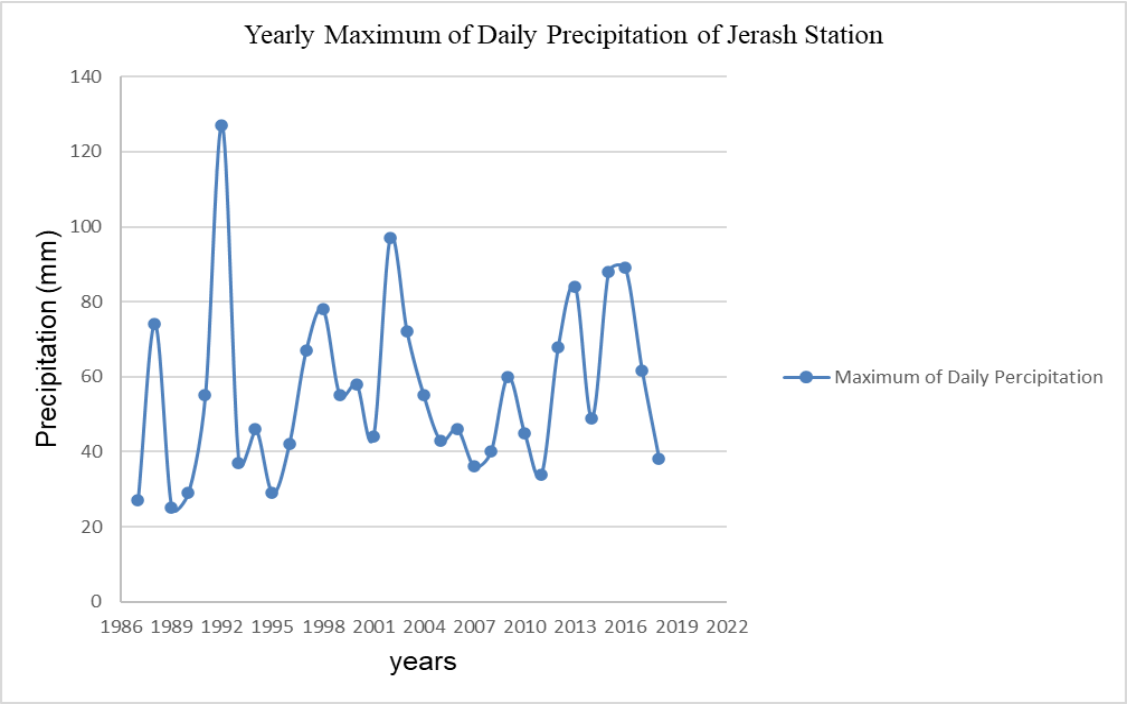

Figure 4.22. Yearly Maximum of Daily Precipitation of Jerash Station.

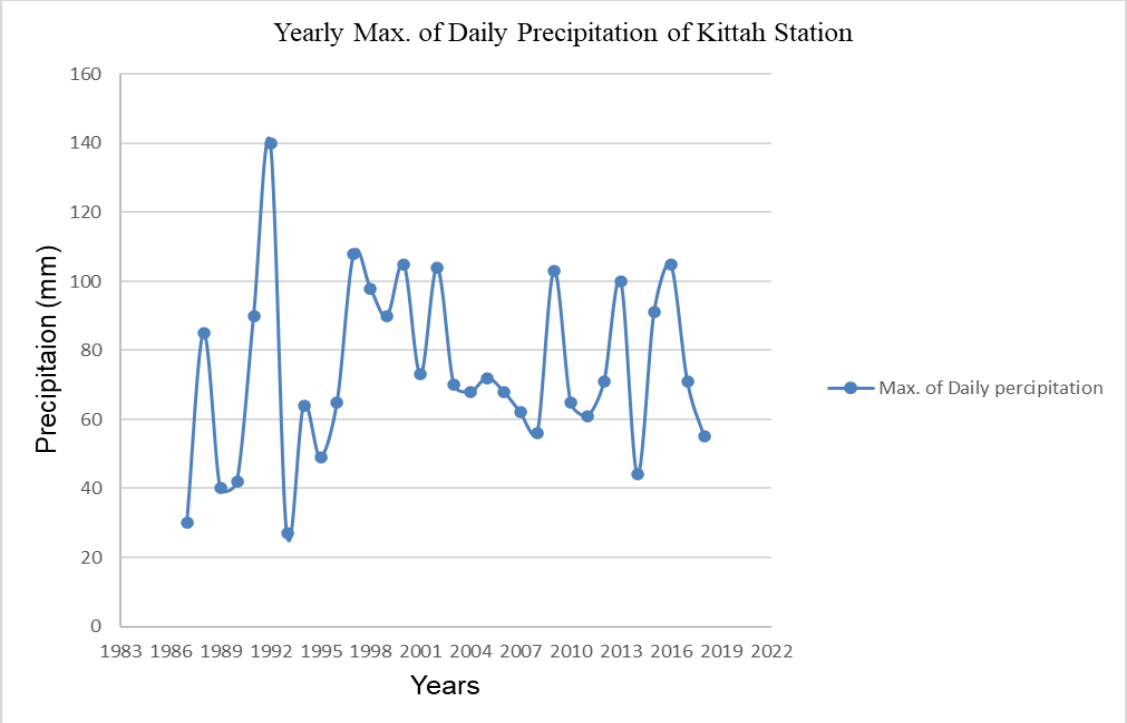

Figure 4.23. Yearly Maximum of Daily Precipitation of Kittah station.

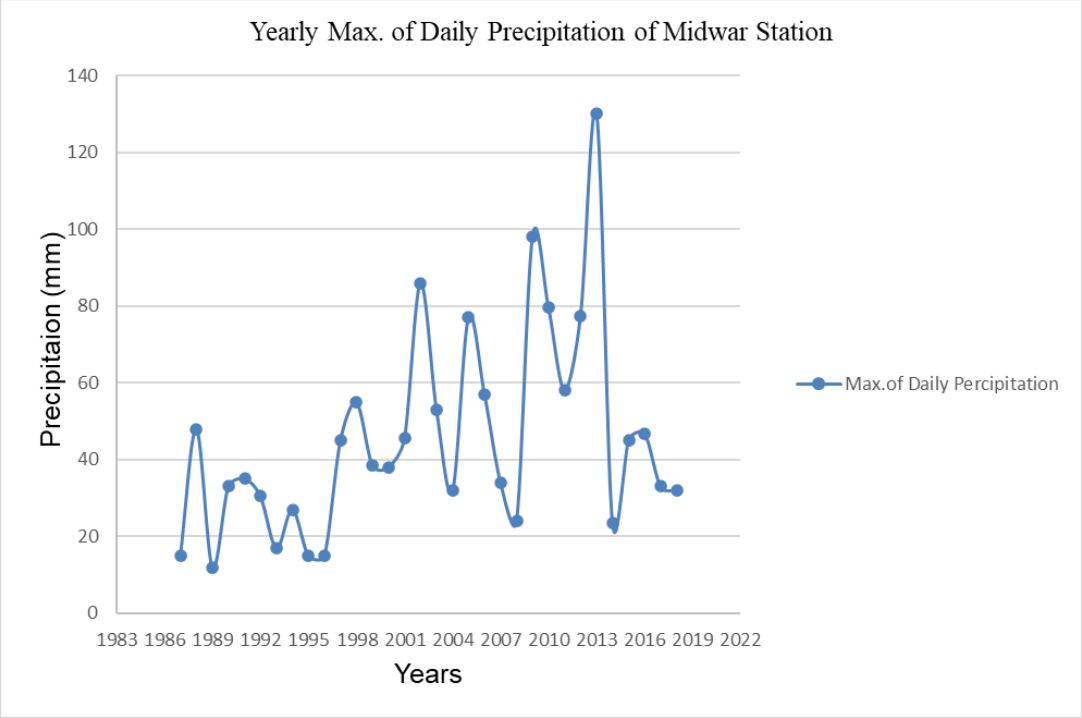

Figure 4.24. Yearly Maximum of Daily Precipitation of Midwar station.

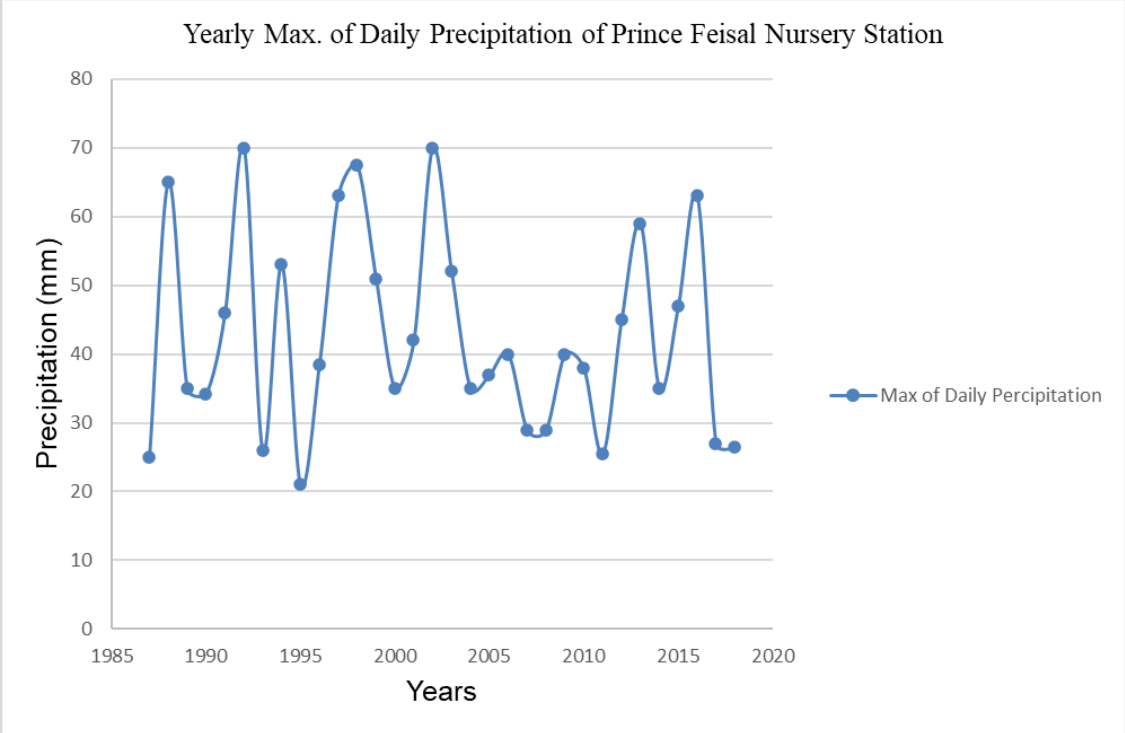

Figure 4.25. Yearly Maximum of Daily Precipitation of Prince Feisal Nursery station.

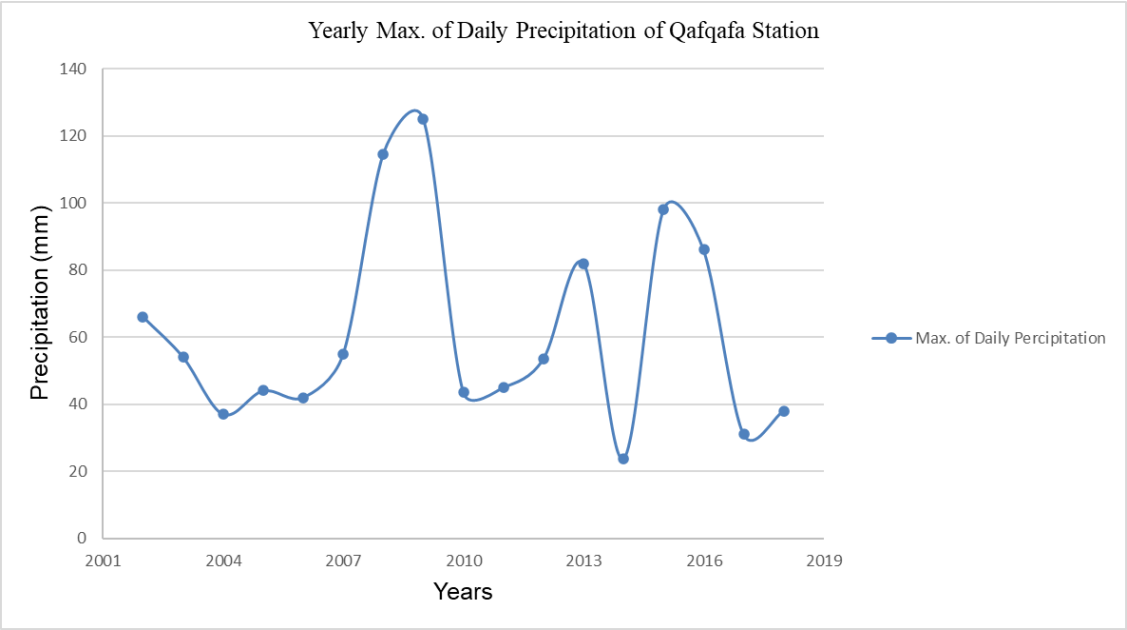

Figure 4.26. Yearly Maximum of Daily Precipitation of Qafqafa station.

4.4.1.2. Monthly Rainfall

Jordan rains in the winter and spring seasons, which explains the lack of records of rain stations in the months of June, July, August, and September. The amounts of rain are at their highest rates in the studied area in January, February, and December (Marques, 1997). In the dry months, rain is absent. This is due to climatic conditions in the watersheds. Figure 4.27 shows the monthly average rainfall, and we can see that January has the biggest amount of average precipitation, February is a rainy month, as it comes second after January. Figure (4.28, 29, 30, 31, 32, 33) show the monthly average rainfall for each station, and we can see those months (June, July, August, September) are not existing in the figures because in Jordan there is no reading for these months, because they are dry months.:

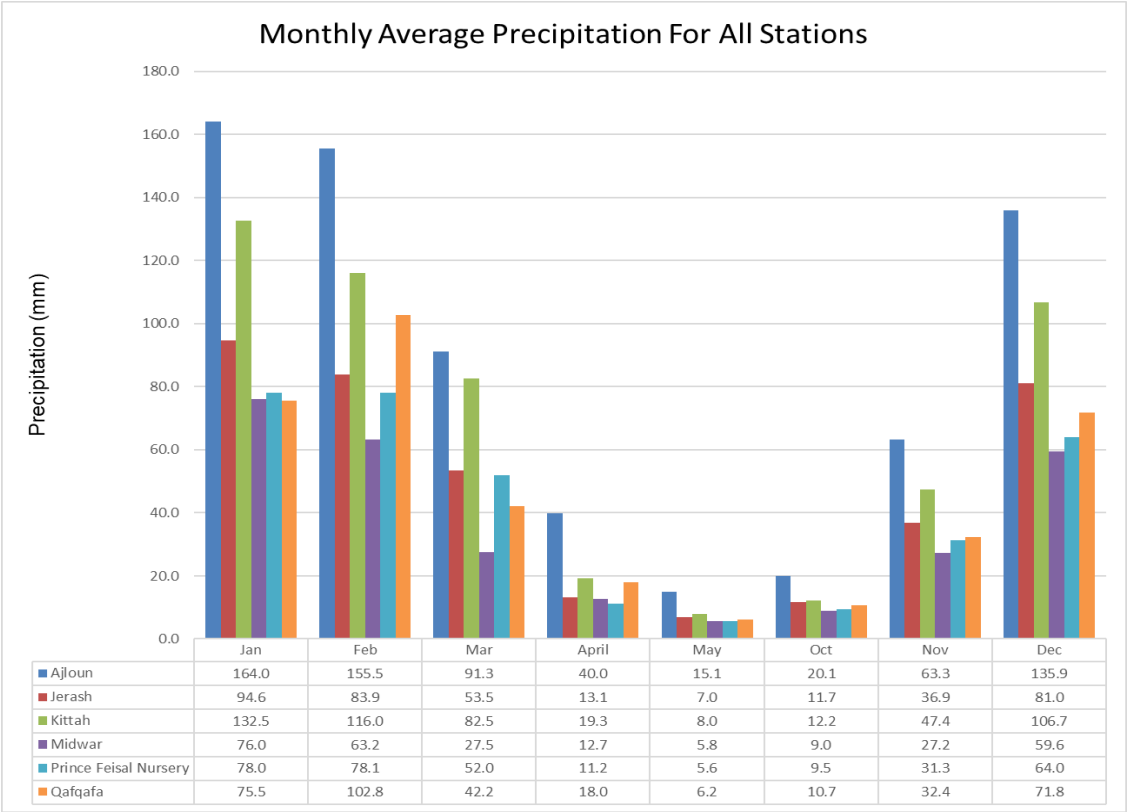

	Jan	Feb	Mar	April	May	Oct	Nov	Dec
Ajloun	164.0	155.5	91.3	40.0	15.1	20.1	63.3	135.9
Jerash	94.6	83.9	53.5	13.1	7.0	11.7	36.9	81.0
Kittah	132.5	116.0	82.5	19.3	8.0	12.2	47.4	106.7
Midwar	76.0	63.2	27.5	12.7	5.8	9.0	27.2	59.6
Prince Feisal Nursery	78.0	78.1	52.0	11.2	5.6	9.5	31.3	64.0
Qafqafa	75.5	102.8	42.2	18.0	6.2	10.7	32.4	71.8

Figure 4.27. Monthly Average Precipitation for All stations.

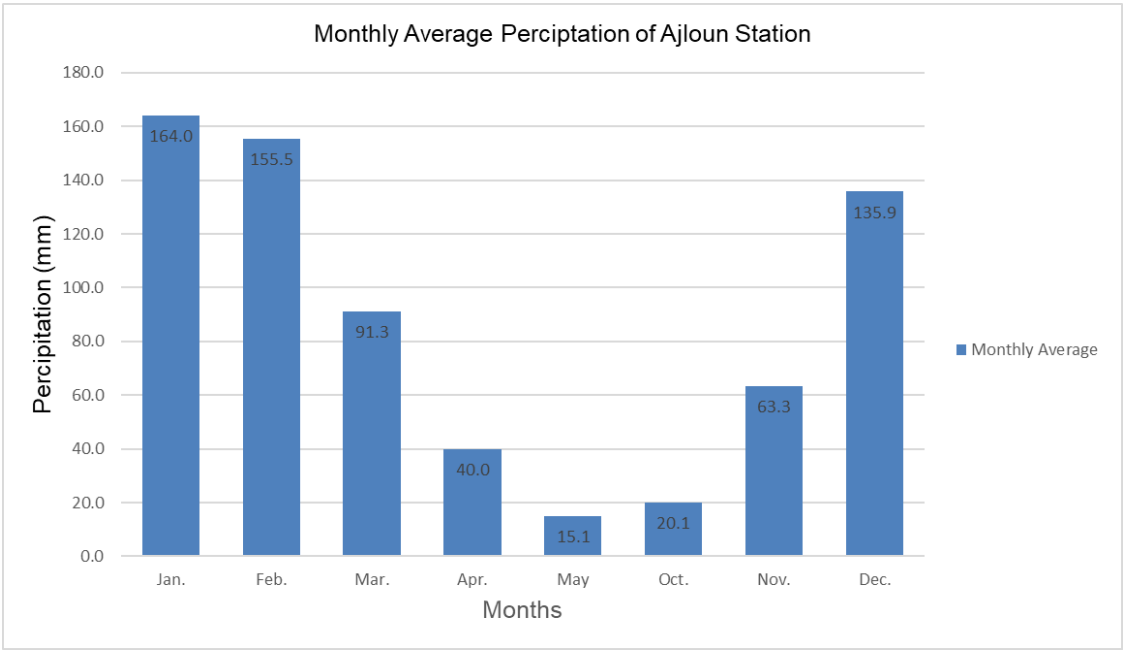

Figure 4.28. Monthly Average Precipitation of Ajloun station.

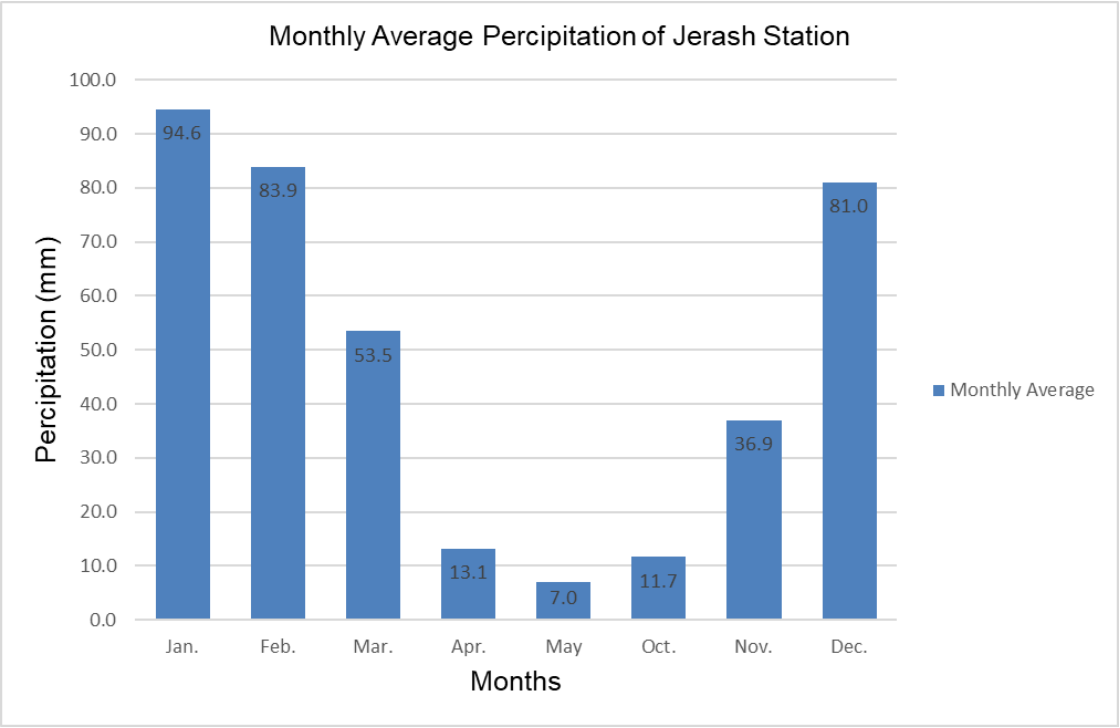

Figure 4.29. Monthly Average Precipitation of Jerash station.

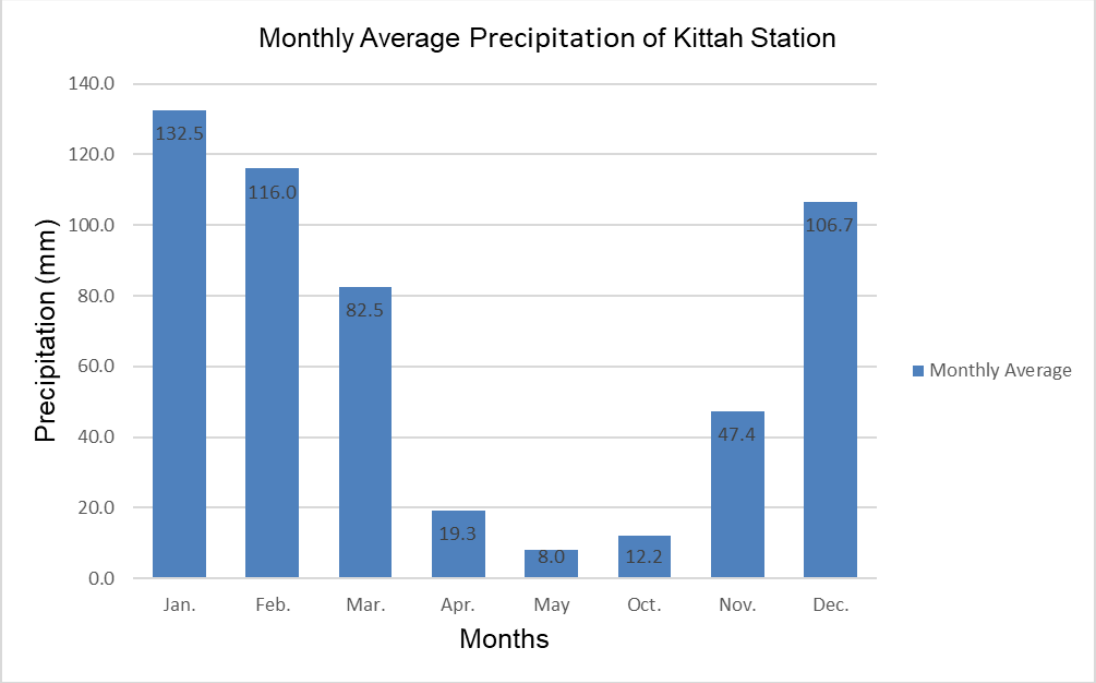

Figure 4.30. Monthly Average Precipitation of Kittah station.

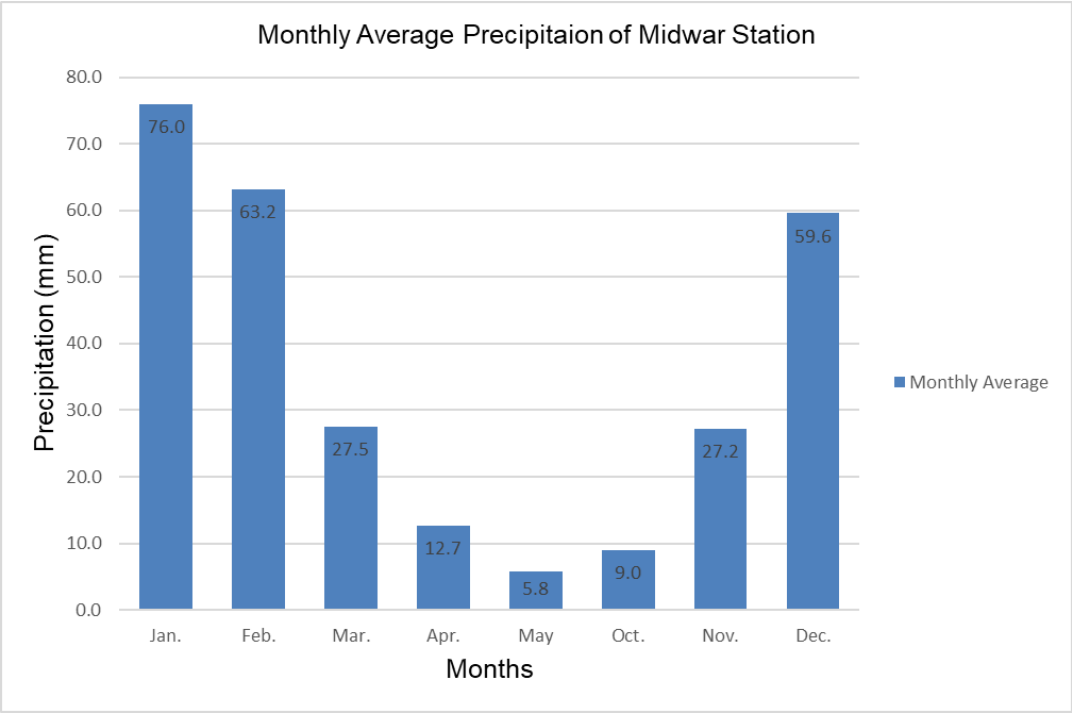

Figure 4.31. Monthly Average Precipitation of Midwar station.

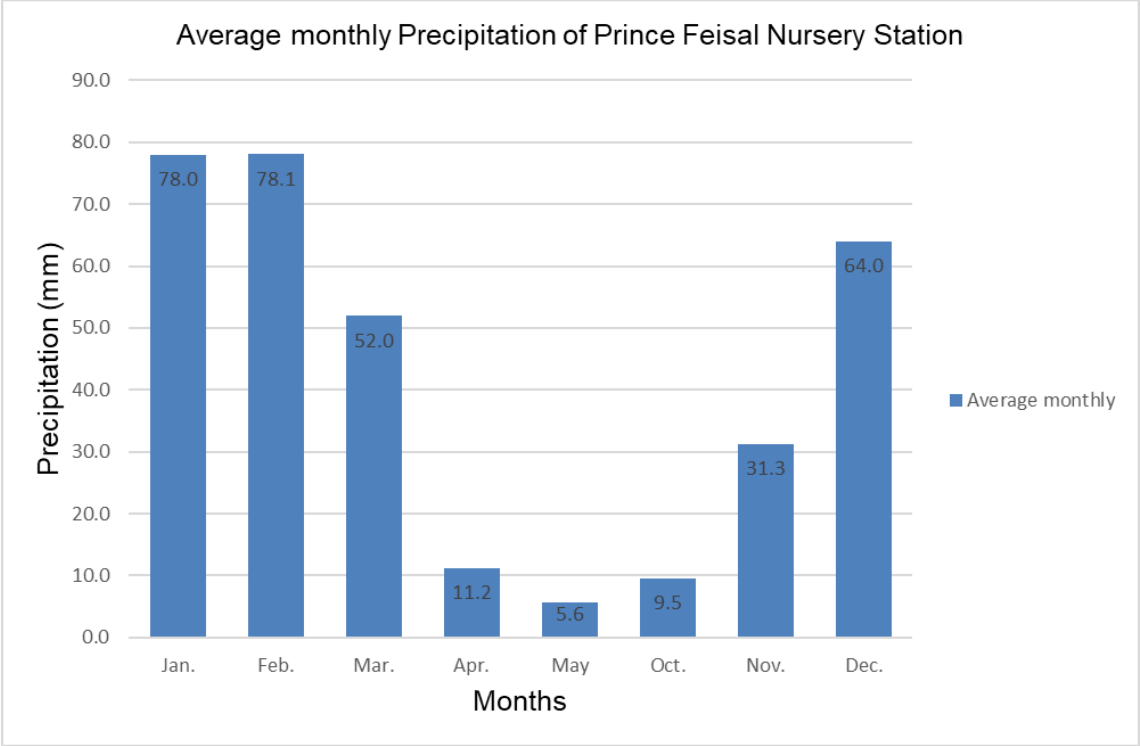

Figure 4.32. Monthly Average Precipitation of Prince Feisal Nursery station.

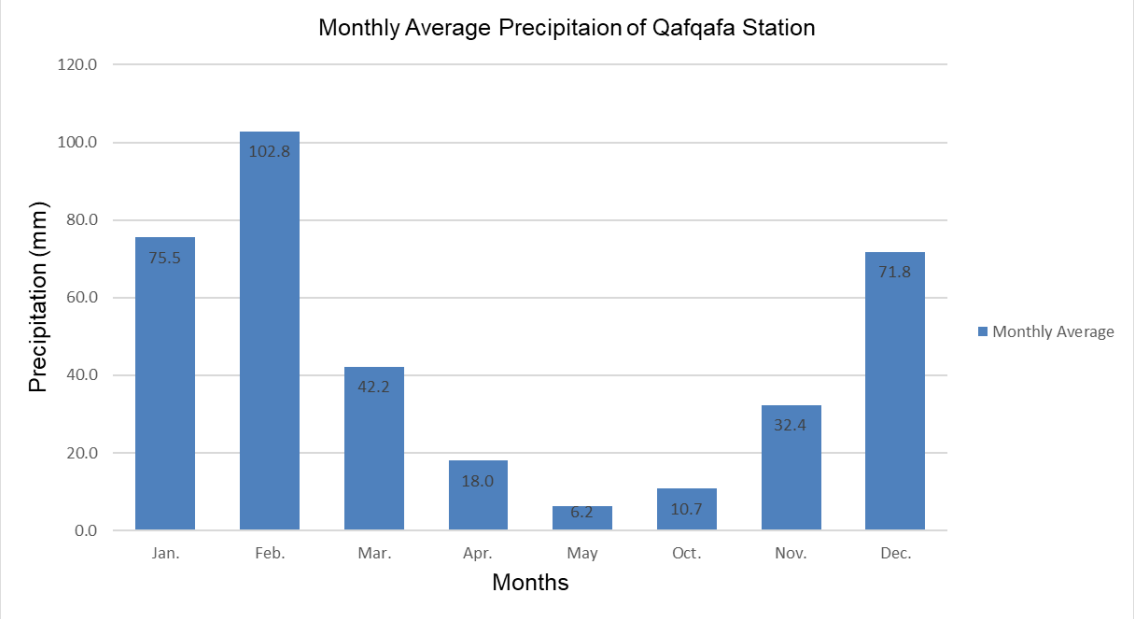

Figure 4.33. Monthly Average Precipitation of Qafqafa station.

4.4.1.3. Annual Rainfall

The amount and distributions of precipitation vary according to different elevations in the region. This is evident when looking at the readings from Ajloun Station and Kittah Station, as the average ranges between 598.18 mm in Ajloun and 498.93 mm in Kittah.

We can notice that four stations were for 31 years and two stations were for a period of 17 years. We found that the highest annual amount of rain was recorded from Kittah station and it was 862 mm in 1992 and the second highest precipitation was for Ajloun station, where it was 823.1 mm in 2003. Figure 4.34 Shows the average annual rainfall for all stations, and we notice that the highest average annual precipitation is in Ajloun with 598.18 mm and the lowest average is in Midwar station with 254.66 mm. Figure 4.35 shows the yearly average rainfall data, From the Figure 4.35 we can see that the highest value of reading refers to Kitta Station reading which is 862 mm and the lowest value is from Midwar Station and it is 54.2 mm. Figure (4.36, 37, 38, 39, 40, 41),Show The annual Rainfall for each station, and the difference between average precipitation and total precipitation. Table 4.3 shows the values of total yearly rainfall in all stations

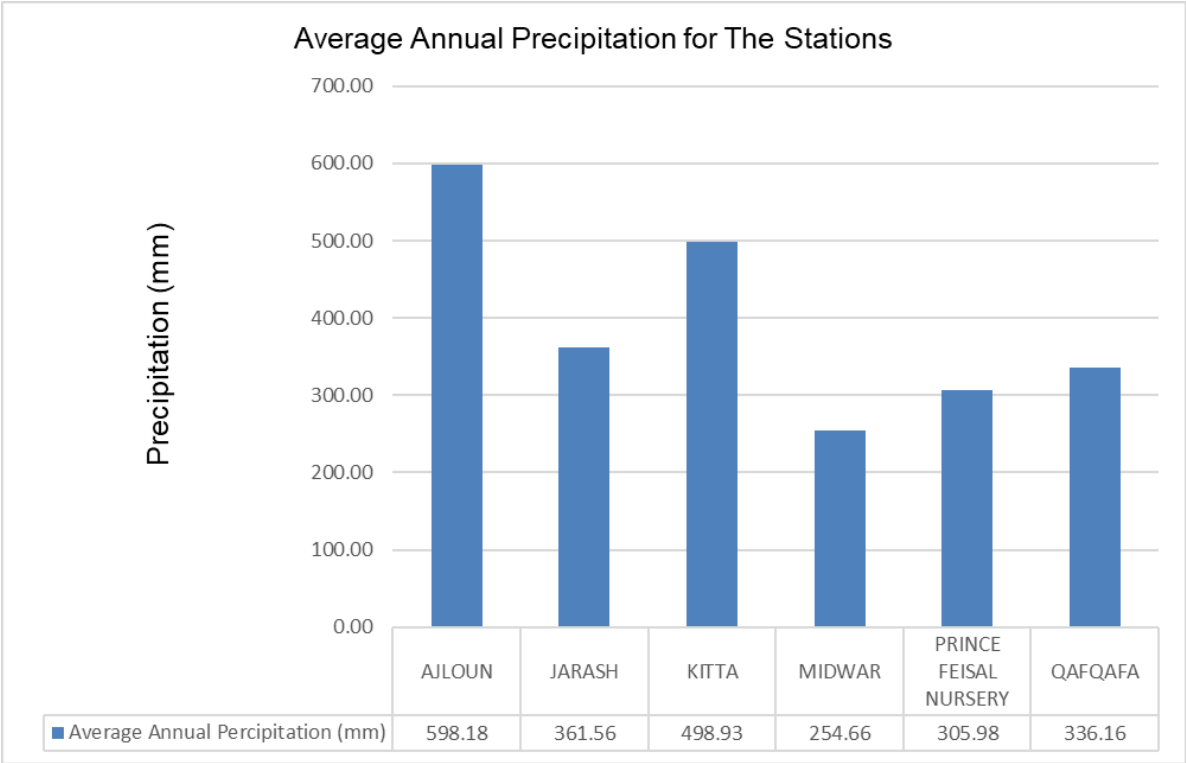

Figure 4.34. Average Annual Precipitation for all stations.

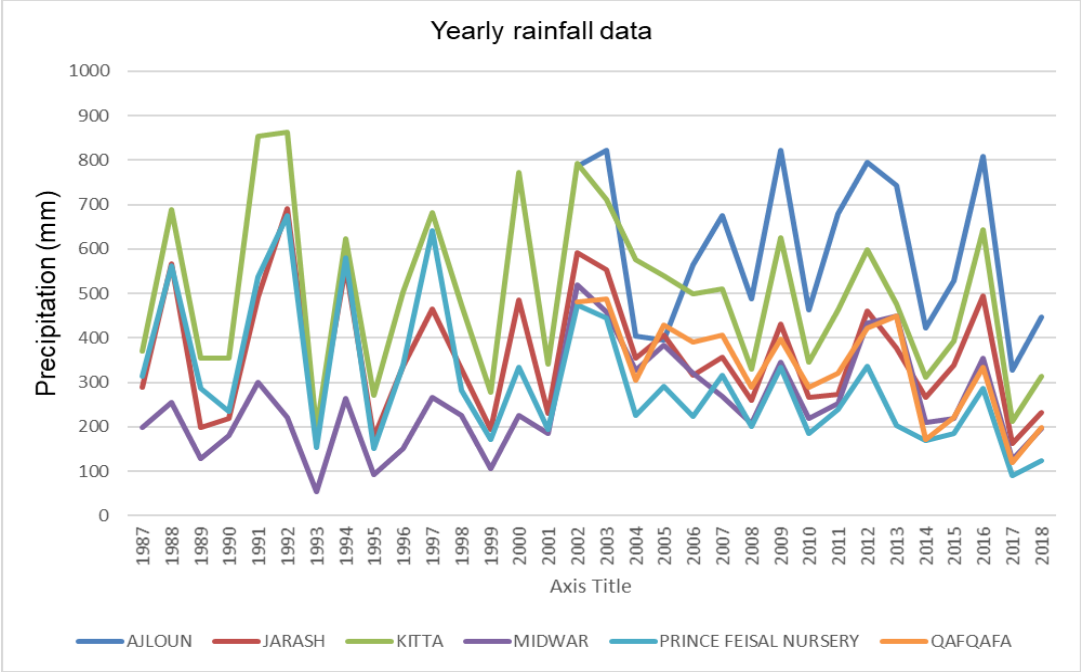

Figure 4.35. Yearly Rainfall Data for All stations.

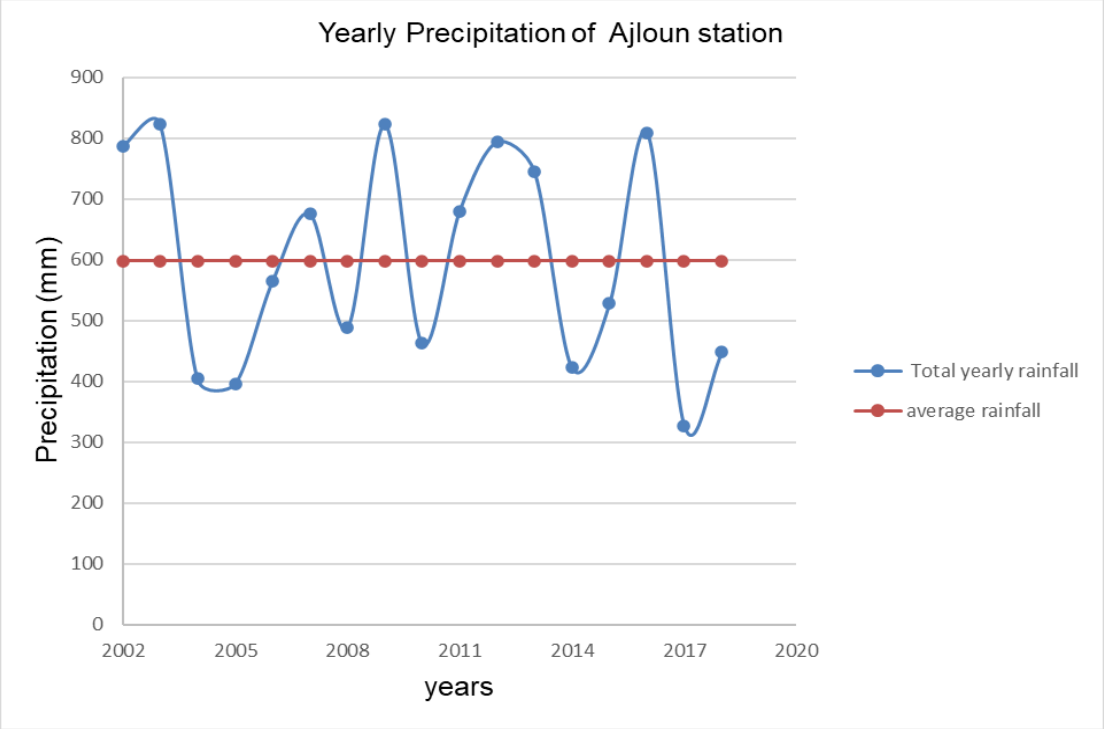

Figure 4.36. Yearly Precipitation of Ajloun station.

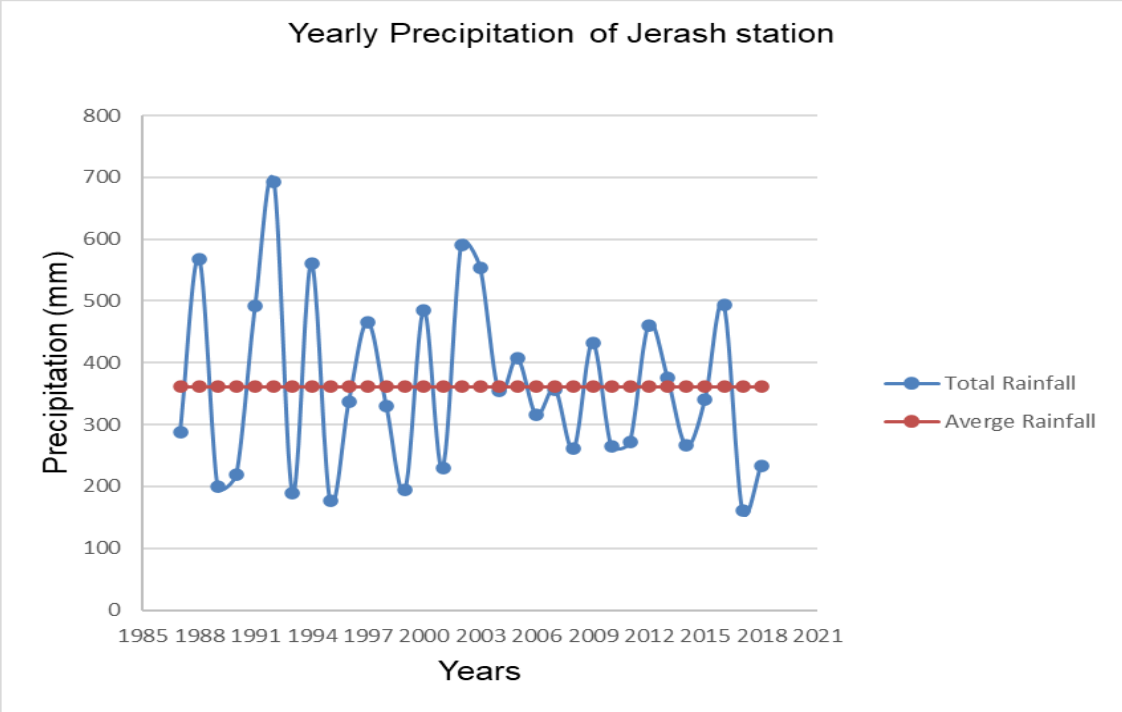

Figure 4.37. Yearly Precipitation of Jerash station.

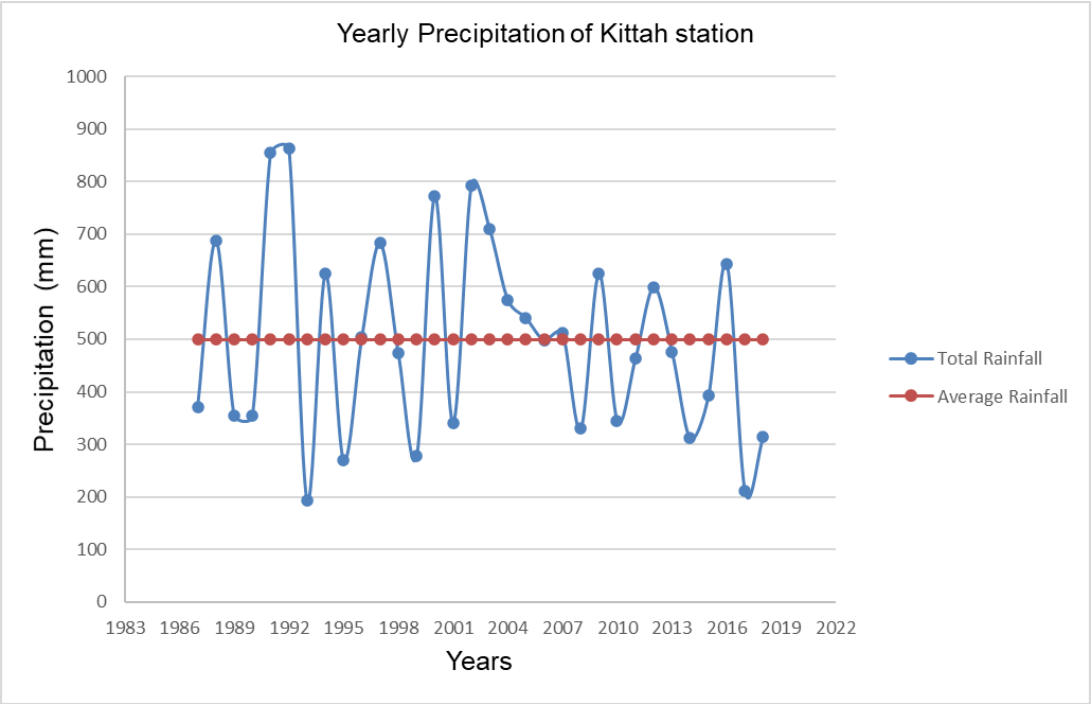

Figure 4.38. Yearly Precipitation of Kittah station.

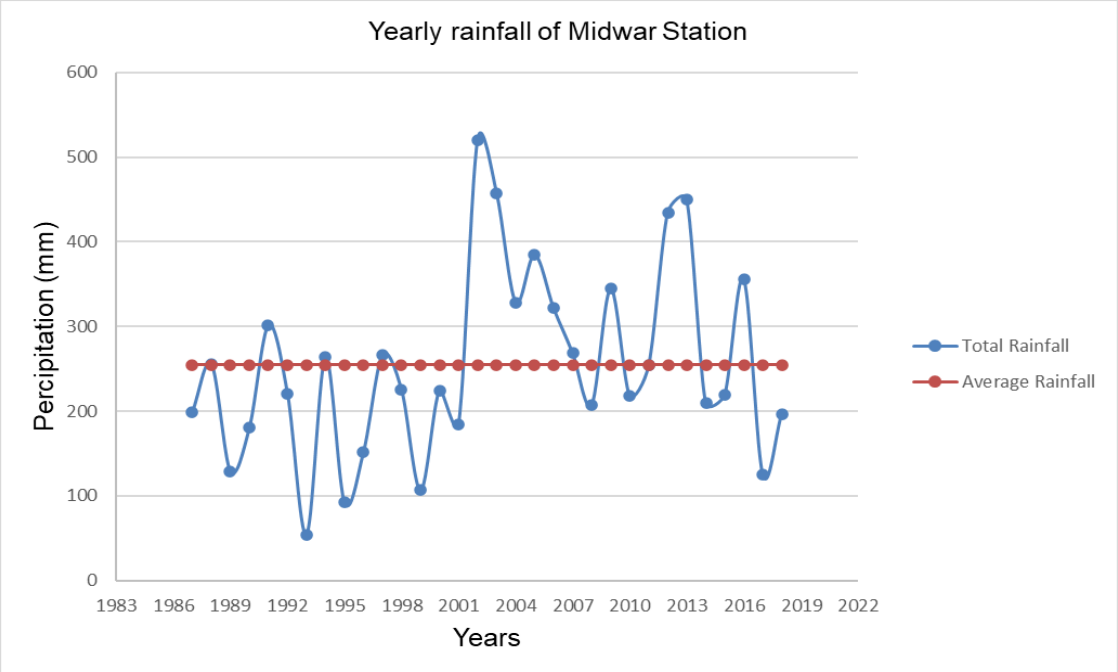

Figure 4.39. Yearly Precipitation of Midwar station.

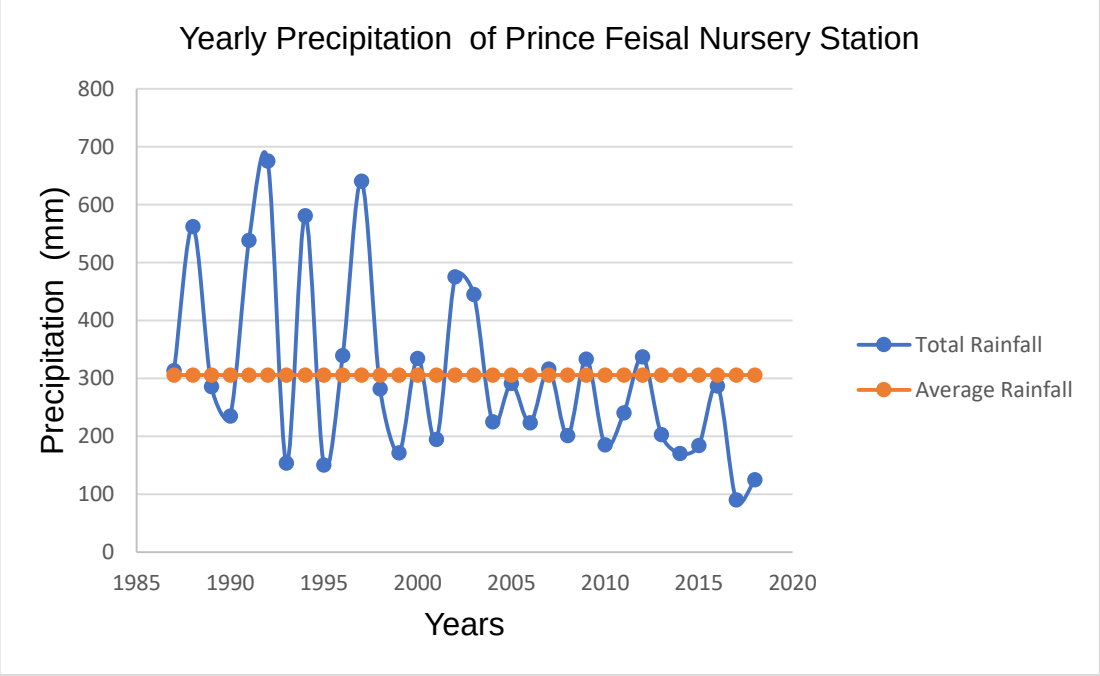

Figure 4.40. Yearly Precipitation of Prince Feisal Nursery station.

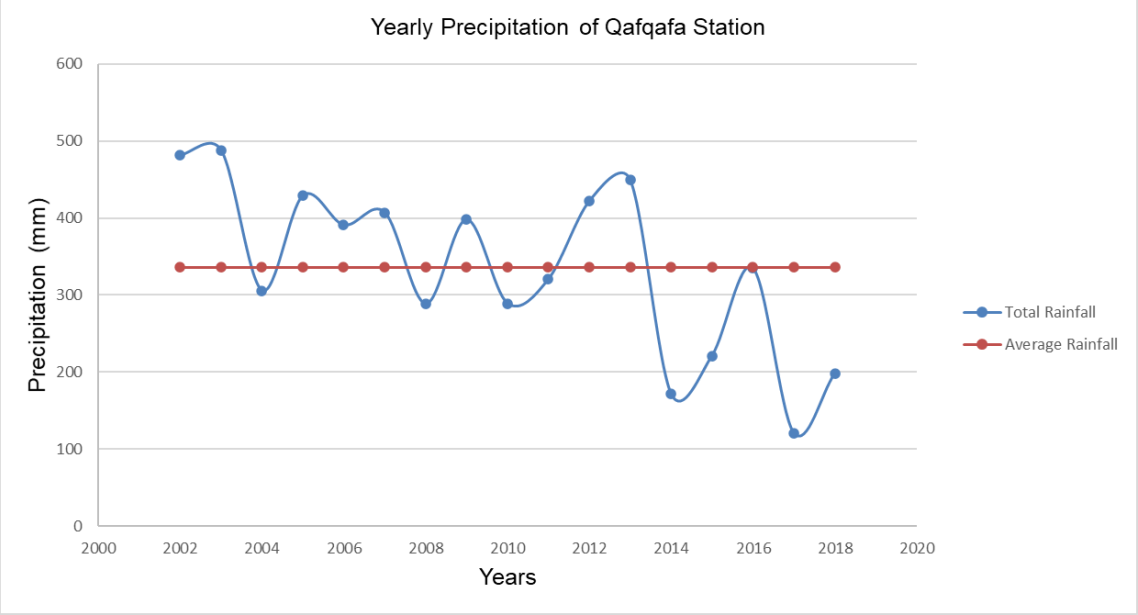

Figure 4.41. Yearly Precipitation of Qafqafa station.

Table 4.3. Total yearly precipitation for all stations.

Year	AJLOUN (mm)	JERASH (mm)	KITTA (mm)	MIDWAR (mm)	P. F. N. (mm)	QAFQAFA (mm)
1987	*	288.5	371.2	199.1	313.5	*
1988	*	567.9	687.8	255.5	562	*
1989	*	199.2	355.5	128.7	286.1	*
1990	*	219.8	354.1	180.6	235	*
1991	*	492	854.1	301.4	538.6	*
1992	*	692	862.5	221	675.2	*
1993	*	189.8	194	54.2	154	*
1994	*	560.6	624	263.5	580.9	*
1995	*	177.2	270.5	92	150.7	*
1996	*	337	504	151.5	339.6	*
1997	*	466.2	683	266.6	640.4	*
1998	*	330	473.4	225.3	281.8	*
1999	*	194.3	277.4	106.5	171.3	*
2000	*	484.9	772.2	224.7	334.7	*
2001	*	229.5	341.1	184.6	194.5	*
2002	785.5	591.2	792.4	520.1	475.3	481.6
2003	823.1	554.2	710.5	457.4	445	487.7
2004	404.2	353.8	575.3	328.5	225	305.7
2005	395.3	406.9	540.6	384.5	291.1	429.1
2006	563.8	315.5	498	321.5	223.3	390.8
2007	675.2	356.7	511.5	268.3	316.3	407
2008	487.4	260.5	329.8	207.5	201.3	288.5
2009	822.1	432.4	624.7	344.4	333.3	397.8
2010	462.1	265.7	345.5	218.2	185.5	289
2011	680	272.1	463.5	253.8	240.3	320.5
2012	794	461	599	434.2	337	421.8
2013	743.7	376.5	476.5	449.5	202.9	449.2
2014	422	265.8	311.5	209.3	170.4	171.5
2015	527.9	339.8	392.4	219.1	184.3	221.1
2016	808.7	494.4	643.7	355.5	287.2	334.7
2017	326.6	161.6	211.4	125.4	90.1	120.7
2018	447.4	232.9	314.6	196.8	124.8	198
Yearly Average	598.18	361.56	498.9	254.66	305.98	336.16

PART 5

RUNOFF MODELING

5.1. RUNOFF

The calculation of the flow chart occupies a large area of scientists' interests, especially as it is considered the main key in the study of streams and floods. Predicting the generation of surface runoff is very difficult for non-pressurized watersheds due to the large spatial variation between soil properties and rainfall intensity. Estimating the volume of runoff and peak drainage resulting from rainstorms is highly dependent on precipitation data (Keskin, 2007), accurate estimates of hydraulic parameters are difficult to obtain due to the short recording period for catchment measurement. Precipitation, vegetation, land cover, soil, height above sea level, and the severity of the watershed slope affect the surface runoff. Rainfall is considered the most influential factor and the most variable, and it affects the link that connects runoff and precipitation. Conditions that are divided into two parts, the first concerned. With rainwater catchments and the other concerned with precipitation. When heavy amounts of rainfall in the large valleys, the runoff forms look like as violent water streams known as flash floods, the rate of rain entering the valleys and the rate of infiltration depend on the characteristics of the shape of the watershed (Hoseini et al., 2016) through the use of precipitation data and hydrograph units derived from them, known techniques are used to estimate the runoff hydrograph at the entrances and exits of the watershed. The reason for using the traditional methods is that the flow measurement stations are out of order and because of the lack of data for them in the study area. In Figure 5.1 we can see a simple sample about runoff in Figure 5.1.

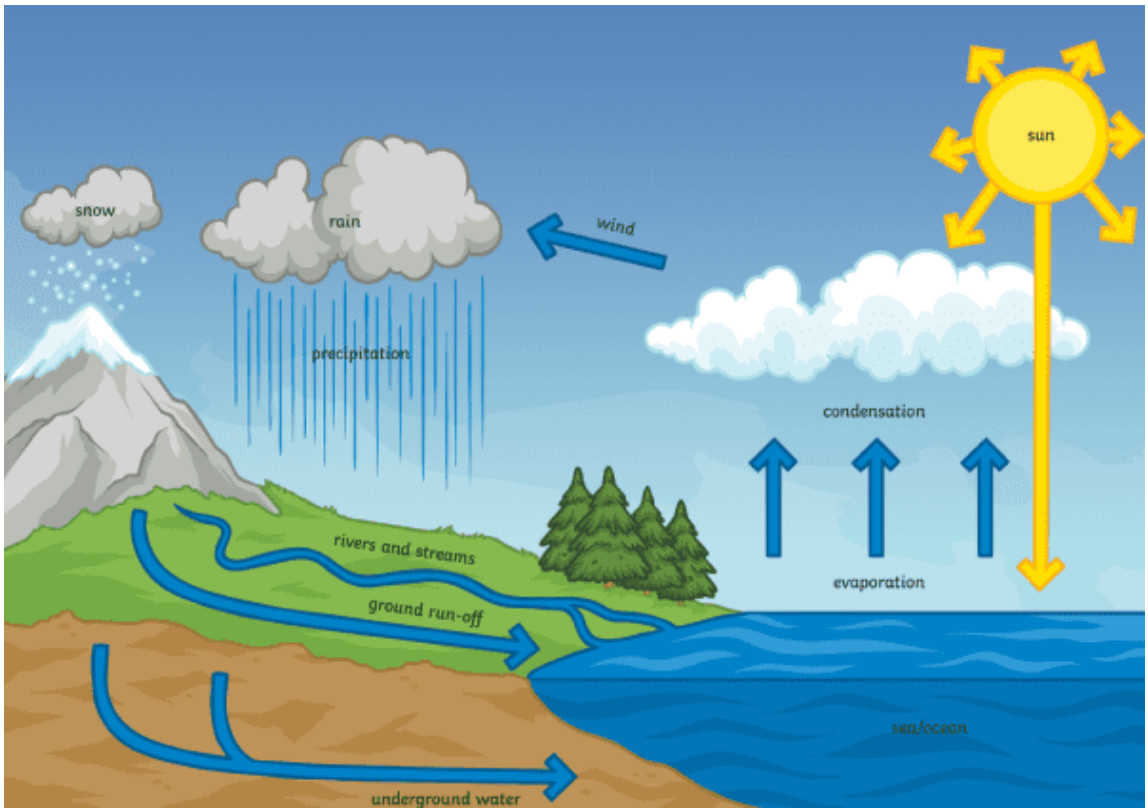

Figure 5.1. Sample of runoff explanation (Twinkl, n.d.).

5.2. CURVES OF FREQUENCY INTENSITY DURATION OF INTENSITY ANALYSIS

IDF is defined as theories to integrate the results from estimates of precipitation levels over several periods. In water resources engineering and management, rainfall intensity-duration-frequency curves have a significant role to play, as they help to check and evaluate rainfall events, arrange and coordinate climatic systems, and even design urban drainage systems in addition to deriving storm design (Sun, Wendig, Kim, & Liong , 2019). The importance of data is to help inform the mapping of the infrastructures on which human life depends. And below we can see table 5.1 that includes Maximum Daily Precipitation for rainfall stations for each year, and accordingly the IDF curves were created after calculating them through a series of steps, which depend on the Gumbel Type I distribution in order to estimate the rainfall events that have correlations

with the specified probability of exceeding. (De Paola, Giugni, Topa, & Bucchignani, 2014).

we will see the formulas that they were used and tables showing the IDF value for each station in the study area (Oosterbaan, 1994) For the design process, we will be asked to divide the periods of rain, and the common division is 5 minutes, 10 minutes, 20 minutes, 30 minutes, 1 hour, 2 hours, 3 hours, 6 hours, 12 hours, and 24 hours.

In the following equation 5.1, we calculated the exceedance probability distribution function of rain intensity for the previously mentioned periods

$$\text{Rain Intensity} = \text{Annual maximum rainfall} \times \sqrt[3]{\frac{\text{Time (hr)}}{24}} \quad (5.1)$$

Equation 5.2 is an application of Gumbel Type I, where (Xt) represents the random variable associated with the return period (T), and (X) represents the mean of observations and the standard deviation of observations is (S)

$$Xt = X + Kt \times S \quad (5.2)$$

We used Equation 5.3 to complete the calculation of precipitation intensity for the return period

$$Kt = -\frac{\sqrt{6}}{\pi}\left(0.5772 + \ln\left[\ln\left(\frac{T}{T-1}\right)\right]\right) \quad (5.3)$$

Table 5.1. Maximum daily precipitation for rainfall stations.

Years	AJLOUN Max (mm)	JARASH Max (mm)	KITTA Max (mm)	MIDWAR Max (mm)	PRINCE FEISAL NURSERY Max (mm)	QAFQAFA Max (mm)
1987	*	27	30	15	25	*
1988	*	74	85	48	65	*
1989	*	25	40	12	35	*
1990	*	29	42	33	34.2	*
1991	*	55	90	35	46	*
1992	*	127	140	30.5	70	*
1993	*	37	27	17	26	*
1994	*	46	64	27	53	*
1995	*	29	49	15	21	*
1996	*	42	65	15	38.5	*
1997	*	67	108	45	63	*
1998	*	78	98	55	67.5	*
1999	*	55	90	38.5	51	*
2000	*	58	105	38	35	*
2001	*	44	73	45.5	42	*
2002	64	97	104	86	70	66
2003	84	72	70	53	52	54
2004	52.3	55	68	32	35	37
2005	136	43	72	77	37	44
2006	80	46	68	57	40	42
2007	73	36	62	34	29	55
2008	64	40	56	24	29	114.6
2009	109.6	60	103	98	40	125
2010	143	45	65	79.5	38	43.5
2011	60	34	61	58	25.5	45
2012	108	68	71	77.5	45	53.5
2013	150	84	100	130	59	82
2014	55	49	44	23.5	35	23.7
2015	117	88	91	45	47	98
2016	168	89	105	46.8	63	86
2017	85	61.5	71	33	27	31
2018	68.8	38.2	55	32	26.4	38

The final results of these calculations are recorded in the tables (5.2, 3, 4, 5, 6, 7) and figures (5.2, 3, 4, 5, 6, 7).

Table 5.2. Rainfall Intensity (mm/min), Duration and Frequency at Ajloun station.

	Duration (min)									
Return Period	5	10	20	30	60	120	180	360	720	1440
2 year	163.01	102.71	64.70	49.37	31.10	19.59	14.95	9.42	5.93	3.74
5 year	221.75	139.72	88.01	67.17	42.31	26.65	20.34	12.81	8.07	5.09
10 year	260.64	164.23	103.44	78.95	49.73	31.33	23.91	15.06	9.49	5.98
25 year	309.78	195.19	122.95	93.83	59.11	37.24	28.42	17.90	11.28	7.10
50 year	346.23	218.15	137.42	104.87	66.06	41.62	31.76	20.01	12.60	7.94
100 year	382.41	240.95	151.78	115.83	72.97	45.97	35.08	22.10	13.92	8.77
1000 year	501.98	316.29	199.23	152.05	95.78	60.34	46.05	29.01	18.27	11.51

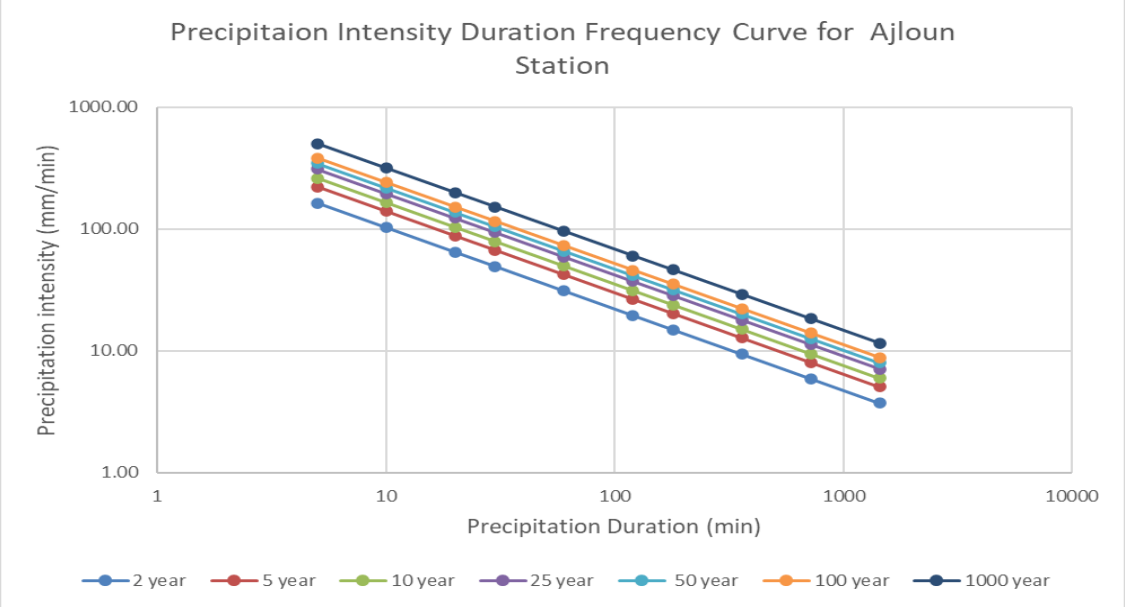

Figure 5.2. IDF Curve for Ajloun station.

Table 5.3. Rainfall Intensity (mm/min), Duration and Frequency at Jerash station.

	Duration (min)									
Return Period	5	10	20	30	60	120	180	360	720	1440
2 year	95.80	60.37	38.02	29.02	18.28	11.52	8.79	5.54	3.49	2.20
5 year	133.38	84.04	52.94	40.40	25.45	16.03	12.23	7.71	4.86	3.06
10 year	158.25	99.71	62.81	47.93	30.20	19.02	14.52	9.14	5.76	3.63
25 year	189.68	119.52	75.28	57.45	36.19	22.80	17.40	10.96	6.91	4.35
50 year	213.00	134.21	84.54	64.52	40.64	25.60	19.54	12.31	7.75	4.88
100 year	236.14	148.79	93.72	71.53	45.06	28.39	21.66	13.65	8.60	5.42
1000 year	312.62	196.98	124.08	94.69	59.65	37.58	28.68	18.07	11.38	7.17

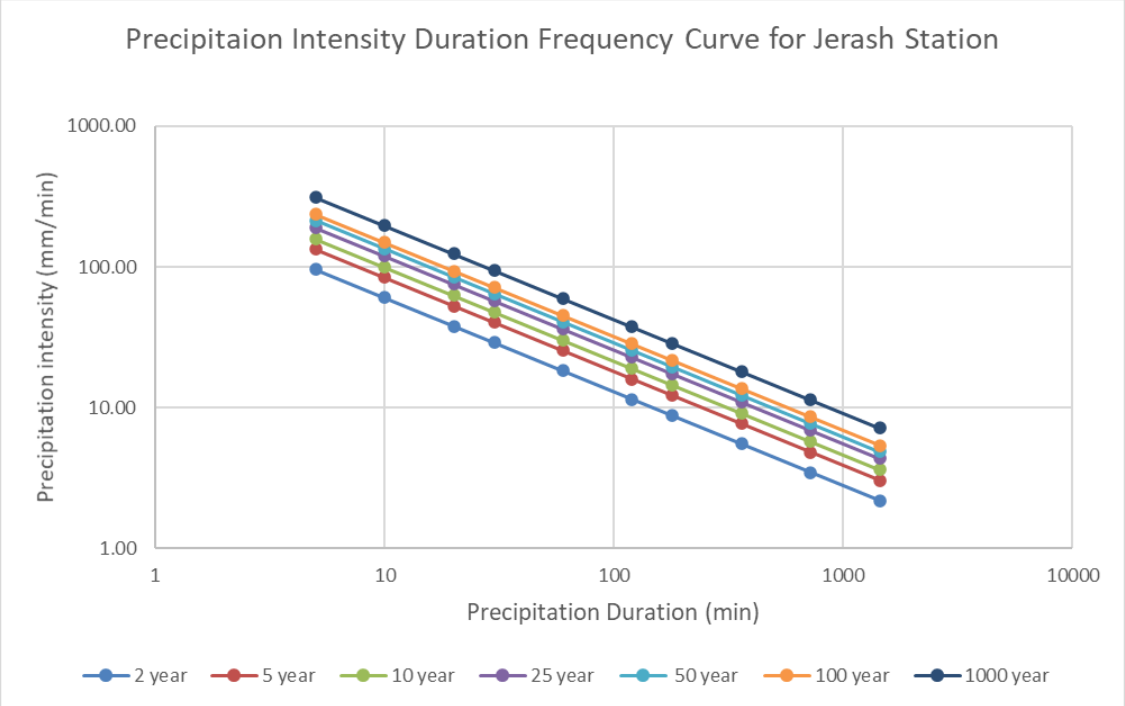

Figure 5.3. IDF Curve for Jerash station.

Table 5.4. Rainfall Intensity (mm/min), Duration and Frequency at Kittah station.

	Duration (min)									
Return Period	5	10	20	30	60	120	180	360	720	1440
2 year	126.98	80.01	50.40	38.46	24.23	15.26	11.65	7.34	4.62	2.91
5 year	168.36	106.08	66.82	51.00	32.13	20.24	15.44	9.73	6.13	3.86
10 year	195.76	123.35	77.70	59.30	37.35	23.53	17.96	11.31	7.13	4.49
25 year	230.38	145.16	91.44	69.78	43.96	27.69	21.13	13.31	8.39	5.28
50 year	256.06	161.34	101.63	77.56	48.86	30.78	23.49	14.80	9.32	5.87
100 year	281.55	177.40	111.74	85.28	53.72	33.84	25.83	16.27	10.25	6.46
1000 year	365.78	230.47	145.18	110.79	69.80	43.97	33.55	21.14	13.32	8.39

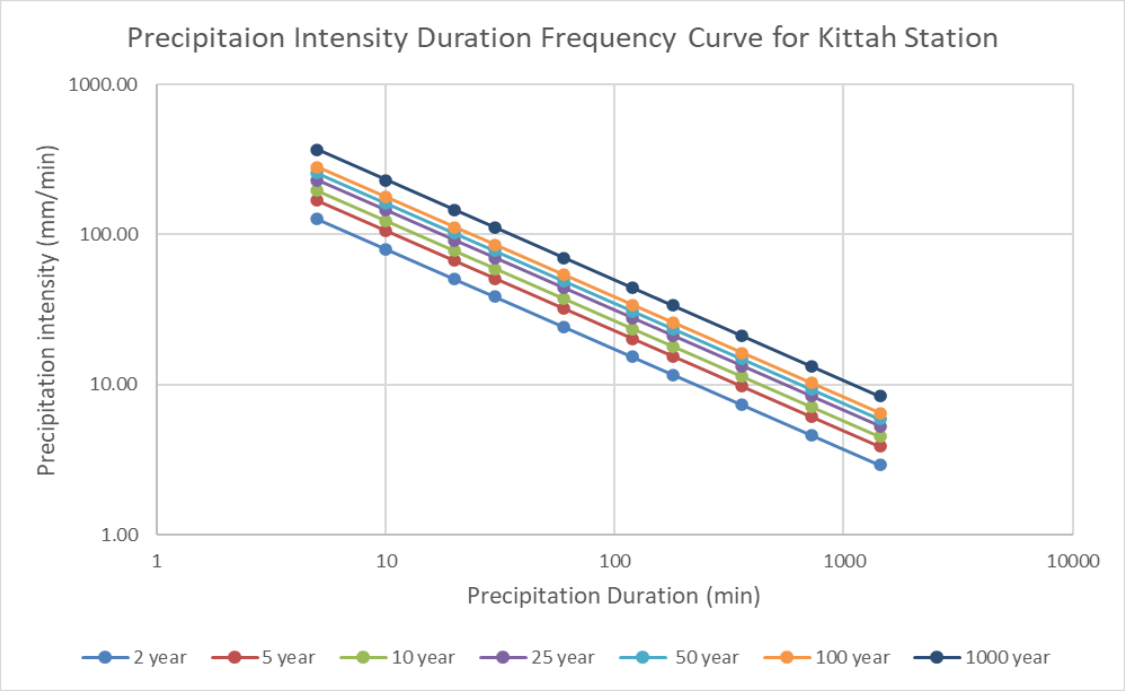

Figure 5.4. IDF Curve for Kittah station.

Table 5.5. Rainfall Intensity (mm/min), Duration and Frequency at Midwar station.

	Duration (min)									
Return Period	5	10	20	30	60	120	180	360	720	1440
2 year	74.38	47.81	29.82	22.83	14.39	9.06	6.92	4.36	2.74	1.73
5 year	117.00	75.21	46.91	35.92	22.63	14.25	10.88	6.85	4.32	2.72
10 year	145.22	93.35	58.22	44.58	28.09	17.69	13.50	8.51	5.36	3.38
25 year	180.87	116.27	72.52	55.53	34.98	22.04	16.82	10.59	6.67	4.20
50 year	207.32	133.27	83.12	63.65	40.10	25.26	19.28	12.14	7.65	4.82
100 year	233.58	150.15	93.65	71.71	45.17	28.46	21.72	13.68	8.62	5.43
1000 year	320.33	205.91	128.43	98.34	61.95	39.03	29.78	18.76	11.82	7.45

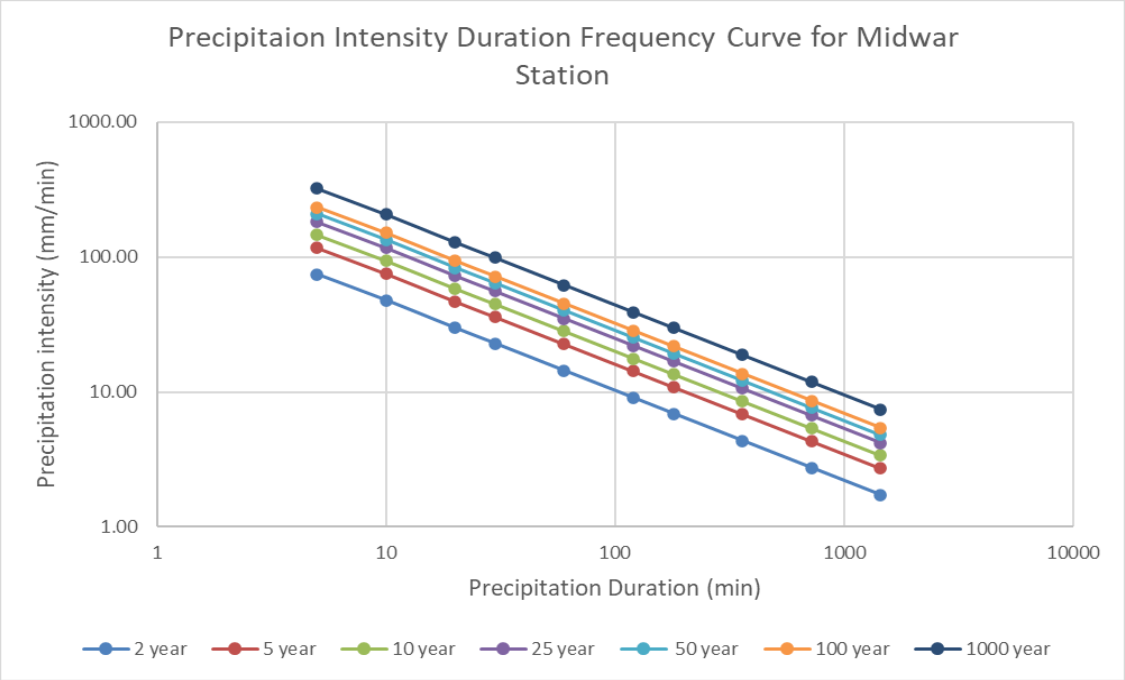

Figure 5.5. IDF Curve for Midwar station.

Table 5.6. Rainfall Intensity (mm/min), Duration and Frequency at Prince Feisal Nursery station.

	Duration (min)									
Return Period	5	10	20	30	60	120	180	360	720	1440
2 year	72.85	46.83	29.21	22.37	14.09	8.88	6.77	4.27	2.69	1.69
5 year	96.03	61.73	38.50	29.48	18.57	11.70	8.93	5.62	3.54	2.23
10 year	111.38	71.60	44.66	34.19	21.54	13.57	10.36	6.52	4.11	2.59
25 year	130.77	84.06	52.43	40.15	25.29	15.93	12.16	7.66	4.83	3.04
50 year	145.16	93.31	58.20	44.56	28.07	17.69	13.50	8.50	5.36	3.37
100 year	159.44	102.49	63.93	48.95	30.84	19.43	14.82	9.34	5.88	3.71
1000 year	206.63	132.82	82.84	63.43	39.96	25.17	19.21	12.10	7.62	4.80

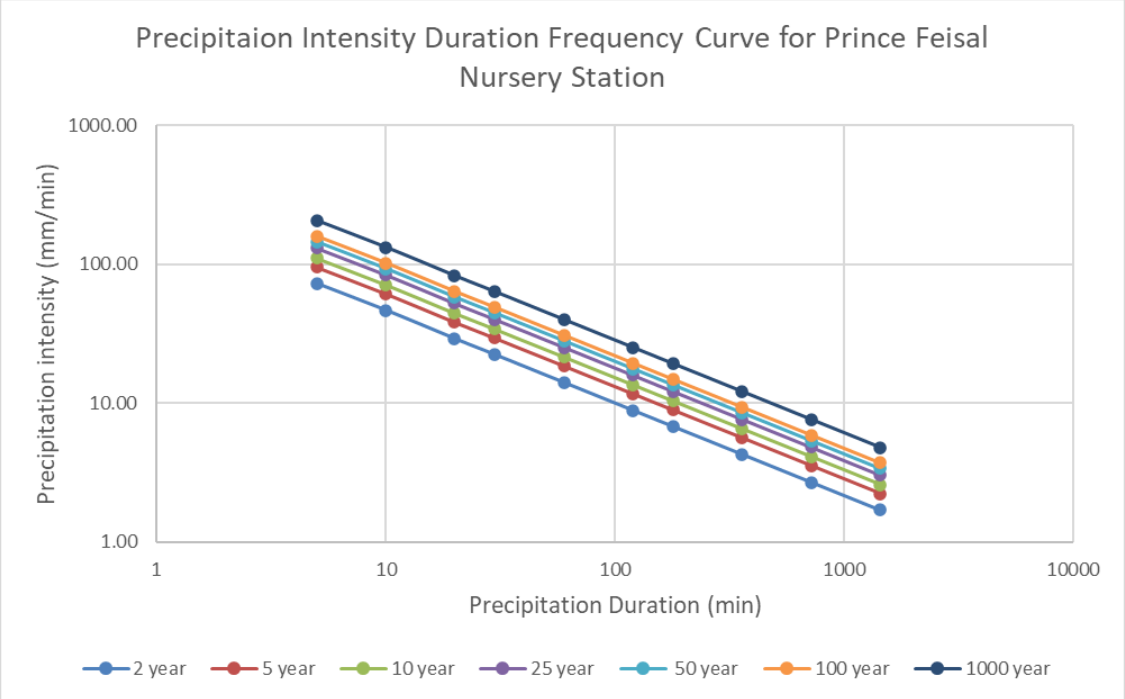

Figure 5.6. IDF Curve for Prince Feisal Nursery station.

Table 5.7. Rainfall Intensity (mm/min), Duration and Frequency at Qafqafa station.

	Duration (min)									
Return Period	5	10	20	30	60	120	180	360	720	1440
2 year	101.55	65.28	40.71	31.17	19.64	12.37	9.44	5.95	3.75	2.36
5 year	148.73	95.60	59.63	45.66	28.76	18.12	13.83	8.71	5.49	3.46
10 year	179.97	115.69	72.16	55.25	34.81	21.93	16.73	10.54	6.64	4.18
25 year	219.43	141.06	87.98	67.37	42.44	26.73	20.40	12.85	8.10	5.10
50 year	248.72	159.88	99.72	76.36	48.10	30.30	23.12	14.57	9.18	5.78
100 year	277.78	178.56	111.37	85.28	53.72	33.84	25.83	16.27	10.25	6.46
1000 year	373.82	240.30	149.88	114.76	72.30	45.54	34.76	21.90	13.79	8.69

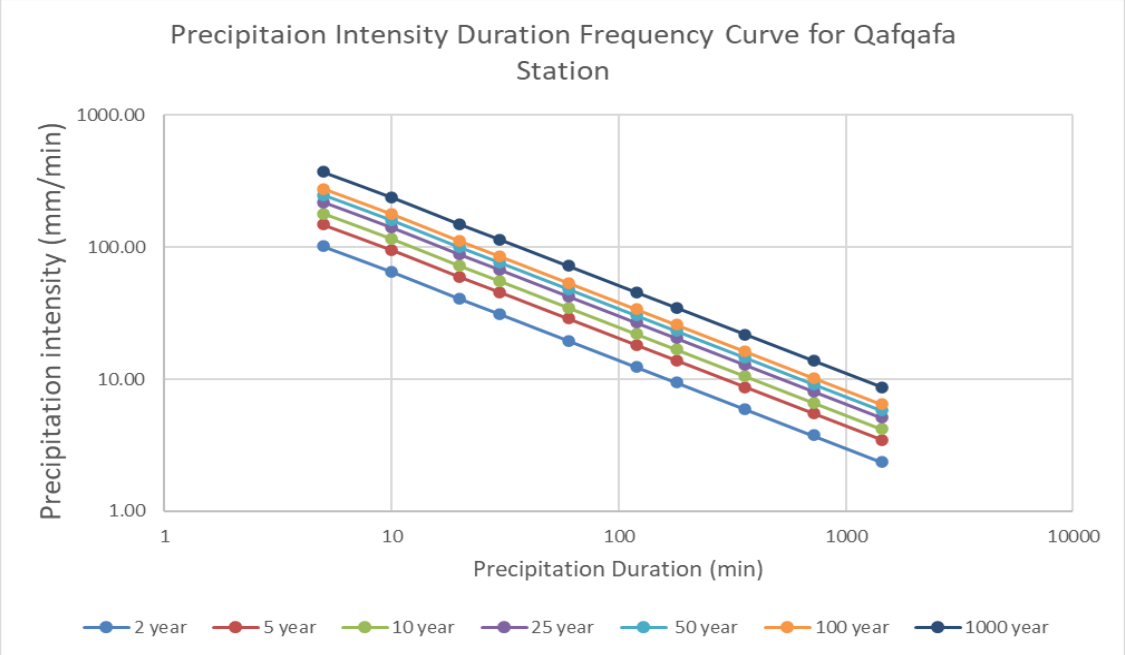

Figure 5.7. IDF Curve for Qafqafa station.

5.3. HYDROGRAPH UNIT AND FLOOD DESIGN METHOD

We created the IDF curves as we have seen before to calculate the effective precipitation quantities in order to complete the process of calculating the runoff drainage, and in

order to find the discharge peak and its value we resort to using the unit hydrograph approach, and the unit graph can be used to refer to the direct runoff of the hydrograph resulting from a unit volume excess sedimentation, and here we will depend on the curve number, time of concentration, and unit hydrograph method.

5.3.1. Curve Number

In order to estimate the runoff, we used the USA Soil conservation services (SCS) method. This method is based on previous rainfall records and on soil moisture percentage, activity and land use, type of soil and its permeability. (engineering purdue, n.d.).

On this basis, we calculated the volume of flow, monthly and yearly. The curve number is defined as a basin parameter that begins with 0 and ends with 100, where the number 0 indicates that the basin is completely permeable and not accompanied by surface runoff, and the number 100 indicates that there is no permeability to the basin and thus all the precipitation turns into surface runoff water, and with this we can Simplify the definition of the curve number as an equation that includes both land use and the amount of moisture present in the soil. In Table 5.8 and 5.9 we can see the Hydrologic Soils Groups, landuse description. (Weaver, 2003).

Table 5.8 Hydrologic Soil Groups and their characteristic (Stone, 2014).

Hydrologic Soil Group	Characteristics of Soils	Minimum Infiltration Rate (mm/hr)
Low Runoff Potential A	High infiltration rates even when thoroughly wetted. Deep, well-drained sands or gravels with a high rate of water transmission. Sand, loamy sand, or sandy loam.	8 - 12
B	Moderate infiltration rates when thoroughly wetted. Moderately deep to deep, moderately well-drained to well-drained, moderately fine to moderately coarse textures. Silt loam or loam.	4 – 8
C	Slow infiltration rates when thoroughly wetted. Usually has a layer that impedes downward movement of water or has moderately fine to fine textured soils. Sand clay loam.	1 – 4
D High Runoff Potential	Very low infiltration rate when thoroughly wetted. Chiefly clay soils with a high swelling potential; soils with a high permanent water table; soils with a clay layer near the surface; shallow soils over near-impervious materials. Clay loam, silty clay loam, sandy clay, silty clay, or clay.	0 – 1

Table 5.9 Hydrologic soil groups and Landuse description (Weaver C. , 2003).

Land Use Description	Hydrologic Soil Grouping			
	A	B	C	D
Commercial houses and town houses	80	85	90	95
Cultivated with conventional tillage	72	81	88	91
Cultivated without conservation treatment	62	71	78	81
Fallow	77	86	91	94
Pastures ore range, poor conditions	68	79	86	89
Pastures ore range, Good Cover	39	61	74	80
Pavement and roofs	100	100	100	100
Wood or forest thin stand, poor cover	45	66	77	83
Wood or forest thin stand, Good Cover	25	50	70	77

In Table 5.10 we have the Hydrologic Soil Group (HGS), Landuse Description, Curve Number (CN), Area (A), and the product of (CN x A), and according to this information we calculated the curve number for whole study area, and this runoff curve number table is generated by WMS.

This method has been proven based on the hypothesis, that the amount of rain losses actually reserved at the time of the start of the drain in relation to the maximum potential retention is equal to the real volume of the actual discharges that can occur.

Table 5.10 Requirements of CN calculation.

HSG	Land Use Description	CN	Area Km^2	Product CN x A
C	Forest	77	12.444	958.151
C	Tree Crops	88	18.972	1669.529
C	Bare Soil	91	0.237	21.603
C	Vegetables	78	0.455	35.491
C	Urban Fabric	98	0.791	77.549
C	Field Crops	88	2.097	184.536
D	Tree Crops	91	22.83	2077.494
C	Pastures	86	0.712	61.248
C	Bare Rocks	91	0.119	10.802
D	Forest	83	6.588	546.783
D	Pastures	89	18.675	1662.09
D	Urban Fabric	98	3.818	374.176
D	Bare Soil	94	1.523	143.19
D	Vegetables	81	1.365	110.567
D	Bare Rocks	94	1.187	111.576
D	Field Crops	91	9.852	896.527

Total products= 8941.312

Total area= 101.665

CN (weighted) = Total products / Total area (5.4)

= 8941.312 / 101.665

= 87.9488

5.4. RUNOFF ANALYSIS

After calculation process, we got that CN value is 87.9488 and this value leads us to know that study area has no enough permeability to absorb the rainwater that falls during winter season, this means that rainstorms with high amounts of precipitation will be accompanied by catastrophic consequences, which is what happened this year, last year, and the year before.

And according to SCS we will calculate runoff data by different intervals:

5.4.1. Daily Runoff

$$Q = \frac{(P-0.2S)^2}{P+0.8S} \quad (5.5)$$

Where:

Q: Runoff depth (mm)

P: Precipitation depth (mm)

S: Potentital maximum retention after runoff begins; $S = \frac{25400}{CN} - 254$ (5.6)

Ia: initial abstraction; Ia = 0.2S (5.7)

Initial abstraction (Ia) is defined as all the losses that occur before the runoff begins and includes all of the water trapped in depressions, evaporation, infiltration, and water that is intercepted by the vegetation, and for this it is a factor that has a significant impact by virtue of it being highly variable.

So that:

$$S = \frac{25400}{87.9488} - 254 = 34.8$$

Ia = 0.2 * 34.8 = 6.96

After that we calculated Q by using Formula (5.5), then according to the results that we got we made the Figures below, zero values refer to that the initial abstraction is bigger than rainfall so that mean we don't have any runoff. And Figures (5.8, 9, 10, 11, 12, 13) were created by using pivot table in Microsoft Excel in order to get the exact numbers without forgetting any number.

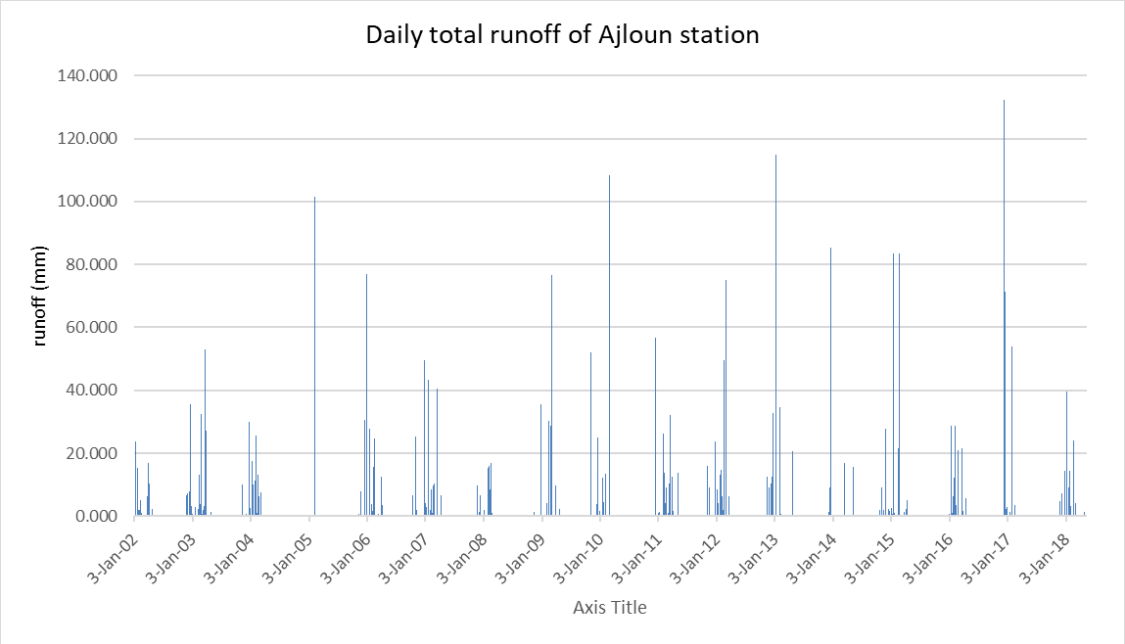

Figure 5.8. Daily runoff of Ajloun station.

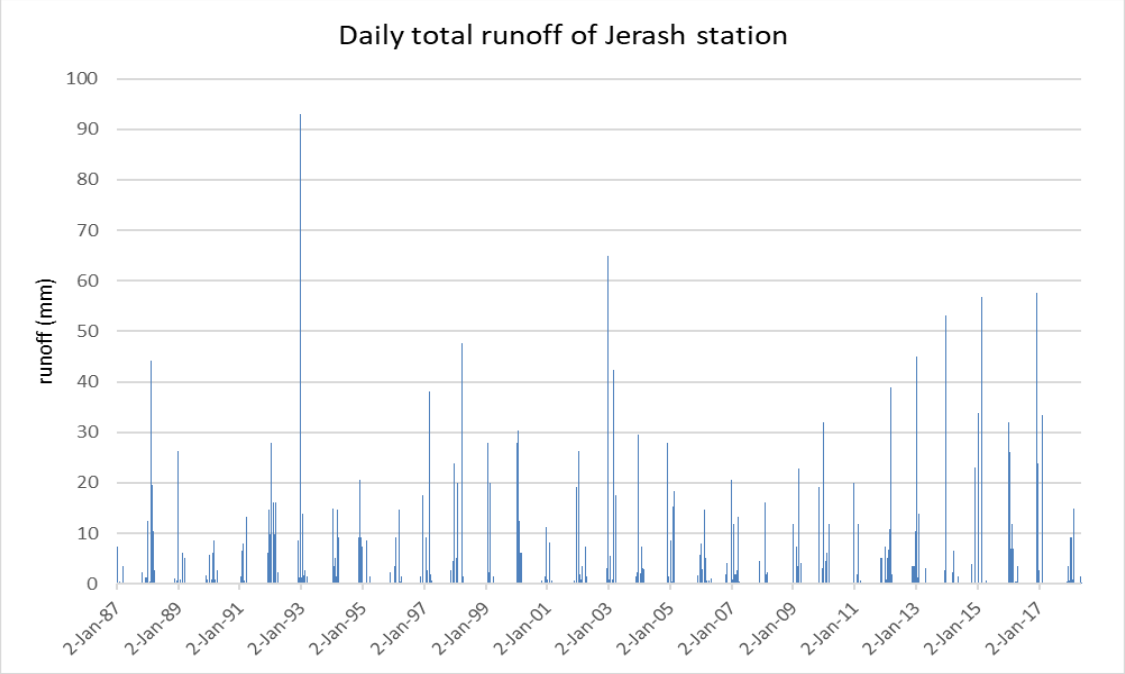

Figure 5.9. Daily runoff of Jerash station.

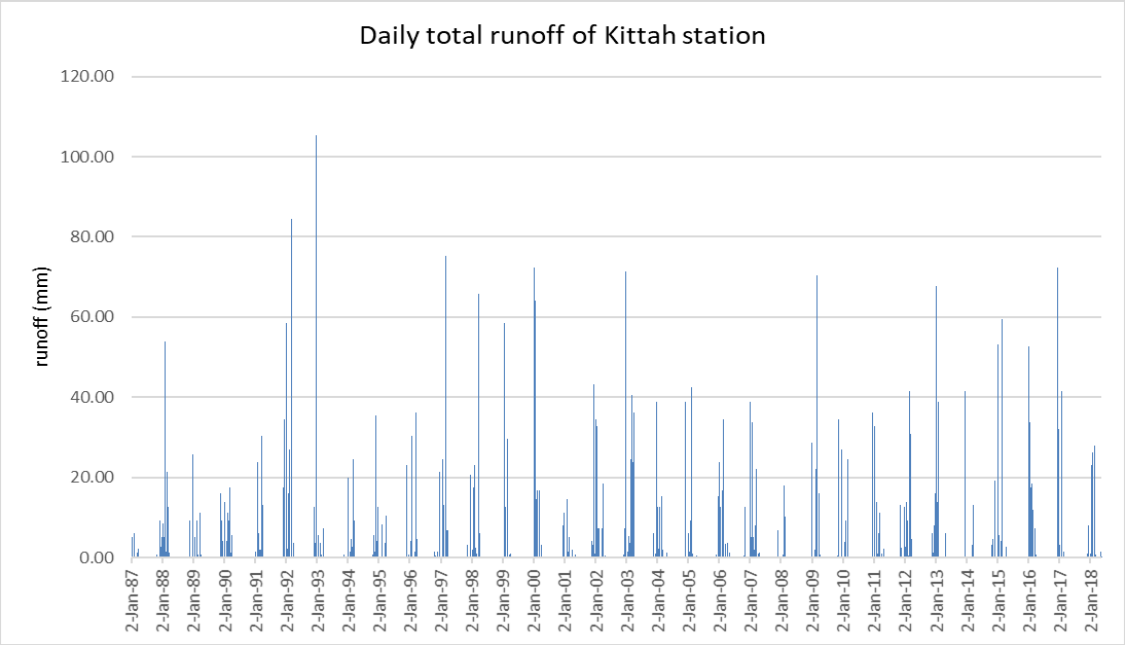

Figure 5.10. Daily runoff of Kittah station.

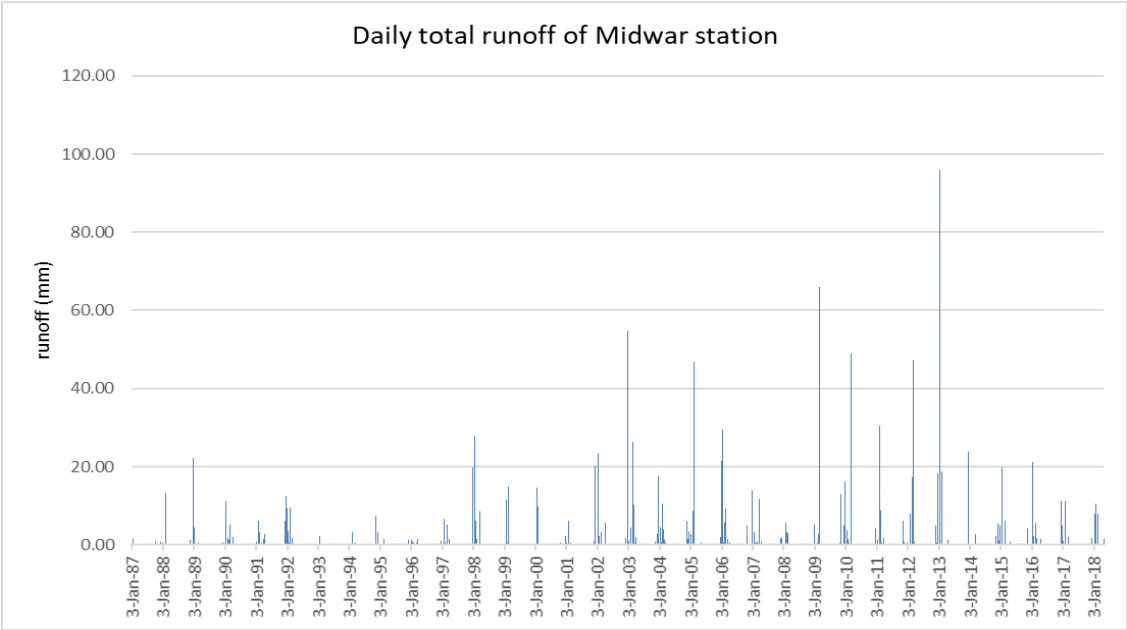

Figure 5.11. Daily runoff of Midwar station.

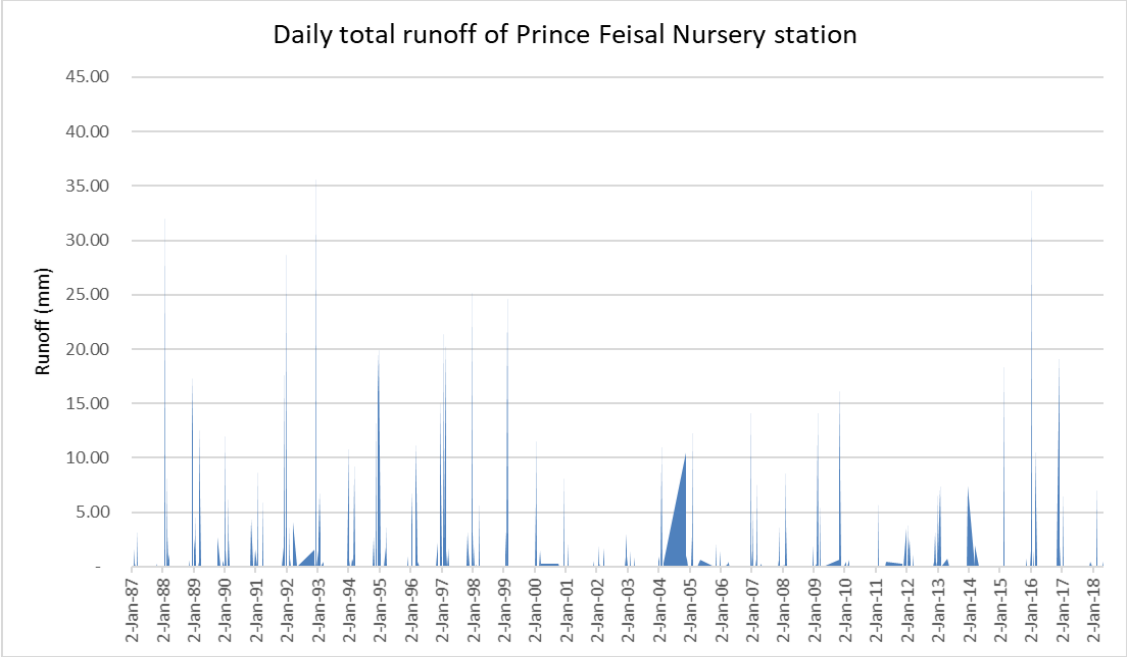

Figure 5.12. Daily runoff of Prince Feisal Nursery station.

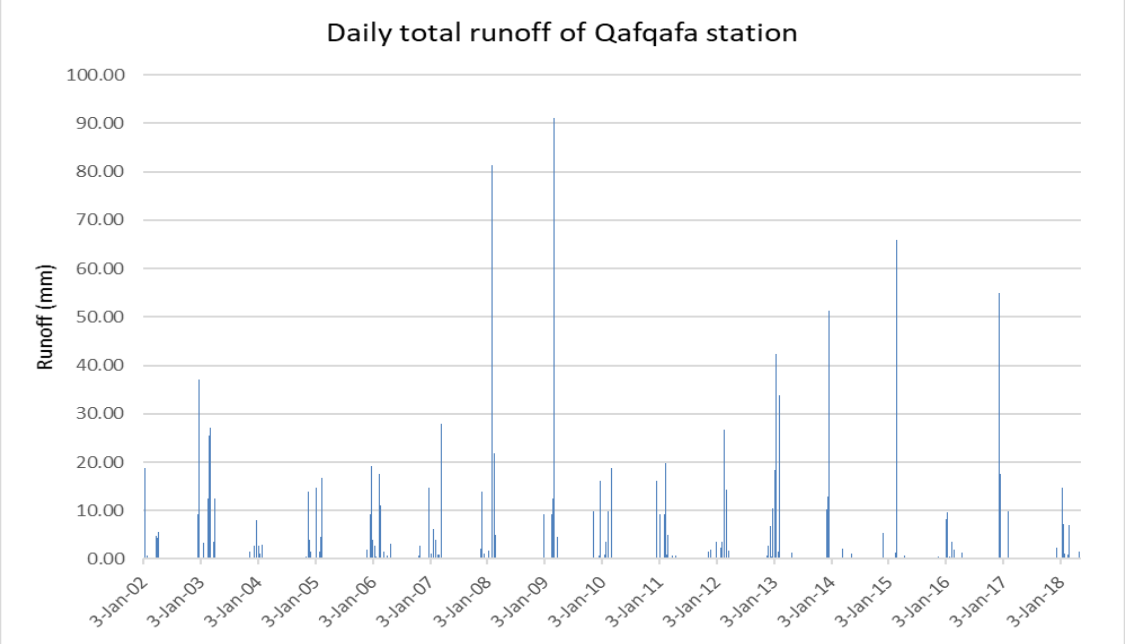

Figure 5.13. Daily runoff of Qafqafa station.

5.4.2. Monthly Runoff

As we noticed in the previous Figures (4.28, 29, 30, 31, 32, 33) that the months of January and February are the rainiest months of the year, and based on this thing, the months of January, February and December witness the largest amount of runoff, as for the rest of the months of the year, we notice that the rate of runoff is declining dramatically, as it is absent from the end of the spring season until the beginning of the autumn season. First, we calculated daily runoff for each station, after that we made a pivot table to get best results, then we organized the numbers to calculate the mean of runoff during each month for whole period (two of them were for 17 years and the rest were for 31 years) and this is what we will see in the next Figures (5.14, 15, 16, 17, 18, 19, 20). From Figure (5.14) we can see that the biggest value of runoff occurred in Ajloun station during February, January then December and this confirms what we talked about above.

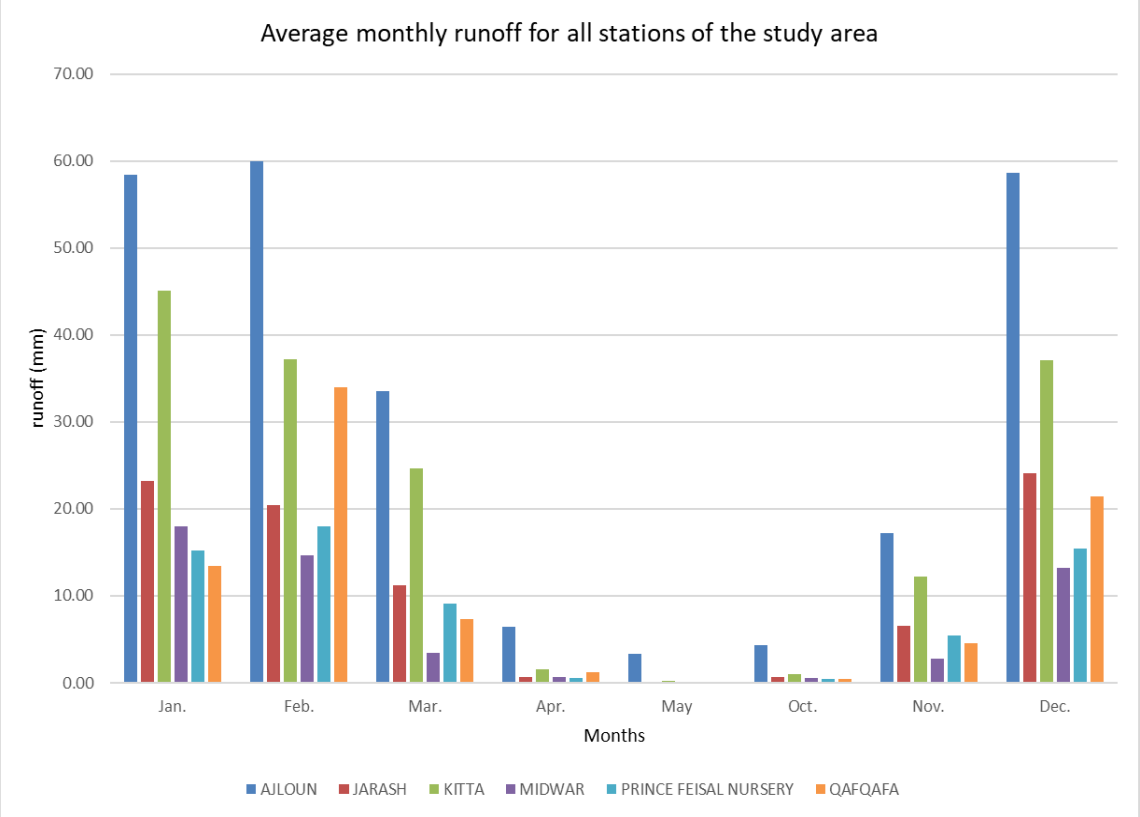

Figure 5.14. Average monthly runoff for all stations of the study area.

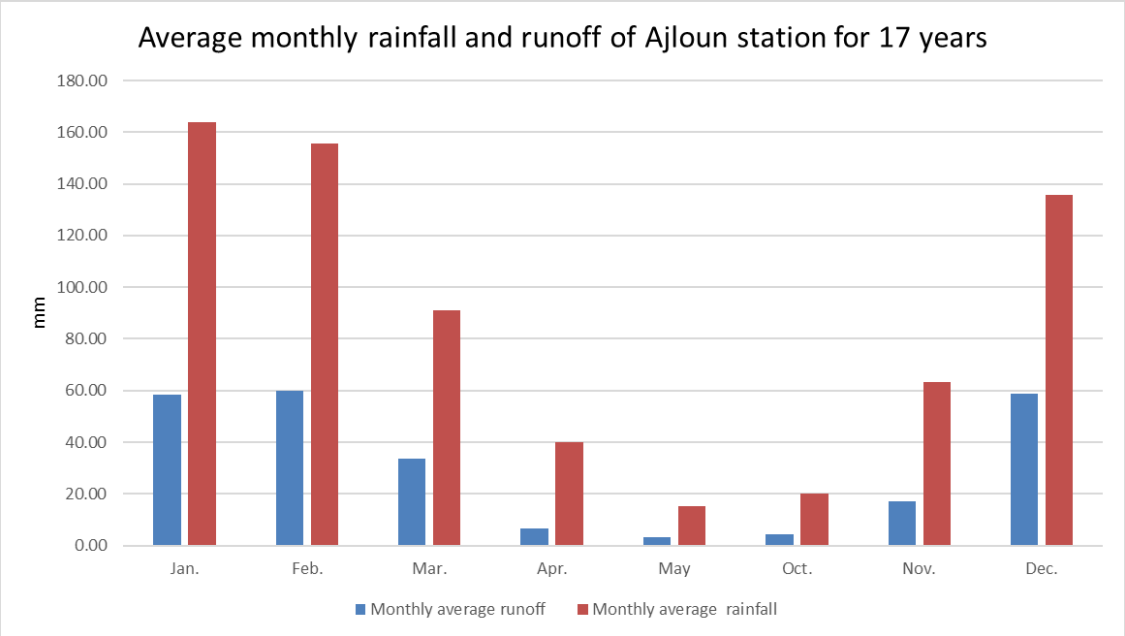

Figure 5.15. Average monthly rainfall and runoff of Ajloun station.

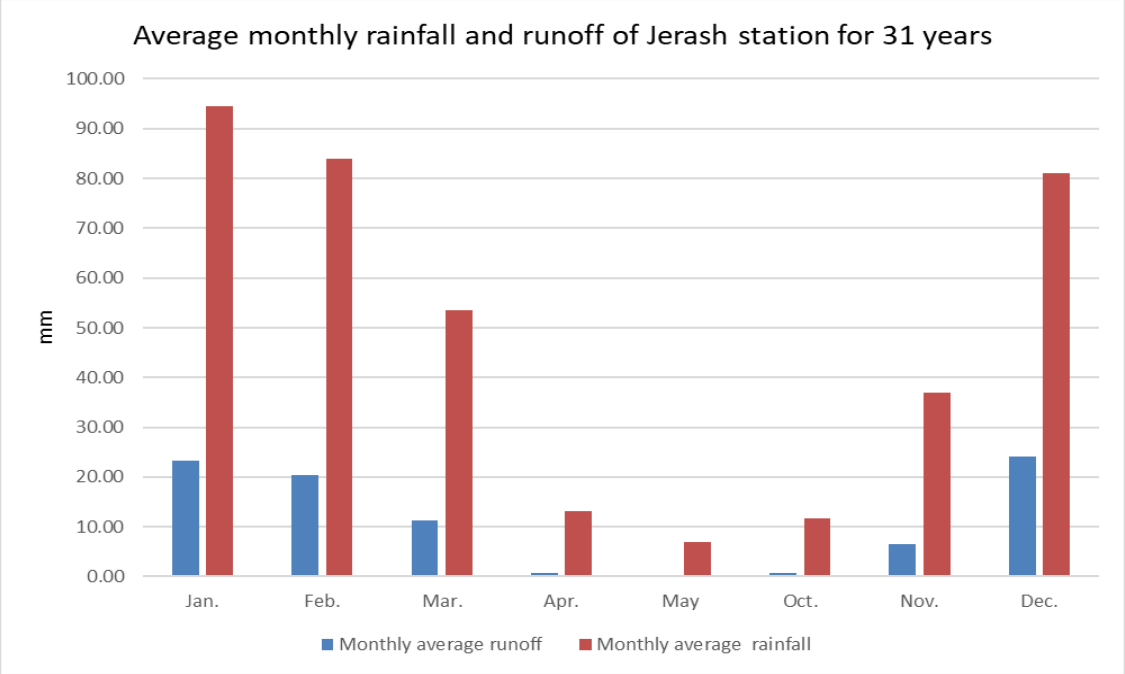

Figure 5.16. Average monthly rainfall and runoff of Jerash station.

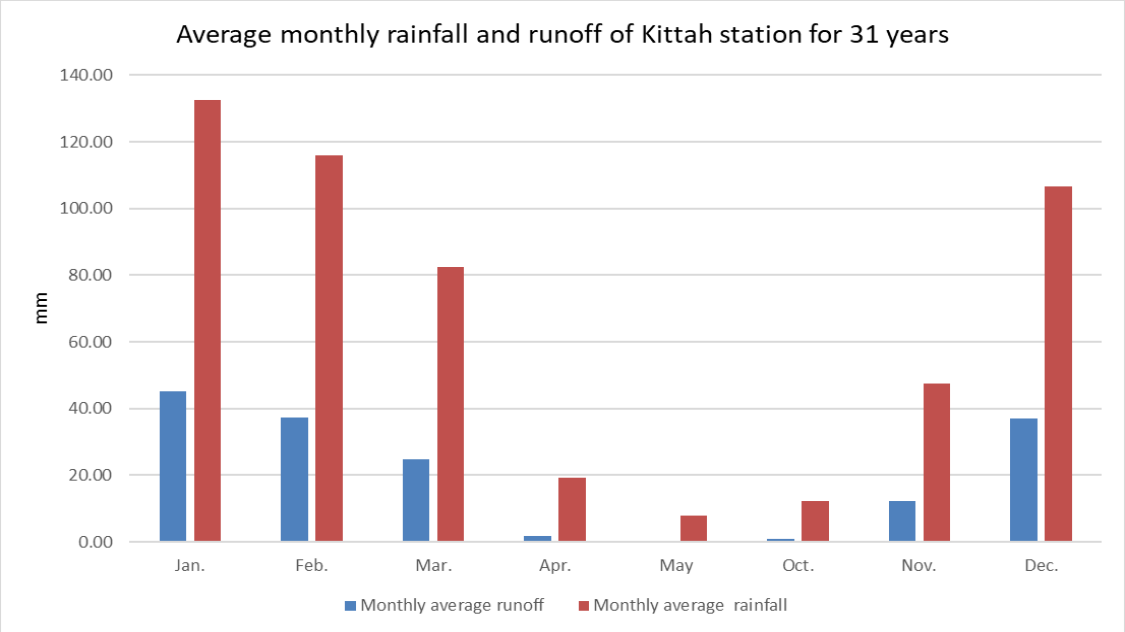

Figure 5.17. Average monthly rainfall and runoff of Kittah station.

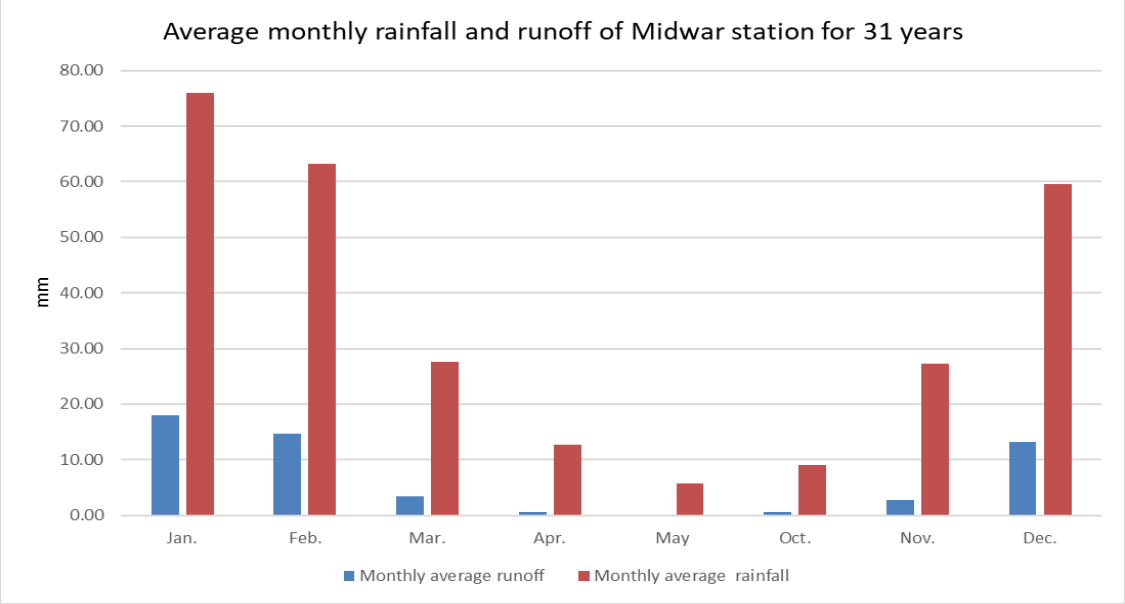

Figure 5.18. Average monthly rainfall and runoff of Midwar station.

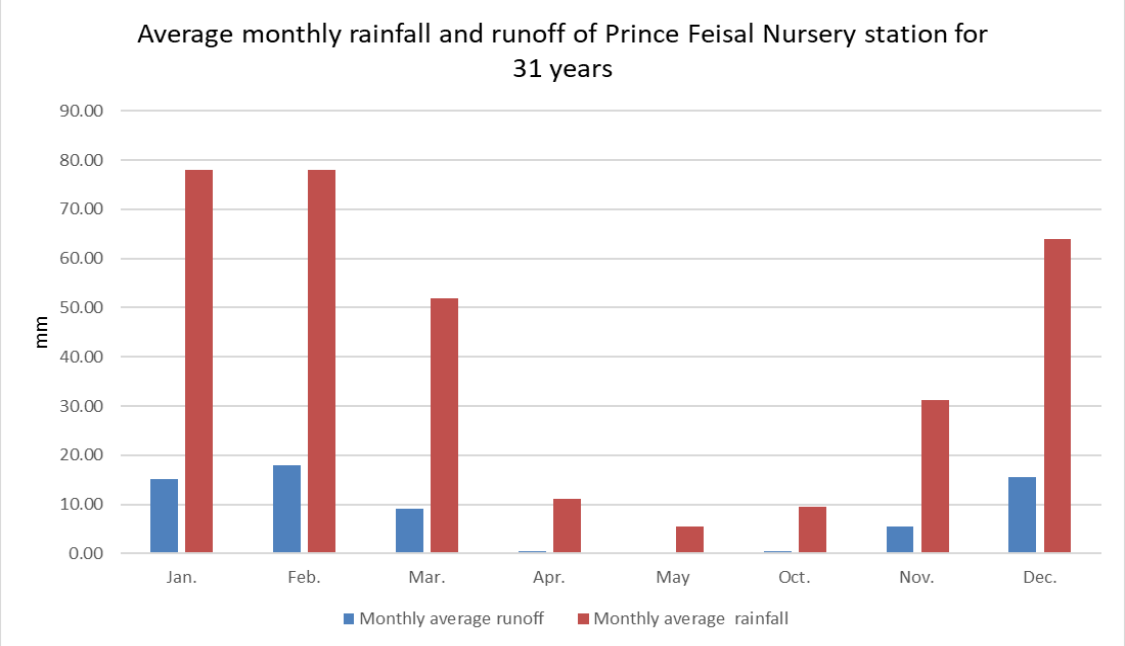

Figure 5.19. Average monthly rainfall and runoff of Prince Feisal Nursery station.

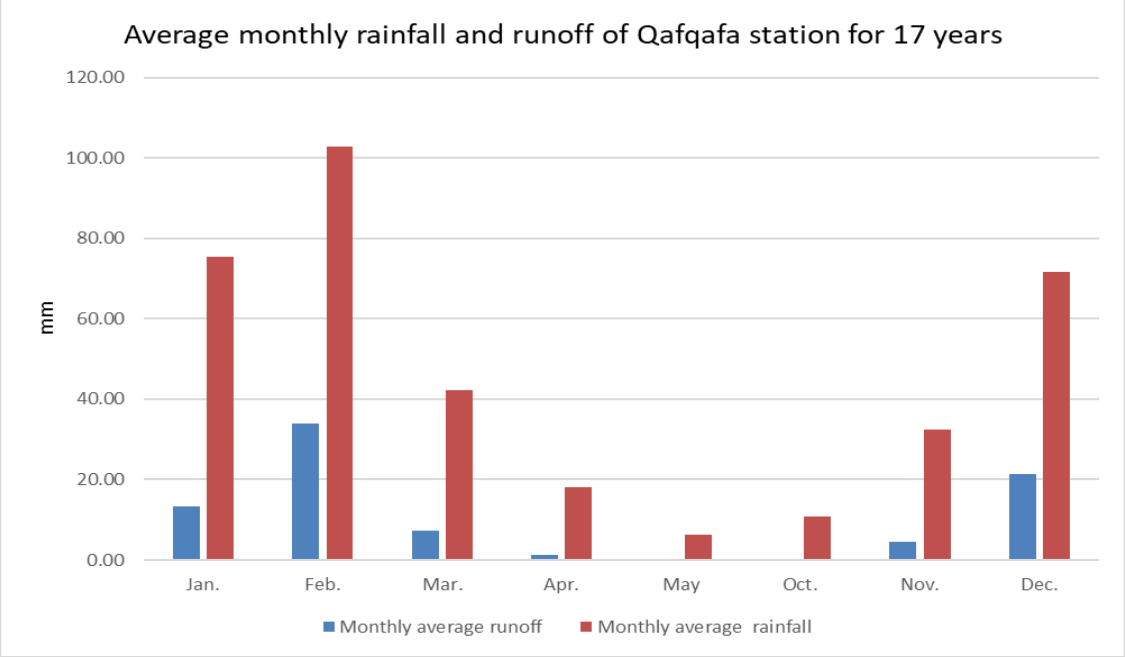

Figure 5.20. Average monthly rainfall and runoff of Qafqafa station.

5.4.3. Annual Runoff

Based on the data related to the annual amount of precipitation and the SCS law, we created figures showing the annual amount of precipitation, average precipitation for each station, the amount of runoff due to rain, average runoff, and the runoff coefficient % that is calculated from the following equation:

Runoff % = [Runoff (mm) / Precipitation (mm)] * 100 (5.7)

The following Figures (5.21, 22, 23, 24, 25, 26) show us that the amount of surface runoff approximates the amount of rain, and this is due to the curve number that guided us to the nature of the study area not conducive to absorbing water, from the figures we can see that the greatest values were from Ajloun station then from Kittah station, for Ajloun station the yearly runoff reached above of 300 mm where the lowest value for this station was a little bit under 100 mm, for Kittah station the yearly runoff reached to above 300 mm where the lowest value was about to be zero, in Table (5.11) we see the

total yearly runoff, max runoff for whole period and average yearly runoff for all stations in study area, and if look at Table 5.11 we can see that the max runoff was 393.37 mm and this number was recorded from Ajloun station, while the greatest value of average runoff was also from Ajloun station and these thing lead us to say that Ajloun station area deserve a huge amount of runoff because off amount of rainfall that fall.

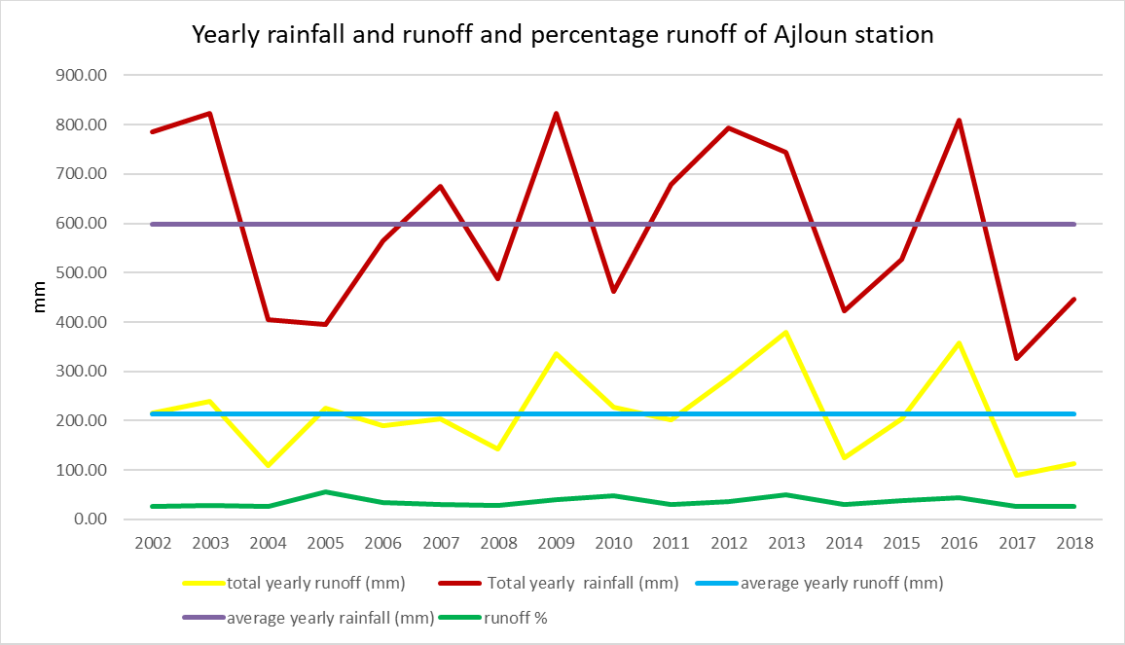

Figure 5.21. Yearly (rainfall and runoff) and runoff % of Ajloun station.

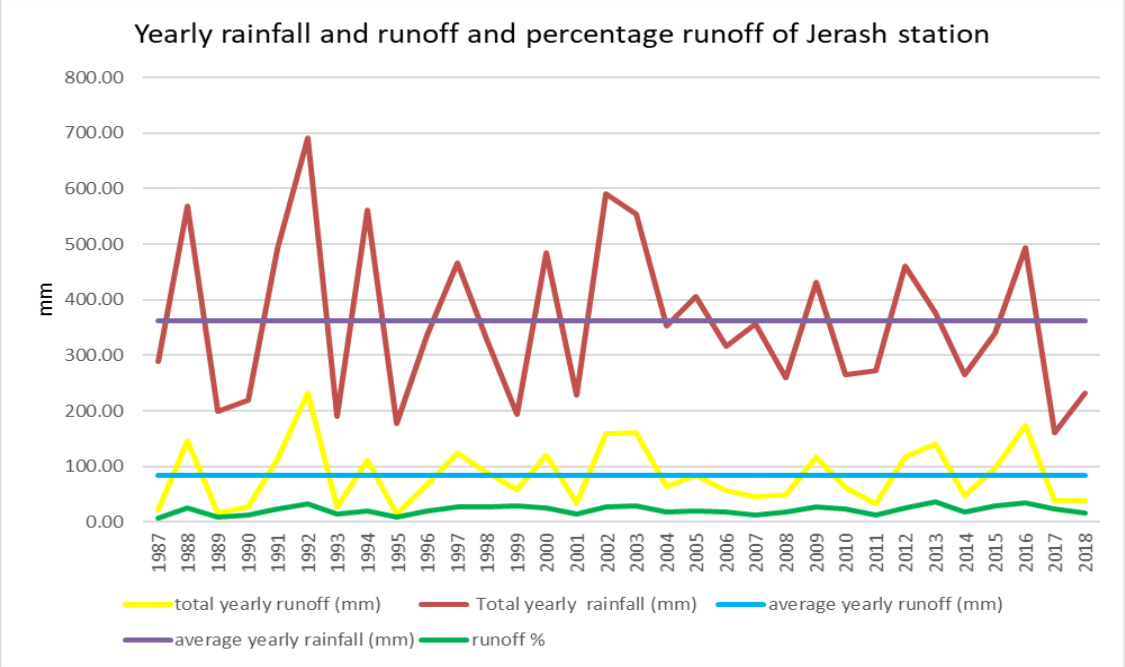

Figure 5.22. Yearly (rainfall and runoff) and runoff % of Jerash station.

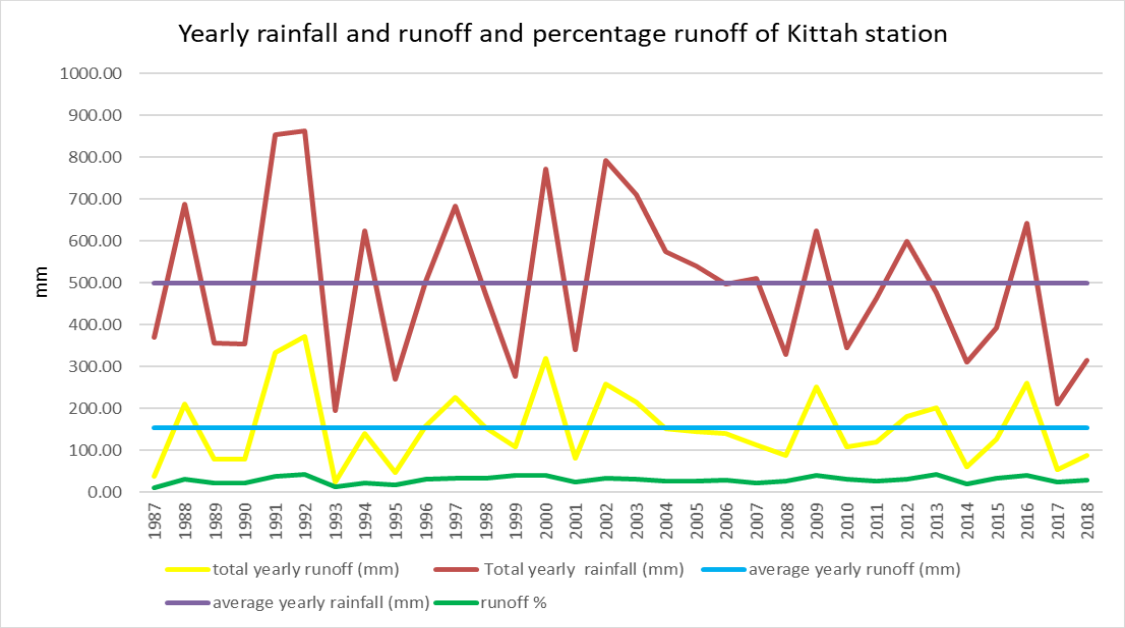

Figure 5.23. Yearly (rainfall and runoff) and runoff % of Kittah station.

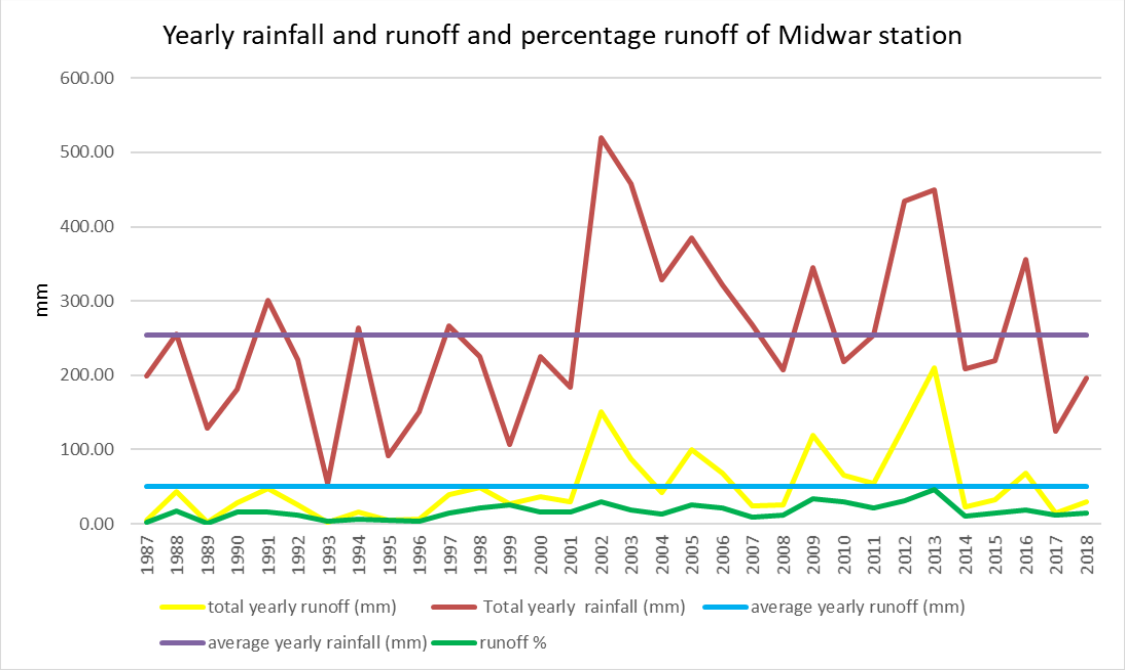

Figure 5.24. Yearly (rainfall and runoff) and runoff % of Midwar station.

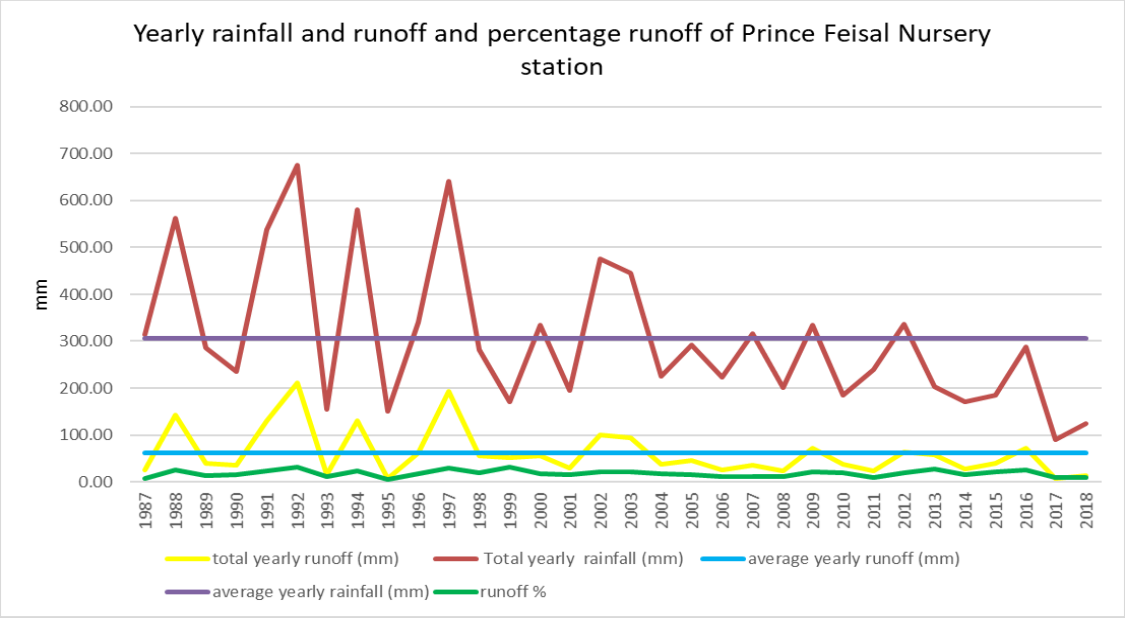

Figure 5.25. Yearly (rainfall and runoff) and runoff % of Prince Feisal Nursery station.

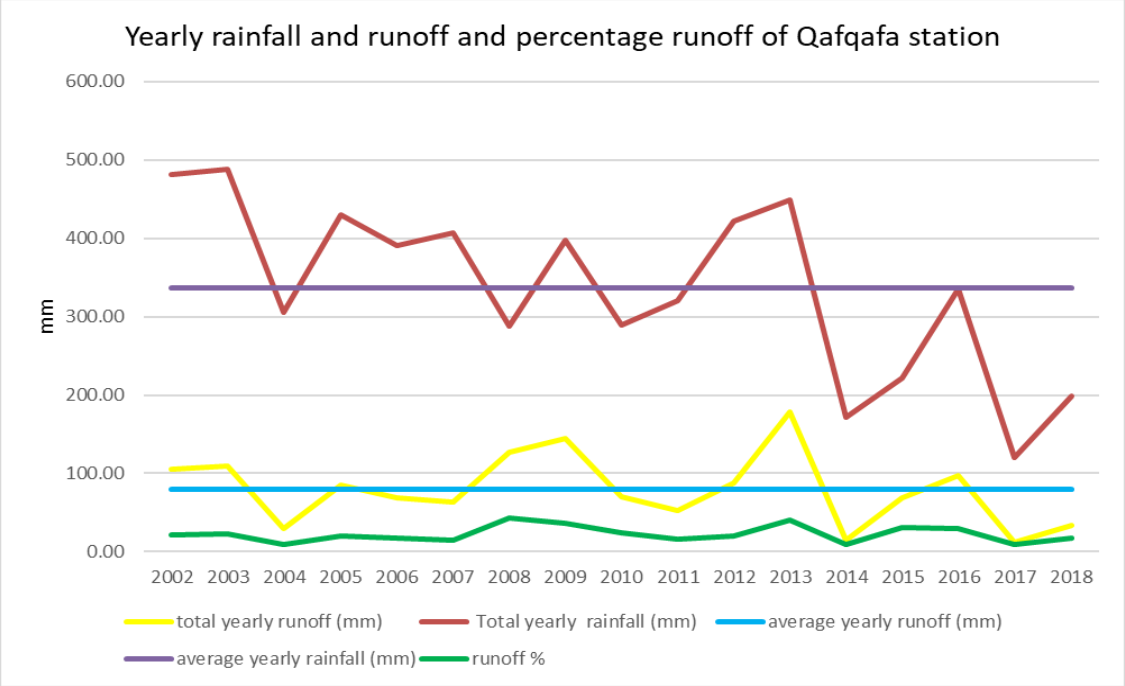

Figure 5.26. Yearly (rainfall and runoff) and runoff % of Qafqafa station.

Table 5.11. Total yearly runoff, average yearly runoff and maximum of yearly runoff for all stations.

Years	Ajloun (mm)	Jerash (mm)	Kittah (mm)	Midwar (mm)	Prince Feisal Nursery (mm)	Qafqafa (mm)
1987	*	22.28	38.36	5.64	25.46	*
1988	*	147.22	210.52	44.07	143.21	*
1989	*	16.54	79.83	1.95	39.53	*
1990	*	26.93	79.78	27.97	35.29	*
1991	*	114.30	334.42	47.98	130.34	*
1992	*	232.98	371.99	25.25	210.95	*
1993	*	27.86	23.95	2.25	16.03	*
1994	*	111.45	141.11	15.55	131.30	*
1995	*	14.70	47.99	4.30	7.80	*
1996	*	66.77	158.39	6.25	61.60	*
1997	*	124.88	227.60	38.91	193.90	*
1998	*	89.72	153.94	48.55	55.62	*
1999	*	57.63	108.95	26.89	52.39	*
2000	*	121.44	319.06	36.68	56.16	*
2001	*	34.10	80.18	29.54	29.67	*
2002	215.30	159.77	257.93	151.57	100.85	105.36
2003	240.06	161.63	214.52	88.23	94.72	109.81
2004	109.86	64.03	151.52	42.78	37.15	30.07
2005	225.21	84.77	144.21	100.18	45.71	84.64
2006	189.36	56.92	139.55	68.58	25.46	68.76
2007	203.21	46.44	112.77	24.43	35.59	62.85
2008	142.67	49.53	88.61	25.03	23.24	126.37
2009	335.81	117.38	252.79	118.89	71.68	144.43
2010	226.76	61.56	108.74	65.37	37.37	70.31
2011	202.32	33.72	119.69	54.49	23.82	53.05
2012	286.74	117.34	181.72	132.51	63.41	88.08
2013	379.37	140.66	202.79	209.63	57.66	179.00
2014	125.10	48.18	61.30	22.44	26.83	15.37
2015	204.45	97.58	127.65	32.28	40.51	68.51
2016	358.26	173.43	260.35	68.70	71.96	97.84
2017	89.53	37.91	53.55	15.19	7.77	12.19
2018	114.18	37.69	88.53	29.47	12.48	33.55
max runoff	379.37	232.98	371.99	209.63	210.95	179.00
average runoff	214.60	84.29	154.45	50.36	61.42	79.42

5.5. TIME OF CONCENTRATION

When it rains, the drainage area needs time to contribute to the runoff, or in other words it is the longest time that the water needs to move to the downstream point, and it depends mainly on the geographical nature of the watersheds (Perdikaris, Rudra, & Gharabaghi, 2018). As if we have rainfall and the duration of precipitation is little compared to with the drainage area, then we can guess the value of the concentration time as the time that starts with the excessive amounts of rain until the turn is reached. And to calculate we can use many formulas and one the mostly used is (Kirpich, 1940)formula which is:

$$Tc= \frac{L^{0.77}}{S^{0.385}} \text{ x } 0.0078; \quad (5.8)$$

Tc: time of concentration (minutes)
L: travel length (km)
S: slope;

As for the lag time: Mathematically, it represents 3/5 of the concentration time. In theory, it is the time between the center of mass of the unit pulse rain and the peak of the hydrograph, and it is calculated by this formula:

$$tI = 0.6 \text{ x } Tc; \quad (5.9)$$

tI: lag time

Because of WMS gave us the lag time which is 1.75 hr so this value leads us to know that we can use Formula (5.10) to calculate Tc

$$Tc= 1.67 \text{ x } tI \quad (5.10)$$

Tc = 1.67 x 1.75 hr

Tc= 2.9 hrs., 175 minutes

And Figure (5.27) shows us what is the difference between lag time and time of concentration, and it shows us where is lag time located on graph, as we see that lag time is located between starting of exceeding precipitation and peak of discharge.

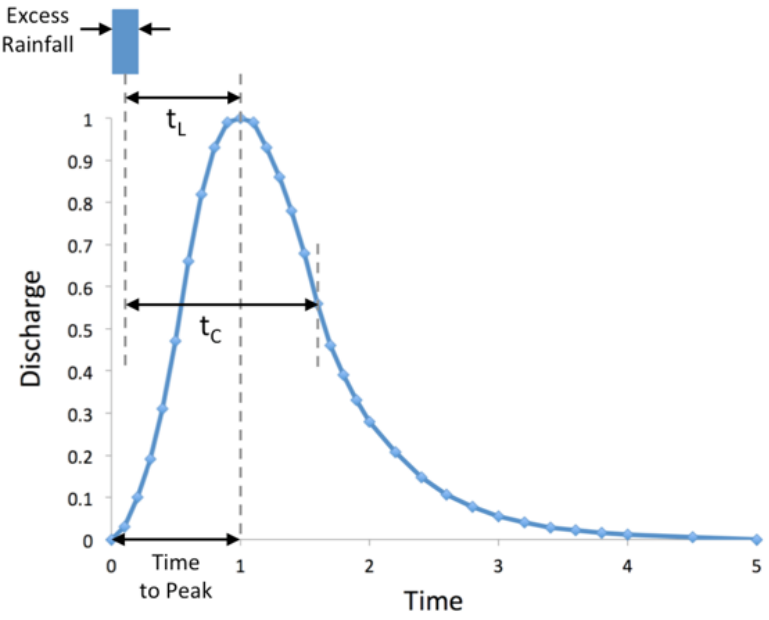

Figure 5.27. Difference between lag time and time of concentration.

5.6. RUNOFF FREQUENCY ANALYSIS

Runoff frequency analysis depends on the use of monitored peak flow discharge data in order to perform calculations on the statistical data. The runoff frequency analysis is one of the most important steps during the modeling process and is used to understand the hydrological behavior of discharges. (MLYNSKI, PETROSELLI , & WALEGA, 2017) In the absence of surface runoff records or insufficient data for the statistical analysis process, surface runoff frequency analysis is used as a way to complete the process of calculating the recorded data for the daily precipitation of the water year.

This method is considered easy in order to deal with the peak rate of runoff and design the hydrograph from the watershed that is not large so that its area does not exceed 5 square miles. The main causes of floods are the type of vegetation cover, vegetation cover, and the topography of the area. By following this method, we can take advantage of the design graph definition as we can determine the total rainfall, and based on this method we can design simple hydraulic structures, and In Figures (5.28, 29, 30, 31) we see the hydrographs that we got from WMS by entering the information that we organized before in Tables (5.2, 3, 4, 5, 6, 7).

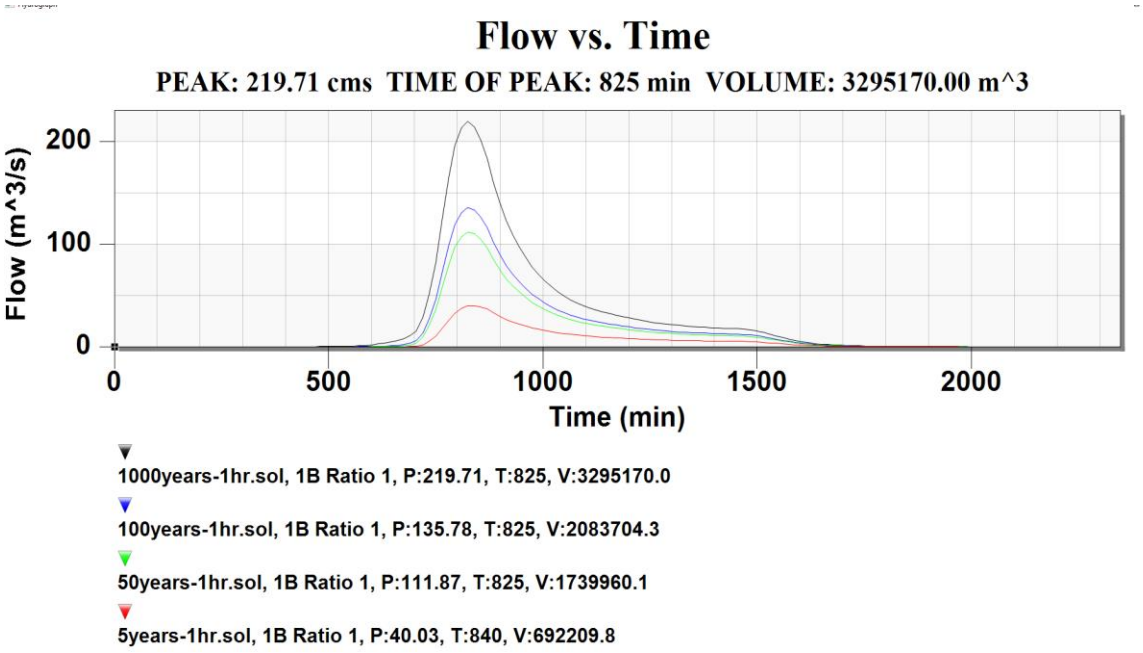

Figure 5.28. The 1-hour hydrograph of the of the different return periods.

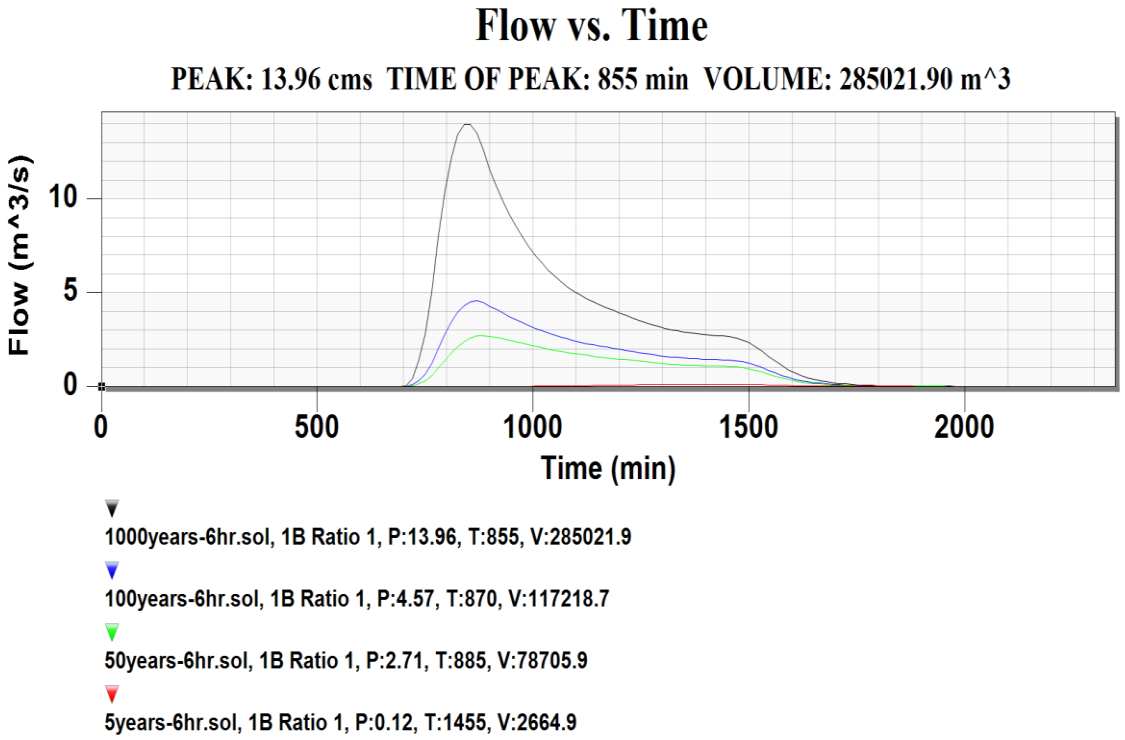

Figure 5.29. The 6-hours hydrograph of the of the different return periods.

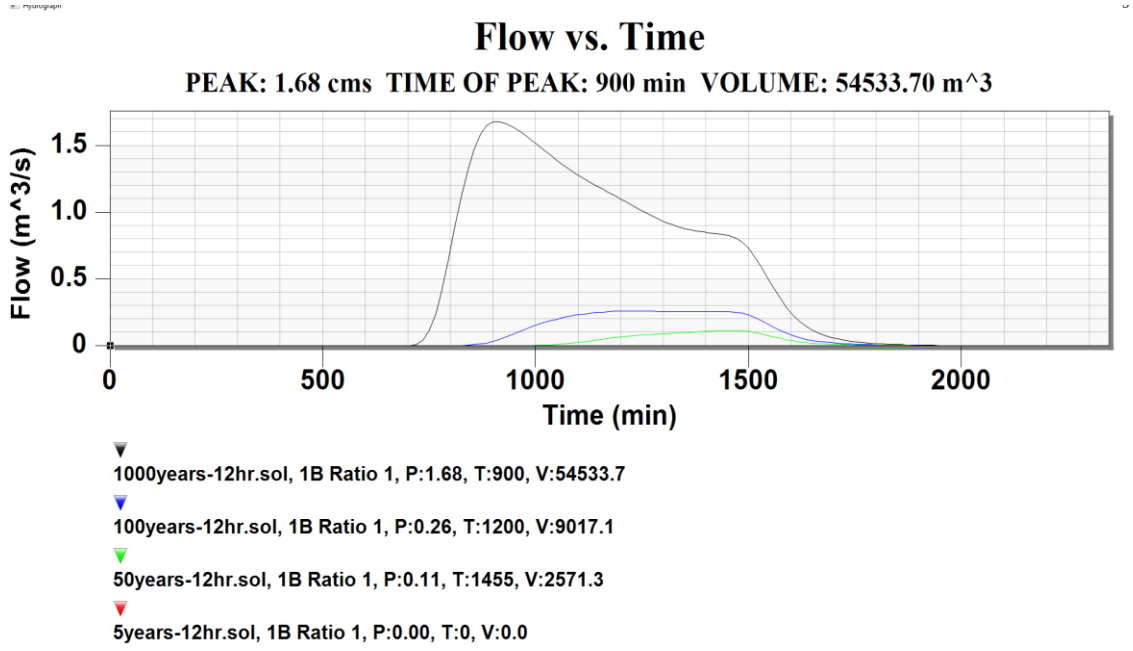

Figure 5.30. The 12-hours hydrograph of the of the different return periods.

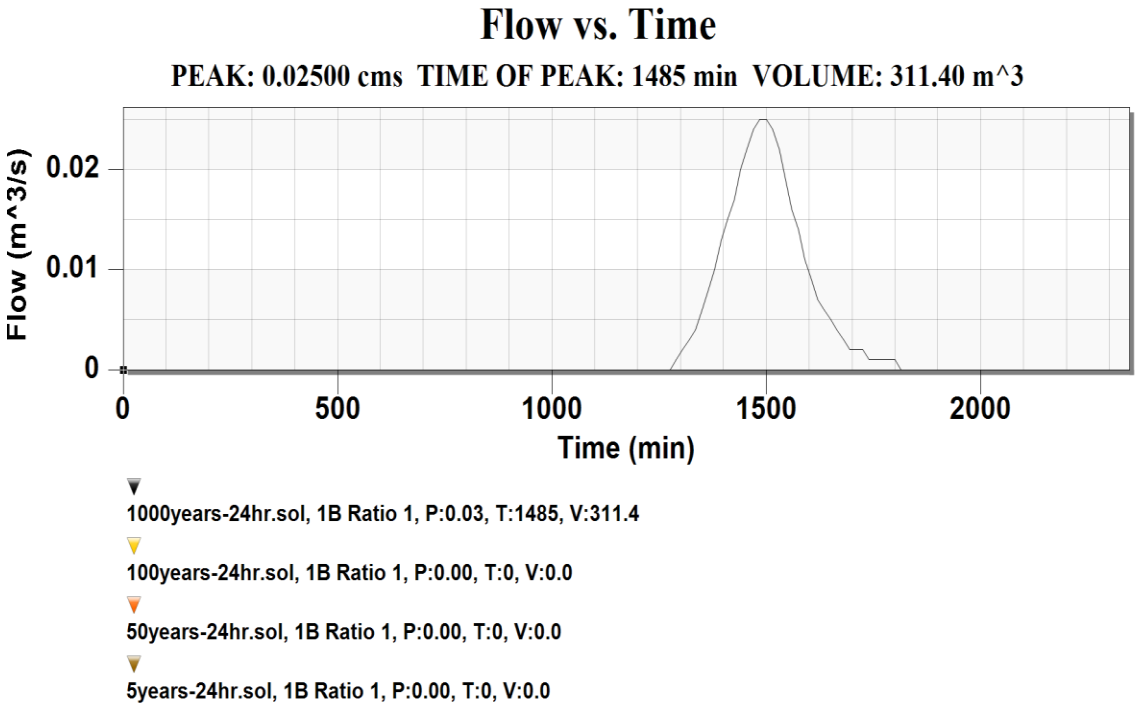

Figure 5.31. The 24-hours hydrograph of the of the different return periods.

5.7. ACCURACY OF METHOD

Through the Jordanian Ministry of Irrigation and Water, we obtained the volume of the floods that occurred during the years 2019 and 2020 in order to ensure that the theory followed during the study is valid or not.

On 27/12/ 2019, a flood occurred in the Jerash Basin area, and the volume of the flood was 765,211 cubic meters, and the duration of the flood until it receded was approximately 23 hours, and by following the same previous steps and replacing the previous precipitation values with the precipitation values that occurred on 27/12/2019, where We get the following Figure 5.32:

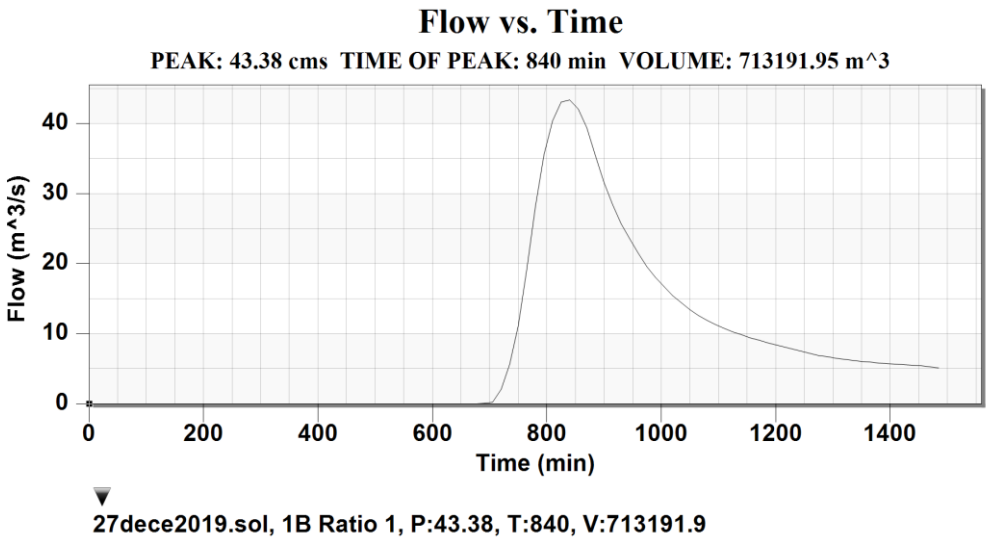

Figure 5.32. Calculated flood on 27/12/2019 by WMS.

In the Figure 5.32 we can see that the volume of the flood was 713191.95 cubic meters, but this value includes only the values of rain, and accordingly we add the volume of water flowing through the ground and surface water as shown in Table 2.1 on the surface and ground flow, where we applied the equation to get the accuracy rate of the WMS program:

$$\frac{\mathrm{Ve} + (\mathrm{B} \times \frac{\mathrm{T}}{60})}{\mathrm{Vr}} \times 100 \qquad (5.11)$$

Ve: Volume from WMS (calculated)

B: Base flow

Vr: Recorded volume (real volume)

T: Duration of flood in min

$$\frac{713191.95 + (310.2 \times \frac{1550}{60})}{765211} \times 100 = 94.2\%.$$

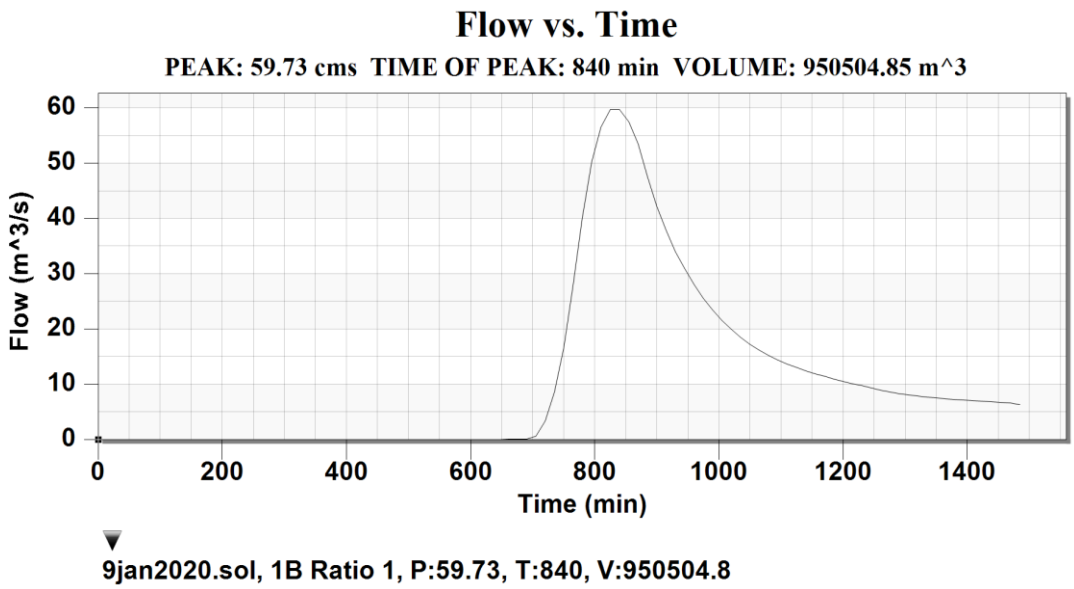

Figure 5.33. Calculated flood on 09/01/2020 by WMS.

On 09/01/2020, as we see in Figure 5.33 a large flood occurred in Jerash, the volume of which was estimated by Jordanian government at 1010220 cubic meters, and it lasted for 24.5 hours. Using the same method, we find that:

$$\frac{Ve + (B \times \frac{T}{60})}{Vr} \times 100$$

Ve: Volume from WMS (calculated)

B: Base flow

Vr: Recorded volume (real volume)

T: Duration of flood in min

$$\frac{950504.85 + (310.2 \times \frac{1560}{60})}{1010220} \times 100 = 94.88\ \%$$

Accordingly, the WMS software and based on the previous parameters (soil type, land use, curve number, concentration time), we can rely on the WMS software in our study because it gave us a similarity rate in both cases more than 94%.

5.8. COMPARISON BETWEEN THE CURRENT FLOODS AND THE EXPECTED FLOODS

Relying on 12/27/2019 and 09/01/2020, we will verify that WMS provided us with correct predictions based on the values we obtained from the Jordanian Ministry of Irrigation and Water.

On 27/12/2019, a flood occurred with a volume of 765,211 cubic meters (precipitation, surface and underground flow), and the WMS software provided us during the hydrograph with a value close to it and it was 874,406 cubic meters (rainfall), and therefore we apply the following equation to make sure that The software has correctly predicted the flood:

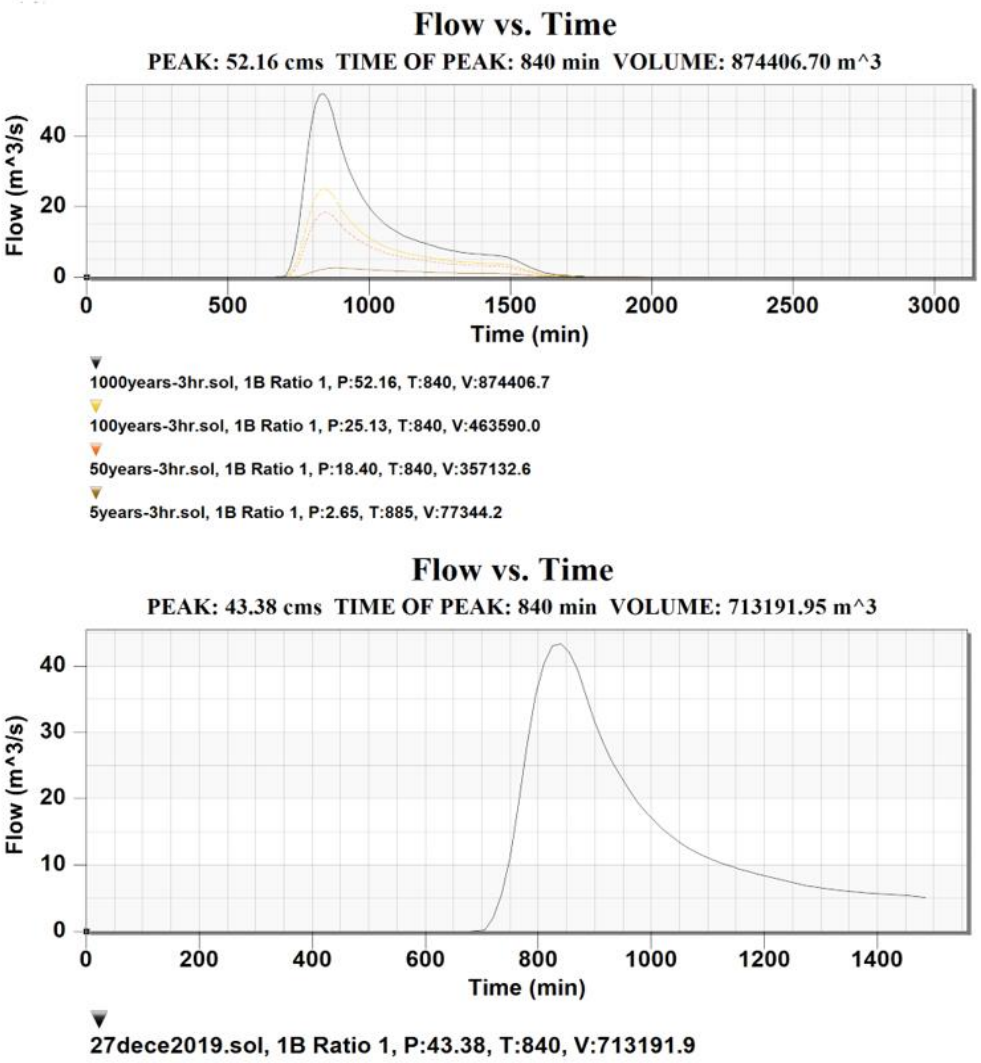

Figure 5.34. Relation between estimated flood and occurred flood (27/12/2019).

$$\frac{\mathrm{Vr}}{\mathrm{Ve}+(\mathrm{B}\times\mathrm{T})}\times 100 \qquad (5.12)$$

Vr: Recorded volume (real volume)

Ve: Volume from WMS (estimated)

B: Baseflow

T: Duration of flood in hr

$$\frac{765211}{874406.7+(310.2\times 29.167)}\times 100 = 86.26\ \%$$

Based on the result we obtained and Figure 5.34, the flood formed 86.62% of the expected flood, and accordingly, WMS provided us with a flood greater than the amount and this is what we want to get, as we want to get the largest possible flood even Official authorities are able to handle matters in emergency situations.

On 09/01/2020 another flood occurred and its volume was 1010220 cubic meters. As for the WMS software, it gave us the value of 950504.85 cubic meters without the ground and surface flows. On the same principle as before, we will make sure that the WMS software provided us with what is It might happen in the future.

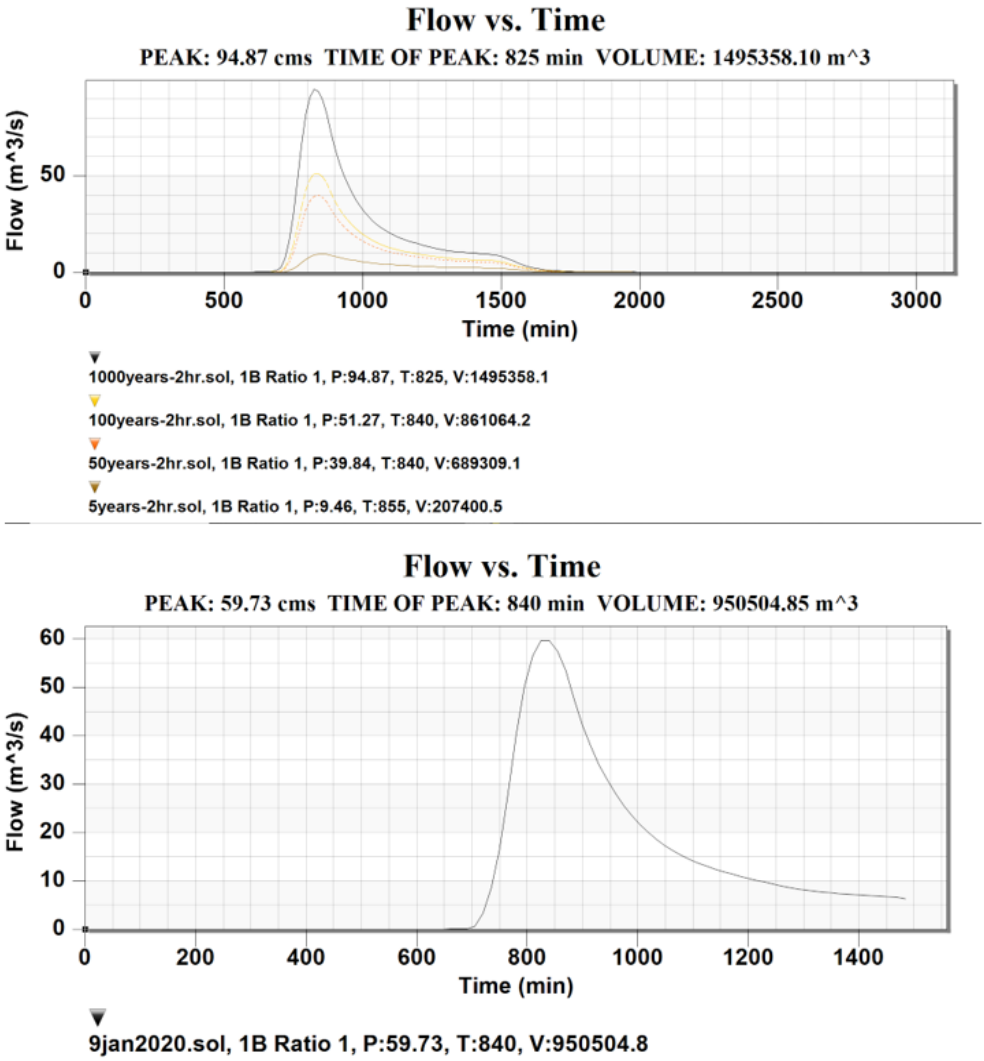

Figure 5.35. Relation between estimated flood and occurred flood (09/01/2020).

$$\frac{Vr}{Ve+(B\times T)}\times 100$$

Vr: Recorded volume (real volume)

Ve: Volume from WMS (estimated)

B: Baseflow

T: Duration of flood in hr

$$\frac{1010220}{1495358.10+(310.2\times 29.167)}\times 100 = 67.16\%$$

By comparing the two graphs in the Figure 5.35, we find that the real flood that occurred on 09/01/2020 was equal to 67.16% of the value of the expected flood from WMS software, and accordingly WMS based on the rainfall values in previous years had expected the occurrence of A flood worse than the flood that occurred on this date, which is what we want to get, as we want to know the worst things that can happen to avoid many physical and human damage.

These Figures done by WMS by applying Theissen polygon method as we chose and we can see it in Figure 5.36.

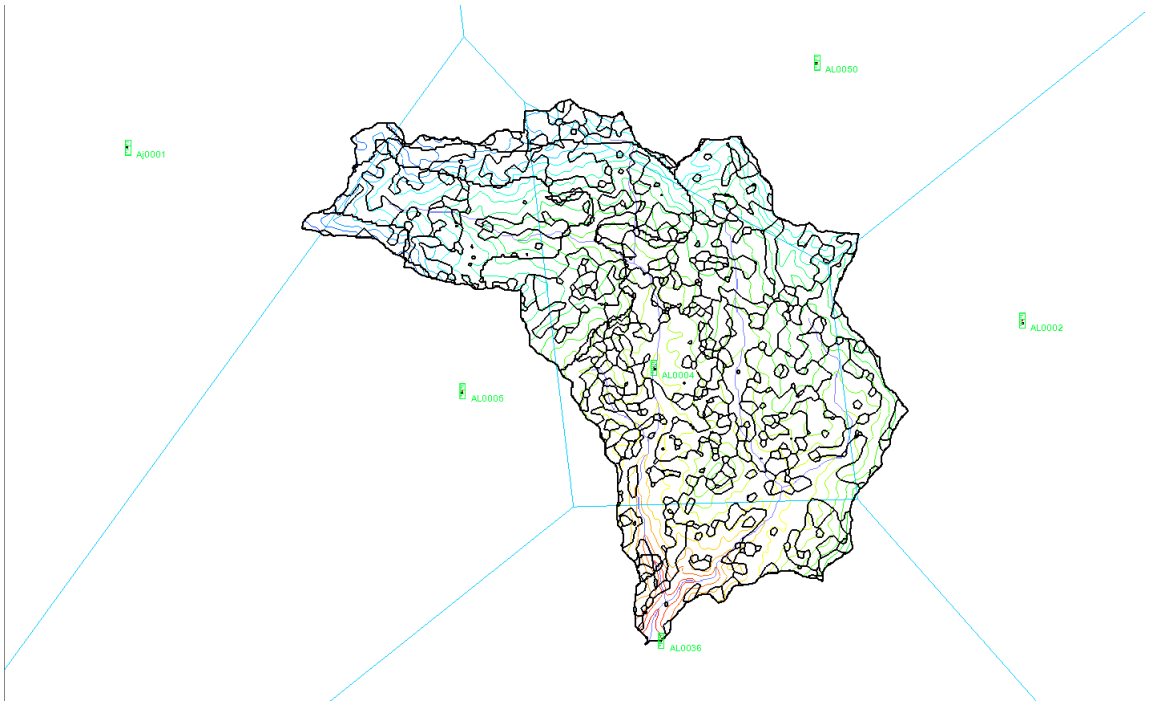

Figure 5.36. Theissen polygons done by WMS.

PART 6

RESULTS

Jordan constitutes the southeastern part of the Levant, meaning it is the link between the Levant, which has a moderate Mediterranean climate, and the Arabian Peninsula, which has a dry desert climate. As for the study area, it is located in the northwestern part of Jordan, which makes it closer than other Jordan to the Mediterranean Sea, and thus It is characterized by a moderate Mediterranean climate, which is characterized by the winter rains extending from October to May.

The study area is characterized by its diversity in heights, as its lowest point reached 261 meters south of the study area, and its highest point was 1268 in the north and north-east, which helped in the occurrence of floods in the past years, as the downstream point is located to the south of the study area. This means that the water flows from north to south due to the difference in elevations and its direction from the highest point to the lowest point.

Based on the data that came from the Jordanian MWI, we have noticed an increase in the average temperature in the last twenty years during the summer months, while during the winter months it did not rise only slightly, and January was the month with the lowest temperatures, reaching lower during the day from seven degrees and at night to less than 3 degrees, and the month of August had the highest temperatures, with the average temperature being above 30 degrees. According to the (IPCC, 2013)report, the increase in precipitation in the winter comes due to the increase in the rates of natural temperatures, as due to the high temperatures that occur, it increases the evaporation process and because of the ability of the air to retain water particles, and thus the precipitation increases, which is the first factor at the beginning of the flood path. Thus,

we will have a good and well-known way to reduce the phenomenon of sudden floods by following the environmental rules and limiting everything that affects the rise in temperatures, and this is what explains the occurrence of many floods in the city of Jerash without warning.

The area of the study area was 101 square km and the study was based on the data coming from the six rain stations (Ajloun- Jerash- Kittah- Midwar- Prince Feisal Nursery- Qafqafa) and it was divided as in the next table, as each station covered a point related to the study area, where the Jerash and Prince Faisal nursing stations were within the study area and the Kittah station was south of The study area and the Ajloun station east of the study area, while the Medawar and Qafqafa stations were north of the study area, where the average annual precipitation for Jerash and Prince Faisal stations was (333.77 mm/year, 498.9 mm/year), and in view of the Ajloun station, although the available readings started in 2002, it had the highest average, which could be a reason for the increase in the intensity of the water current during the floods, as we said by virtue of the movement of water from the north to the south.

According to what (Zregat, 2014) found, she said that the percentage of agricultural lands in Jerash Governorate in 2009 was 48%, and thus the percentage of agricultural lands increased after it was 33% in 2009, where agricultural lands were concentrated in places whose height is between (500 -1000 m) Its decline is between (3-18%) due to government legislation that recommends increasing the area of agricultural land in an attempt to confront the threat of desertification that threatens large lands in Jordan, and taking into account the increase in the area of agricultural land increases the air humidity.

By looking at the hydrological soil classification for the study area, we realize that the study area is located in classifications D and C, which gives the study area the advantage that it is not drainable, but it is a suitable environment for the occurrence of floods, as the classification D is characterized by the permeability of (1.8 mm / hour). Classification C is characterized by its permeability (1.56-4.34 mm/hour), which is why

the soil of the study area was (silty clay and loam, Silty clay and clay) and based on the WMS program, we used our land use map and soil map We can now find the curve number, which was approximately 88, where the values of the curve number are between 0-100, when the value of the curve number is 0, this means that the permeability of the earth is large and it is difficult for the runoff to occur in it, and when the value of the curve number is 100, this means that the permeability of the earth few and the possibility of a very large run-off.

Relying on the curve number, we calculated IDF for all stations for a period of 5-10-20-30-60-120-180-360-720-1440 and each for a return period of 2-5-10-25-50-100-1000 years for each A station and on the basis of it we prepared the Figures (5.2, 3, 4, 5, 6, 7), and by checking the Tables (5.2, 3, 4, 5, 6, 7) we find that there is a relationship that with the increase in the return and time periods, the height of the water will increase in the different cross-sections studied in the catchment area water.

After taking the initial abstraction into consideration, we calculated the runoff rates for each station daily, monthly, annually, and the highest rates were coming from Jerash station, where the average yearly surface runoff is (214 mm/year) then followed by Kitta station (154.45 mm/yea)r, and the highest rates were recorded The value of surface runoff is (379.37 mm/year) this value represents the annual surface runoff, but the hydrological life in Jordan begins in October and ends in May, and this means that the surface runoff is distributed over 8 months per year only and not over 12 months.

We also relied on WMS to find the curve number. The program helped us calculate the delay time, which was 1.75 hours. We also found the time of concentration, which we extracted from WMS, and it was (2.9 hours) which corresponded to the practical calculation of it, as it had the same value of (2.9 hours). Through the WMS program, and by entering both the time of concentration and the lag time, with the IDF we got what we were looking for, which is the amount of peak flow when the surface runoff will start and how long it will take until it reaches its peak, which we will mention in detail below, which we will mention in detail below.

In Figure (5.28) we can see that the time required to start the special runoff for the duration of the frequency intensity of 1000 years – 1hr was approximately after 600 minutes, and that the time required to reach the peak was 825 minutes, while the peak was 219.71 cubic meters per second, the volume of runoff was 3295,170 cubic meters, and the runoff ends after 1700 minutes.

Figure (5.29) shows that the time required to start the special surface runoff for a period of frequency intensity 1000 years - 6 hr. was after 725 minutes and that the time required to reach the peak is 855 minutes, while the peak was 13.96 cubic meters per second, the volume of runoff was 285021.9 cubic meters, and the runoff ends after 1700 minutes.

Figure (5.30) shows that the time required to start the special surface runoff for a period of frequency intensity 1000 years - 12 hr. was after 600 minutes and that the time required to reach the peak is 900 minutes, while the peak was 1.68 cubic meters per second, the volume of runoff was 54,533 .7 cubic meters, and the runoff ends after 1700 minutes.

Figure (5.31) shows us that the time required to start the surface runoff for a period of frequency intensity 1000 years - 24 hours was after 1290 minutes and the peak is 1485 minutes, while the peak was 0.025 cubic meters per second, the volume of runoff was 311 .4 cubic meters, and the runoff ends after 1800 minutes.

WMS provided us with the graph 5.32, and we obtained from it that the volume of the flood that occurred on 27/12/2019 was equal to 713191.95 cubic meters, knowing that the real flood that occurred on this date was equal to 765,211 cubic meters and when we entered this number into the equation 5.11, we concluded that the accuracy of the WMS software was equal to 94.2%, and accordingly we were able to make sure that the software provided us with a figure that is as close as possible to the flood that occurred in this period, and the same applies to the 5.33 graph of the flood that occurred in 09/ 01/2020, where the software with equation 5.11 was able to provide a working accuracy of 94.88%.

When we compared the expected floods with the floods that occurred in the period after the rainfall readings, we got that the software provided us with more devastating floods than the floods that occurred, which we got when we applied equation 5.12, based on graphs 5.34 and 5.35 because in Such a pattern of studies always seeks to find out what are the worst floods that can occur, so that the official authorities concerned with these matters can take the necessary precautions in the event of sudden floods to avoid catastrophic consequences.

PART 7

CONCLUSION AND RECOMMENDATIONS

7.1. CONCLUSION

When looking at the digital elevation model in Figure (3.3), we find that the difference in elevations between the northeastern and northern regions with the southern region, we note that there is a difference in altitudes about 1000 meters, which explained the existence of a difference between the average of the northern and southern rain stations, as the difference that was between the Ajloun station and the Prince Faisal Nursery station is 293 mm/year due to the difference in heights between the two areas as mentioned above.

During the period of global warming, the average temperature increased throughout Jordan, including the study area, which helped to increase the evaporation rates. When rainstorms occur, the amount of rain increases due to the water evaporated by the temperature.

After looking at the Figure (3.1), which represents the map of Jordan that we obtained from the University of Jordan in the Department of Geography, we found that the study area is divided into two parts, a southern and a northern section, the southern section consisting of the soil of Jerash, which is soil (clay loam and clay) and a northern section consisting mostly of soil (clay and silty clay), and according to the characteristics of (clay and silty clay), it is considered a porous soil, but it is of little permeability. As for the soil of clay, it is characterized by having small pores and its drainage of water is very slow, and this is one of the reasons why water does not seep quickly into the ground during the period of rainstorms.

After analyzing land use map, we note that the areas of agricultural land with tree crops control a large proportion of the area of the study area and throughout, and the urban fabric are concentrated in the south of the study area, which is the same as what (Zregat, 2014) spoke about, however, the increase in the urban invasion of agricultural land It still poses a threat to Jordan, as the urban growth rate in Jerash in 2009 compared to 1952 amounted to about 608%, which is not a small number at all, as most of the urban growth was at the expense of agricultural lands, which will contribute in the future to the exacerbation of global warming.

From IDF chart, we note that the frequency of long storms is less than the incidence of short storms, by following the formula of Gamble type I. Ajloun station had the highest rainfall rate, due to its mountainous nature and being higher than the study area. It is considered the first resort in Jordan, as it is a mountainous city, with mild weather in summer. Relying on the map of soil characterization and the map of land use in the WMS program, we calculated the curve number, which is considered the best description of the nature of the area during the period of rainstorms, where the curve number was equal to 88, which means that the permeability of the study area is very small, which was a major reason for the occurrence of flash floods as the initial abstraction was 6.96mm. Since the initial abstraction of the study area is 6.96 mm, this means that any precipitation rate that is less than this figure will not result in surface runoff, and that the surface runoff will start after the precipitation rate exceeds the initial abstraction.

We have obtained the simplest description of the runoff of different durations at different intervals in WMS program, and from it we concluded that the surface runoff to start and exceed the initial abstraction needs at least 700 min to start.

7.2. RECOMMENDATIONS

We must rely on previous experiences in order to avoid the catastrophic results of flash floods, pay attention to cleaning the sewage channels before the start of the hydrological

season, and work on developing the channels so that the drainage channels can withstand the excess water that forms the beginning of the surface runoff and the subsequent flash floods.

Relying on technology to simulate the occurrence of floods, as it can provide realistic models of floods and can provide a complete and comprehensive study of earthquakes, which is what we applied to the WMS program and the ArcGIS program, thanks to which we were able to provide a hydrological study, and we also have to update and develop geological and hydrological maps until We can provide quick and valid studies for any study area.

Relying on the construction of housing units for emergency times in anticipation of material damage as a result of floods, reliance on warning devices that precede the occurrence of rainstorms to avoid human damage.

REFERENCES

Green, T. R., Taniguchi, M., Allen, D. M., & Gurdak, J., "Beneath the surface of global change: Impacts of climate change on groundwater". ***Journal of Hydrology*** (2011).

Youssef, A. M., Alsefry, S., & Pradhan, B., "Analysis on causes of flash flood in Jeddah city (Kingdom of Saudi Arabia) of 2009 and 2011 using multi-sensor remote sensing data and GIS" (2015).

Internet: Retrieved from Arabnews: **https://www.arabnews.com/node/1402051/middle-east** (2018).

Ababsa, M., "Atlas Of Jordan" (2013).

Abdulla, F., "21st Century Climate Change Projection of Precipitation an Temperature in Jordan" (2020).

Abed, A. "Jordan's geology, environment and water" (2000).

Akkawi, E., & Hadadin, N., "The geological model and the groundwater aspects of the area surrounding the eastern shores of the Dea Sea (DS) - Jordan". p. 670 (2009).

Al-Smadi, M., "Incorporating Spatial And Temporal Variation of Watershed Response in a Gis-Based Hydrologic Model" (1998).

Anderson, R., Hansen, J., Kukuk, K., & Powell, B., "Development of a Watershed-Based Water Balance Tool For Water Supply Alternative Evaluations" (2006)

Aswathy, S., Sajikumar, N., & Mehsa, M., "Watershed Modelling Using Control System Concept"**,** 39-46 (2016).

Bhaskar, N. R., James, W. P., & Devulapalli, R. S., "Hydrologic Parameter Estimation Using Geographic Information System. Journal of Water Resources Planning and Management" (1992).

Internet: Britannica. Retrieved from **https://www.britannica.com/place/Jordan/Climate** Chang, H., Franczyk, J., & Kim, C., (2009).

De Paola, F., Giugni, M., Topa, M. E., & Bucchignani, E., "Intensity-Duration-Frequency (IDF) Rainfall Curves, for Data Series and Climate Projection in African Cities" (2014).

Internet: Earth data. (n.d.). Retrieved from **https://search.asf.alaska.edu/#/**

Internet: engineering purdue. Retrieved from **https://engineering.purdue.edu/mapserve/LTHIA7/documentation/scs.htm**

Internet: ESRI. (n.d.). Retrieved from **https://doc.arcgis.com/en/arcgis-online/get-started/what-is-agol.htm**

Fardous, A.-N., Mudabber, M., Jitan, M., & Badwan, R., "Harnessing Salty Water to Enhance Sustainable Livelihoods of the Rural Poor in Four Countries in West Asia and North Africa: Egypt, Jordan, Syria and Tunisia" (2004).

Internet: Gisgeography. *gisgeography*. Retrieved from gisgeography: **https://gisgeography.com/what-gis-geographic-information-systems/** (2021).

Internet: Weather in JERASH, JORDAN, **Google Search: jerash temperature** (2021).

Hoseini, Y., Azari, A., & Pilpayeh, A., "Flood modeling using WMS model for determining peak flood discharge in southwest Iran case study: Simili basin in Khuzestan Province" (2016).

IPCC., "The Physical Science Basis Contribution of Working Group I to the Fourth Assessment Report of the IPCC" (2007).

IPCC., *Climate change 2013 the physical science basis:* " Working Group I contribution to the fifth assessment report of the intergovernmental panel on climate change" (2013).

Keskin, F., "Hydrological Model Study in Yuvacik DAM Basin By Using GIS Analysis" (2007).

Kirpich, P., "Time of concentration of small agricultural watersheds" (1940).

Marques, R. Climate, "Hydrology and Water Resources; Angolan Sector" (1997).

MLYNSKI, D., PETROSELLI , A., & WALEGA, A., "Flood Frequency Analysis by an Event-based Rainfall-Runoff Model in Selected Catchments of Southern Poland" (2017).

Moumany, K., Abed, A., & Ibrahim, K., "Geology of Jordan- Field Guidebook. Amm***an***" (2011).

Naidu, D. S., "Use of Gis in Hydrological Investigations" (2015).

Namrouqa , H., "Floods 'only beginning' of severe climate change impacts on Jordan" (2018).

Internet: National Geographic. Retrieved from **https://www.nationalgeographic.org/encyclopedia/geographic-information-system-gis/**

Oosterbaan, R. J. "Drainage principles and applications" (1994).

Perdikaris, J., Rudra, R., & Gharabaghi, B., "Reference Time of Concentration Estimation for Ungauged Catchments" (2018).

Sawarieh, A., Chen, C., Beinhorn, M., & Gronewold, J., "GIS based model for groundwater flow and heat transport in Zarqa Ma'in and Jiza area, central Jordan" (2009).

Shawabkeh, K., "The geology of Ma'in Area. Amman, Jordan" (1998).

Sippel, S., Zscheischler, J., Heimann, M., Otto, F. E., Peters, J., & Mahecha, M. D., "Quantifying changes in climate variability and extremes" (2015).

Stone, R. J., "Rainfall-Runoff Analysis Using the Soil Conservation Service Curve Number Method" (2014).

Sun, Y., Wendig, D., Kim, D. E., & Liong , S.-Y., "Deriving intensity–duration–frequency (IDF) curves using downscaled in situ rainfall assimilated with remote sensing data" (2019).

Internet: Tashta, N. *onlinenews*. Retrieved from **https://onleinnewos.com/%D8%A7%D9%84%D8%A3%D9%85%D8%A7%D9%86%D8%A9-%D9%85%D8%B4%D8%B1%D9%88%D8%B9-%D9%8A%D8%AE%D9%81%D9%81-%D8%AE%D8%B7%D8%B1-%D8%A7%D9%84%D9%81%D9%8A%D8%B6%D8%A7%D9%86%D8%A7%D8%AA-%D8%A7%D9%84%D9%85%D9%81/** (2020).

Internet: Teach Engineering. Retrieved from **https://www.teachengineering.org/lessons/view/cub_watershed_lesson01**

Internet: The European Space Agency. Retrieved from **https://www.esa.int/ESA_Multimedia/Images/2009/02/The_water_cycle**

The National Severe Storms Laboratory. Retrieved from **https://www.nssl.noaa.gov/education/svrwx101/floods/**

Times, T. N., Death Toll in Jordan Flood Reaches 21, but Grief Quickly Turns to Anger" (2018).

Internet: Toaimat, S. Retrieved from Alghad: **https://alghad.com/%D8%AC%D8%B1%D8%B4-%D8%B4%D9%83%D8%A7%D9%88%D9%89-%D9%85%D9%86-**

%D9%81%D9%8A%D8%B6%D8%A7%D9%86-
%D9%85%D9%8A%D8%A7%D9%87-
%D8%A7%D9%84%D8%B5%D8%B1%D9%81-
%D8%A7%D9%84%D8%B5%D8%AD%D9%8A-%D8%A8%D8%B4/ (2021).

Internet: Twinkl. Retrieved from **https://www.twinkl.com.tr/teaching-wiki/runoff**

Weaver, C., "Geological Survey Water-Resources Investigations" (2003).

Weaver, J., "Methods for Estimating Peak Discharges and Unit Hydrographs for Streams in the City of Charlotte and Mecklenburg County, North Carolina. United States Geological Survey" (2003).

Internet: Wienner, J. B., World History Encyclopedia. Retrieved from **https://www.worldhistory.org/Jerash/** (2018).

Youssef, A. M., Pradhan, B., & Hassan, A. M., "Flash flood risk estimation along the St. Katherine road, southern Sinai, Egypt using GIS based morphometry and satellite imagery" (2011).

Zregat, D. "*Land cover change in Jerash governorate between 1952-2009 using* geographic information systems and remote sensing. *Jordanian Journal of Social Sciences*" (2014).

RESUME

Albaraa Shanati was born in Homs finished his school 2012/2013, and studied one year in Albaath University as a Mechatronic Engineering, after that transferred to North Cyprus to continue as Civil Engineering in Eastern Mediterranean University, and graduated from EMU in 2018. Finally started studying Master Degree in Karabuk University in 2019.